HYDROGEN PRODUCTION STUDY USING AUTOTHERMAL REFORMING OF BIODIESEL AND OTHER HYDROCARBONS FOR FUEL CELL APPLICATIONS

By

Mónica Ospinal-Jiménez

A thesis submitted in partial fulfillment
of the requirements for the degree of

MASTER OF SCIENCE

In

Chemical Engineering

UNIVERSITY OF PUERTO RICO MAYAGÜEZ CAMPUS - 2006

Approved by:

_____	_____
Julio Briano, PhD *Member, Graduate Committee*	Date
_____	_____
Arturo Portnoy, PhD *Member, Graduate Committee*	Date
_____	_____
José A. Colucci-Ríos, PhD *President, Graduate Committee*	Date
_____	_____
Julio Quintana, PhD Representative of Graduate Studies	Date
_____	_____
Nelson Cardona, PhD *Chairperson of the Chemical Engineering Department*	Date

ABSTRACT

During the last few years concerns with distribution, supply and cost of conventional liquid fuels increased considerably. Several developed countries are seriously considering using hydrogen (no fossil combustible) as an automotive energy source as part of the global effort to preserve the environment. An alternative methodology to provide renewable source energy in the transportation sector is Autothermal Reforming (ATR) in combination with fuel cell technologies. Presently, the department of Chemical Engineering of the University of Puerto Rico (UPRM) in collaboration with Argonne National Laboratory (ANL) works in the development of a reforming catalyst characterization program. The purpose of this research is to study the viability of using a new catalyst to convert Biodiesel, Glycerin and Methanol to a hydrogen rich product gas and compare their production potential, identify the conditions for the accumulation of coke and determine the influence of reactor temperature and water to carbon and oxygen to carbon ratios. A Basket Stirred Tank Reactor (BSTR) and Plug Flow Reactor (PFR) with Pt and Rh-based catalysts synthesized at ANL were used.

Hydrogen can be produced from vegetables oils and glycerol by catalytic ATR using Pt-based catalyst. Exit gas concentrations of 45%, 26% and 20% H_2 for methanol, glycerol and biodiesel respectively were obtained. The use of catalyst and increases in reactor temperatures favors H_2 production for ATR of methanol and biodiesel. In glycerol experiments without catalyst, it was observed that at 0.4 O_2/C and 0.5 O_2/C and 900 °F the highest hydrogen concentration was obtained. Also, H_2 was obtained from biodiesel at temperatures higher than 950°F. All biodiesel and glycerol experiments performed had shown coke formation. In ATR methanol, coke formation was not detected in the fittings. In addition, Scanning Electron Microscopy (SEM) was used for surfaces analysis on Pt-based catalysts. Soot deposition on catalyst surface was detected in all samples analyzed. Also, Rh-based catalysts did not increase hydrogen production. Heavy solvents were detected below 4500 ppm in the liquid organic waste.

Keywords: *Hydrogen, ATR, biodiesel and glycerol*

RESUMEN

Durante los últimos años, la preocupación por la distribución, el suministro y los costos de los combustibles líquidos convencionales se ha incrementado. Muchos países desarrollados están considerando seriamente el uso de hidrógeno (combustible no fósil) como una fuente de energía para aplicaciones automotrices como parte del esfuerzo global para conservar el ambiente. Una metodología alterna para proveer una fuente de energía renovable en el área de transportación es la combinación de la reformación autotérmica (ATR*) con la tecnología de celdas de combustibles.

Actualmente, el Departamento de Ingeniería Química de la Universidad de Puerto Rico (UPRM), en colaboración con el Laboratorio Nacional Argonne, trabaja en el desarrollo de la caracterización de catalizadores usados en procesos de reformación. El propósito de esta investigación es estudiar la viabilidad de usar nuevos catalizadores para convertir Biodiesel, Glicerina y Metanol en un producto gaseoso rico en hidrógeno; comparar su potencial de producción, identificando las condiciones para la acumulación de carbono y determinar la influencia de la temperatura del reactor y de las razones agua/carbono (H_2O/C) y oxígeno/carbono (O_2/C). Para ello se usaron un reactor de agitación continua (BSTR*), un reactor de flujo pistón (PFR*) además de catalizadores a base de Pt y Rh sintetizados en ANL.

Es posible producir hidrógeno a partir de aceites vegetales y glicerina utilizando ATR y catalizadores a base de Pt. En experimentos usando metanol, glicerina y biodiesel como combustibles se obtuvieron concentraciones de gases de salida de 45%, 26% y 20% de H_2 respectivamente. El uso de catalizador en base platino al igual que el incremento de la temperatura del reactor favorece la producción de hidrógeno en experimentos con metanol y biodiesel. En experimentos con glicerina se observo que a 0.4 O_2/C y 0.5 O_2/C y 900°F se obtuvo la mayor concentración de hidrógeno. También se obtuvo H2 a partir del biodiesel a temperaturas mayores de 950°F. Todos los experimentos realizados con biodiesel y glicerina mostraron formación de carbón. Sin embargo, con metanol, el sistema de

* Por sus siglas en inglés

tuberías no evidenció presencia de carbón. Además, se practicó microscopía de barrido de electrones (SEM*) para analizar la superficie de los catalizadores a base de Pt. Se percibió deposición de carbón en la superficie de todas las muestras analizadas. Por otro lado, los catalizadores a base de Rh no aumentaron la producción de hidrógeno. Se detectaron solventes pesados por debajo de 4500 ppm en el residuo orgánico líquido.

Palabras Claves: *Hidrógeno, ATR, biodiesel y glicerina*

Copyright@2006 by Mónica Ospinal-Jiménez.
All rights reserved.

Now faith is assurance of things hoped for,
proof of things not seen. - Hebrews 11:1-

To my parents and Jorge Eduardo

ACKNOWLEDGMENTS

I wish to express my gratitude to everyone who contributed to the development and conclusion of this project. I must single out Argonne National Laboratory who gave their approval and economical support. Hats off to Dr. Jose Colucci who provided me enough freedom, personal and academic advises, and encouragement to complete this work. And especially because he was not merely my mentor, he ended up been my academic father. Many thanks to my graduate committee, Dr. Briano, Dr. Portnoy, and Dr. Quintana for their advices and considerations.

I am also grateful to Hewlett Packard, particularly Julio Cartagena who gave permission to use their SEM equipment and Gabriel Cruz who provided his expert advice in the pictures' acquisition. Also, thanks to Dr. Castro from the Dept. of Chemistry by the use of his SEM.

Thanks to Efrén Mercado, Ernesto Borrero, Angel Zapata and María G. Gómez for all their help, suggestions and ideas related with the assembly and procedure analytical.

It is also a pleasure to recognize the cooperation of the undergraduate research group: Jesús García, Edgar Caro, Teresa Rosa, Chaila Rodríguez, Raquel Mejía, Luis Moux, and Vanessa Ayala. This project would not be finished without their extraordinary help. Also, I want to mentioned my gratefulness to my friends; Joma, Wanda, Andrya, Denisse, Carmelo, Abner, Mattei, Kristia and Ivelisse, who are part of our R&D group.

I am deeply indebted to my friends Ritsdeliz, Juan Carlos, Jesús, and Luis who painstakingly read and edited my drafts. A special debt of gratitude is owed to M. Schwarz, O. Santos, M. López, Y. López, R. Pérez, A. Alegría, J. Rivera, D. Hernández, JC Sáez and M. Gómez those who offered their friendship and brotherhood. They always reminded me that I had a family here and that there are things in life beyond doing experiments.

I would like to warmly thank Jaime Benítez, Antonio Estévez and Moses Bogere for their guidance and thank the Dept. of Chemical Engineering for the sponsorship and allowing the opportunity to pursue my MS studies.

Last, but not least, I thanks to my extended family for their sincere encouragement, despite having no actual knowledge in the subject.

TABLE OF CONTENT

LIST OF FIGURES

LIST OF TABLES

LIST OF SYMBOLS AND ABBREVIATIONS

Symbols

ATR	Autothermal Reforming
ATR's	Autothermal Reformers
ANL	Argonne National Laboratory
UPR	University of Puerto Rico
EU	European Union
NREL	National Renewable Energy Laboratory
FASTER	Feasibility of Acceptable Start Time Experimental Reactor
SR	Steam Reforming
Ox	Oxidation
POx	Partial Oxidation
FC	Fuel Cell
PSA	Pressure Swing Adsorption
NOx	Nitrogen Oxides
S/C = W/C = H_2O/C	Steam to Carbon ratio = Water to Carbon ratio
O_2/C	Oxygen to Carbon ratio
H/C	Hydrogen to Carbon ratio
CO	Carbon monoxide
O_2	Oxygen
H_2O	Water
H_2	Hydrogen
N_2	Nitrogen
HC's	Hydrocarbons
$C_nH_mO_p$	Hydrocarbon with *n* mol of carbon, *m* mol of hydrogen and *p* mol of oxygen
η_{ref}	Efficiency of the reformer
ΔH	Finite change in a total enthalpy [J/mol, J/kg]
Ni	Nickel
Pt	Platinum
Rh	Rhodium
Co	Cobalt
Ru	Ruthenium
DOE	Department of Energy
BP	British Petroleum
GM	General Motors
ppm, ppb	Part per million and part per billion
BSTR, PFR	Basket Stirred Tank Reactor and Plug Flow Reactor
PEM	Proton Exchange Membrane
R&D	Research and Development

CHAPTER I

Introduction

We are living in a planet of fast and accelerating adjustments. The technological advances are transforming the manner that we live. As more and more areas of the globe develop, the demand for energy will continue to increase considerably, impacting the overall environment in unpredictable ways. It is pertinent to develop an energy strategy for the world's energy future that could be economical and environmentally sustainable. Fossil fuels are a finite resource. More than a century ago, the writer J. Verne recognized hydrogen as a potential energy carrier [88]. Hydrogen contains no carbons that can form pollutants or greenhouses gases. Considerable efforts have being focused on research intended in introducing hydrogen into the transportation sector as a competitive and useful fuel. The Bush Administration is focused on overcoming the technical obstacles that would allow affordable hydrogen fuel cells vehicles. The goal is to make hydrogen fuel and its applications competitive in the 2015-2020 time frames [95]. David Garman, of the U.S. Department of Energy (DOE), in his speech concerning the future of energy and transportation issues (March 12, 2004) emphasized, "Hydrogen is far less expensive than in the past…".

There are many alternatives that would allow hydrogen to be used as the feed of the fuel cell. Some of them are: H_2 gas cylinder, H_2 refill in a gas station or H_2 generation inside the car. In the latter, Autothermal Reforming (ATR) is an excellent option to generate H_2 from hydrocarbons (HC's) fuels such as CH_3OH, Biodiesel, Glycerin and Natural gas. Since 1980, Argonne National Laboratory (ANL) has been paying attention to fuel processors and is working to develop reformer catalysts in order to improve their performance.

Presently, the Department of Chemical Engineering of the University of Puerto Rico at Mayagüez (UPRM), in conjunction with ANL work in a reforming catalyst characterization program. Its purpose was to establish the viability of using a new catalyst in order to: convert Biodiesel and glycerin to H_2 and compare the production of H_2 with and without catalyst. A basket Stirred Tank Reactor (BSTR), Bed Flow Reactor (BBR), Pt and Rh-based catalysts synthesized at ANL was used.

I.1 Justification

Recently, the scientific international communities representing the energy, transportation and academic sectors are developing alternative processes to produce energy in order to reduce greenhouse gas emissions and reduce the dependence on crude oil. The world is moving toward fuels that contain less and less carbon and are looking for oil independence technology. Among all fuel cells, the proton exchanged membrane (PEM) fuel cell is an interesting technology, because it has lower environmental impact. It uses hydrogen and oxygen as reactants to produce water and electricity. The easier way to obtain the hydrogen gas is to be reformed from hydrocarbons or biofuels. Figure 1, illustrates the combination of a reforming process with fuel cell technology to produce renewable energy.

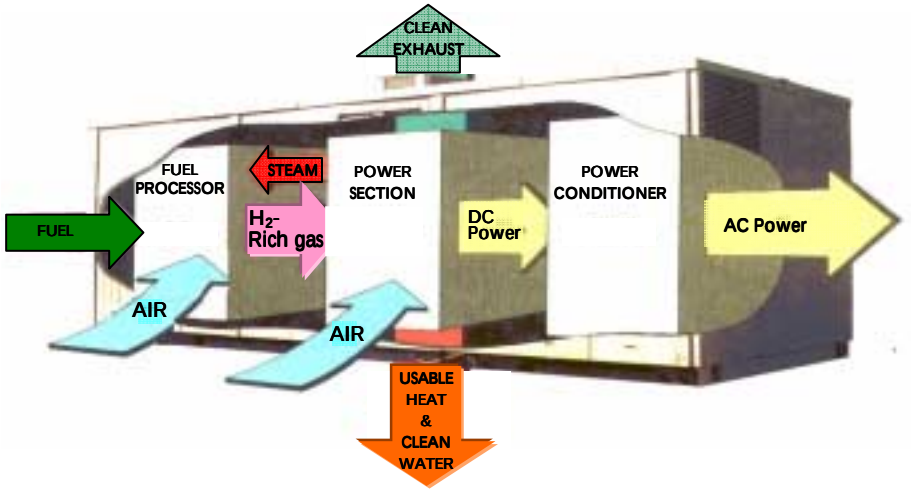

Figure I.1 Illustration of clean energy production

There is a lot of interest in converting hydrocarbons known in transportation such as methanol, bioethanol, methane, diesel and biodiesel into a hydrogen rich gas acceptable for automotive fuel cells applications. The hydrogen infrastructure and regulations necessary for its utilization as a fuel for road transportation still have some issues to solve. Many alternatives need to be analyzed focusing on market necessity. Some of the issues include alternatives to the hydrogen storage and the

selection of a good combination between HC's and catalysis, capable to produce higher performances.

Hydrogen rich gas can be produced via reforming technologies. Three major processes are: Steam reforming (SR), Oxidation (Ox) and the combination of both, called Autothermal reforming (ATR). These have been increasingly accepted as the most appropriate processes for future fuel cell vehicles and are also used in chemical processes. Hydrogen is obtained in large scale by the SR process with methane as the hydrocarbon fuel. This reaction is endothermic. In large chemical plants, normally there are excess heats available from other process that can be used, but in automotive applications it must be internally generated. At a smaller scale, an attractive alternative is ATR. The heat generated by the Ox can be controlled directly by adjusting the proportions of fuel, air and oxygen in the feed.

An important issued in the commercial viability of the automotive fuel cell technology, is the feasibility of reforming the hydrocarbon outside or inside the car. Department of Energy (DOE) through their national laboratories in collaboration with universities and industry partners are collaborating to overcome critical technical barriers to fuel cell commercialization and decrease the infrastructure problems.

One of the main problems with reforming systems is the formation of coke and the presence of gases that can poison the cell. ANL research involves the development of new catalysts that could be effective for all HC's reforming. They should be capable to minimize methane formation, avoid coke formation in the catalyst surface and be selective to hydrogen and carbon dioxide. They have developed Pt and Rh-based catalysts. ANL is very interested in utilizing these catalysts with alternative fuels such as ethanol and Biodiesel.

There is preliminary evidence that hydrogen can be obtained by catalytic steam reforming with rapeseed, corn, soybean and sunflower oil (renewable fuel). This suggests that fats and other refined vegetable oils might be appropriate for hydrogen production such as Biodiesel (methyl ester or vegetable oil derived).

In this context, the Department of Chemical Engineering of the UPRM in collaboration with Argonne National Laboratory in Chicago, IL is developing and

implementing a Reforming Catalyst Program. In this investigation the reforming method of interest is the ATR, which combines the endothermic SR (part of the fuel reacts with water) with the exothermic Oxidation (part of the fuel reacts with oxygen) with the purpose to balance the heat loads. Autothermal reforming refers to the heat exchange between the steam reforming and the oxidation process. HC's react with a mixture of oxygen and steam in a reactor with a catalyst. Argonne National Laboratory (ANL) has been developing systems that are capable of reforming many conventional fuels into a hydrogen-rich gas for feeding fuel cells using ATR. This process will be similar to the automotive catalytic converters, using reactors of lower cost and easy manufacture. Vaporized fuel is mixed with steam and oxygen inside a catalyst packed reactor.

The principal objectives of this work are to convert biodiesel and glycerin to a hydrogen rich product gas and to identify hydrocarbons such as C_2's, C_3's and aromatics (benzene, toluene and xylene's). Also, to establish the better combination of furnace temperature, flow rate of O_2, water and fuel in order to optimize fuel conversion and maximize H_2 production. And determine the deactivation operating window of the catalyst due to soot and coke formation.

I.2 Objectives

The main objectives of this study are:

- To convert biodiesel and glycerin to hydrogen rich product gas.
- To study the combination of experimental variables O_2/C and reaction temperature in order to obtain the highest hydrogen rich gas production.
- To identify the other hydrocarbons formed in the reaction (C_2's…C_{10}'s).

The specific objectives of this study are:

- To establish the feasibility of reforming biodiesel and glycerin using a Pt-based and Rh-based catalysts synthesized by ANL.
- To determine the efficiency of the process to convert biodiesel and glycerin to hydrogen.
- To compare the production of carbon monoxide, carbon dioxide and other hydrocarbons in the product gas at all conditions analyzed.
- Identify the operation window conditions that lead to coke formation.

CHAPTER II

Background and Literature review

II.1 Fuel Cell Technology

The fuel cell (FC) was first conceived by Sir William Grove in 1839, but it has taken more than a hundred years for FC's to become seriously considered for commercial applications [77]. FC, first used in the U.S. space and military programs, are an attractive power source for mobile applications. Now, with support from DOE and other federal agencies, early commercial fuel cells are being used today in an amazing variety of ways.

Due to unstable oil price situation in the world market, many countries have been looking for alternative energy to substitute petroleum. The union of hydrogen and oxygen (air) in a fuel cell is an ideal alternative to replacing existing carbon based technologies. Although FC has been known for more than 167 years, it is still in a development stage. One reason why it has taken so long to introduce the technology into the market, are the high costs.

The advance of material science, engineering techniques and development of better design methods are leading to cost reductions. Presently, Proton Exchange Membrane FC (PEMFC) has the biggest potential for cost reduction and implementation in automotive applications. So far test applications in cars proved good acceleration performance up to 90 km/h and a maximum speed of 110 km/h. The driving range is 250 km [73].

Considerable effort is being dedicated on research and demonstration projects aimed at introducing hydrogen into the transportation sector as a fuel. Any hydrogen-rich material can serve as a possible fuel source of hydrogen. Right now, energy companies and researchers are exploring various methods and resources for hydrogen production in an effort to determine the most cost-efficient, environmentally-friendly way to provide power for fuel cell vehicles.

Reformer technology is a key player on the future development of hydrogen production. Although the earth has many natural sources of hydrogen, unfortunately it is

not a primary source of energy as fuel to be used in transportation vehicles. Hydrogen generation from water by electrolysis is not economic at the moment [73]. It has to be produced by conversion of hydrocarbons such as natural gas, alcohols or bio-oils.

Because of its similarity to fossil diesel, vegetable oil derivates are an alternative in automotive engines either with a reformer or as direct fuel. Usually, the ethyl or methyl ester (biodiesel) derivates are preferred. Steam Reforming (SR), Oxidation (Ox) and Autothermal Reforming (ATR) are the options to reform hydrocarbon (HC's) fuels.

In general, hydrogen obtained from vegetable oils or HC's must pass through clean treatments before they are fed to a FC to avoid membrane poisoning. The future of FC in transportation is not guaranteed. FC will be in competition with current technologies such as gas turbines, steam turbines, combined cycles and diesel engines. The commercialization will require improvements in costs, durability, materials, system design and manufacture to be competitive. Advantages of FC are its high energy conversion efficiency (50–70%) and nearly zero emission (clean power) [8]. It is an interesting candidate to compete and replace the conventional power source (petroleum and derivates).

II.1.1 Fuel Cell (FC)

Fuel Cells (FC) are an attractive but challenging technology. It transforms chemical energy directly to electrical energy, with less pollution when compared to burning fossil fuels. Although the fundamentals of FC as an electrochemical system and an energy conversion device are out of the scope of this work, a brief discussion of the different types of FC will be given. A FC is classified by the type of electrolyte which plays an important role in the transport of the electrons upon oxidation of hydrogen at the anode and reduction of oxygen at the cathode. The typical design is based on: an anode, to which the fuel is supplied, a cathode, to which the oxidant is supplied, and an electrolyte, which allows the flow of ions (but not electrons and reactants) from the anode to the cathode. The net chemical reaction is exactly the same as if the fuel were burned, but by spatially separating the reactants, the fuel cell intercepts the stream of electrons that

spontaneously flow from the anode (fuel) to the cathode (oxygen) and diverts it for use in an external circuit. Figure II.1 illustrates a standard Fuel Cell. As mentioned earlier there are different classes of fuel cells, which operate at different temperatures and are generally distinguished by their electrolytes. The main fuel cells include: Phosphoric Acid FC (AFC), Molten Carbonate FC (MCFC), Solid Oxide FC (SOFC), Proton Exchange Membrane FC (PEMFC), and Direct Methanol FC (DMFC). Some of them show promise for use in industrial power generation as MCFC and SOFC and other may be useful for small portable applications as PEMFC [53].

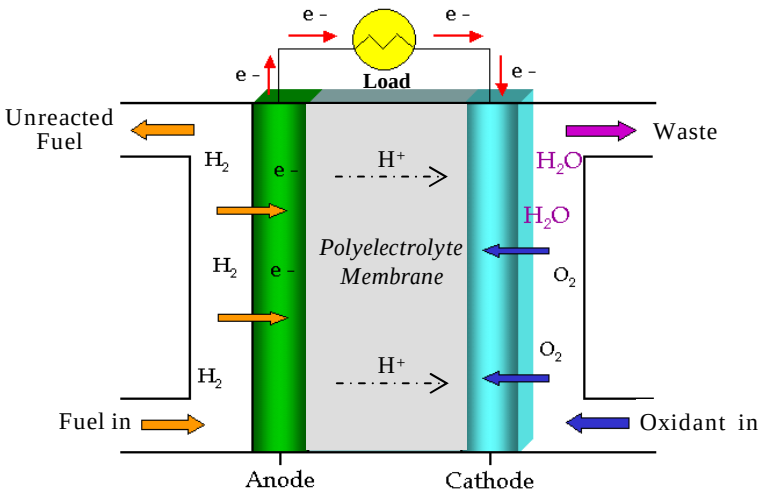

Figure II-1 Scheme of Fuel Cell [34]

The polymer electrolyte FC has the potential to replace the internal combustion engine for propulsion power. A number of companies have developed compact steam methane reformers to reform natural gas with closely coupled FC as Haldor-Topsoe, International FC (IFC), Osaka Gas Company and Sanyo electric. Likewise, countries as Hawaii and Iceland are considering supplying a high percentage of their power energies requirements with FC. Although this technology is newly commercialized, it shows the promise of reduced capital cost when compared to conventional small-scale reformers and compactness.

II.1.2 Hydrogen for FC

Hydrogen is flexible, affordable, safe, domestically produced, used in all sector of the economy, clean option and emerges as a particularly attractive long term alternative to be a suited fuel for FC system.

This technology have the following desirable characteristics: hydrogen vehicles have near zero tailpipe emissions, can be made from widely available primary energy sources (including solar, wind, nuclear and natural gas power), greatly reduced full fuel cycle emissions of air pollutants are ongoing rapid development worldwide, and is expected to result in good performance and low costs in mass production.

Approximately 40 million tons of hydrogen gas are produced annually on a global scale, but very little of this is used as an energy source. Most of the hydrogen produced is used in oil refining, in methanol and ammonia production [21]. Despite its abundance in Earth specifically in the hydrosphere, H_2 generation must be evaluated and studied, because it is not a resource; is an energy carrier that must be manufactured. Hydrogen does not exist freely in nature, but it can be obtained from fossil fuels, biomass, or water [88]. Ogden *et al.*[31], reported that approximately 95% of the hydrogen produced today comes from carbonaceous raw material, principally fossil in origin and only a fraction of this percent is currently used for energy purposes.

More recently, Farrell *et al*.[13] and the web site Edmunds [9], presented a revision of the costs of building, distribution, infrastructure, transportation over large distances and manufacture of hydrogen at large scales in the near future. They concluded that the principal economic barriers are the costs, currently unacceptably high compared to the existing natural gas or petroleum distillate technologies.

In the transportation sector storage and delivery of hydrogen has its limitations. Since it has low volumetric energy density, it is difficult to compress and requires extremely low temperatures for liquefaction. A key question is how to supply hydrogen to vehicles. A number of near term hydrogen supply options exist, including the following processes: compressed gas, liquefied hydrogen, chemical hydrides and carbon nanotubes [21].

Each one has advantages, disadvantages and issues to solve like the accommodation of vessels inside the cars, boiling during refueling, safety concerns and heating/cooling to

deliver the fuel. A list of ongoing and future supply options to delivery hydrogen prepared by Ogden *et al.* [31] is given in appendix C.

The cost of supplying hydrogen to vehicles depends on a host of factors including the local energy prices and the size of the hydrogen demand [2, 9, 13, 18, 31-33]. Hydrogen really doesn't need to be storage. It can be produced and fed online to the fuel cell using hydrocarbons reforming as a process. A review of the ongoing research at Princeton University's, ANL, Alamos Laboratory and others, suggest that small-scale steam reforming with natural gas might offer the lowest delivered hydrogen cost and efficient results for hydrogen production.

Farrell *et al.*[13], explained some policy considerations about the incursion of hydrogen in the transportation sector since it is a product with few benefits compared with petroleum fuels. Based on this point of view many authors recommended that the introduction of hydrogen into the market must require forceful government action or substantial economic incentives. Detailed descriptions of the advancement in this technology are presented by Naidja *et al.*[14], Sommer *et al.*[45] and Borup *et al.*[30].

Hydrogen gas produced by reforming has inherent poisons that result in fuel cell deactivation. Some purification processes are suggested by the authors that can be used to correct it: water gas shift reactions, methanation, selective oxidation, membrane reactors and pressure swing adsorption (PSA).

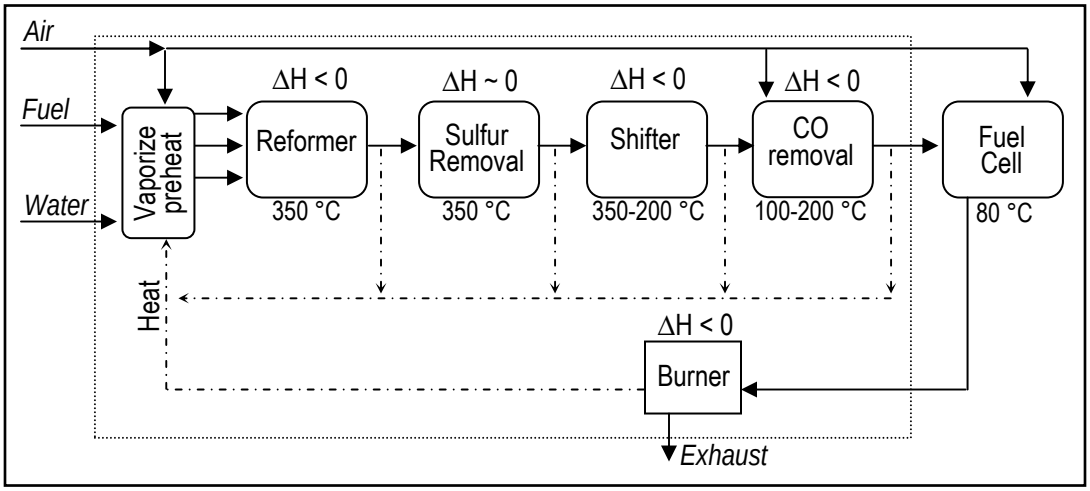

Figure II-2 Typical fuel processor requirements

Additionally, limitations of poison also will be diminished or eliminated with a correct combination between fuel types and catalysts used. All reformed outlet gases will need to include significant gas conditioning. One alternative is to clean the reformate product before the FC feed to guarantee a good performance of the unit. Furthermore, stream recycle could improve the selectivity and conversion of the fuel. Figure II.2 depicts one option for H_2 production. [14, 30, 45].

Another interesting hydrogen production process was developed by Johnson Matthey [69]. They developed the HotSpot™ system to reform fuels such as methanol, natural gas, LPG and higher hydrocarbons, including gasoline. Additionally, the research center *IWV* [53], has been working on the development of a compact reformer whose specific weight must not exceed 3 kg/kW, their configurations consisted in an electric drive system with PEFC.

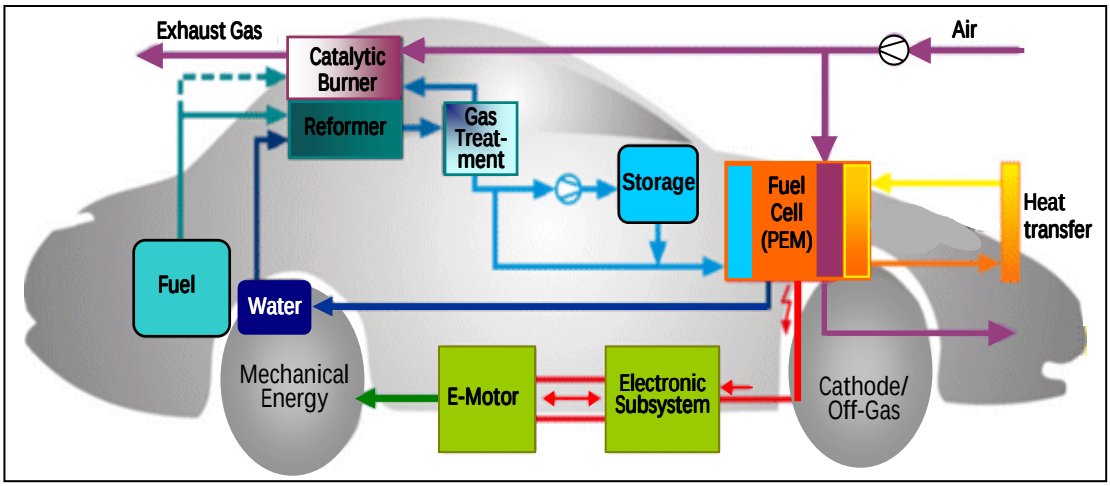

Figure II-3 Schematic configuration of a FC passenger car with on-board production of H_2 from CH_3OH by steam reforming [53]

Figure II.3, describes a schematic configuration of a FC with on-board hydrogen production, which in addition to the fuel cell also contains the reformer, catalytic burner, a secondary gas treatment unit, an electronic regulator and an electric motor. It must be able to compete with conventional technology concerning volume, weight, dynamics and costs.

In order to meet the economical requirements, future research in this field must concentrate on the development of a compact reformer whose specific weight must not exceed 0.3 kg/kW. This comprises 0.13 kg/kW for the reformer and 0.17 kg/kW for the catalytic burner.

II.1.3 Argonne National Laboratory (ANL)

ANL is one of the U.S. Department of Energy's (DOE) largest research centers. The investigations in ANL are distributed in five wide programs: basic science, energy resources, scientific facilities, environmental management and national security. The 2nd one helps assure a reliable supply of efficient and clean energy for the future. Batteries, FC, catalysts and storage systems are studied in this program. ANL conducted research in conjunction with DOE in fuel reforming, computer modeling and H_2 infrastructure.

In fact, ANL has developed a lightweight fuel processor, capable of rapid start-up and shutdown and energy efficient that combines a liquid fuel with oxygen to produce hydrogen stream. They have been studying a wide variety of organic compounds and catalysts. Alcohols and HC's such as bioethanol, aromatics, cyclohexane and biofuels have been used. The catalysts play a key role in fuel reforming and are selected to maximize hydrogen production and minimize undesirable byproducts, such as carbon monoxide, methane and others.

In order to enhance the knowledge in catalytic routes, some catalysts studied and synthesized by ANL are: Pt, Rh, Ru, Ni and Pd in substrates as ceria, zirconia and lanthanum gallate. Catalysts studied by ANL meets the DOE targets for performance, conversion and selectivity of CO, durability and activation. ANL increased the activity and stability of Pt catalyst and less stability in the samples after air exposure.

At the same time, Argonne is doing alternative developments in sulfur removal, design, to optimize and validate a reliable and safe integrated hydrogen refueling system. The ANL research team [1, 12, 16, 18, 29, 35], has been continuously publishing progress and ongoing works attained in the energy resources program.

Moreover, *Perez, R.* [25] performed a literature review of research and improvements made by ANL. She identified a chronological evolution on subjects related to Reforming Process. ANL is continuing research to find alternative combination of fuels, catalyst and processes that will permit a small, light and efficient reformer capable of being introduced in transportation markets.

They are part of FASTER (Feasibility of Acceptable Start Time Experimental Reactor) project supported by DOE [35]. Argonne has developed an award-winning catalyst that is licensed to an industrial firm, and continues to focus efforts on developing new reforming and water-gas shift catalysts specifically tailored for use in emerging fuel cell applications.

II.1.4 Global economy of hydrogen and dependence of oil

Almost 40% of all the energy demand in the United States including the one needed for transportation systems is met by liquid fuels such as gasoline, jet fuel and diesel. All these fuels are derived from petroleum. British Petroleum (BP) published the proven oil reserves in 2001 and the majority is in the Middle East as depicted in figure II.4.

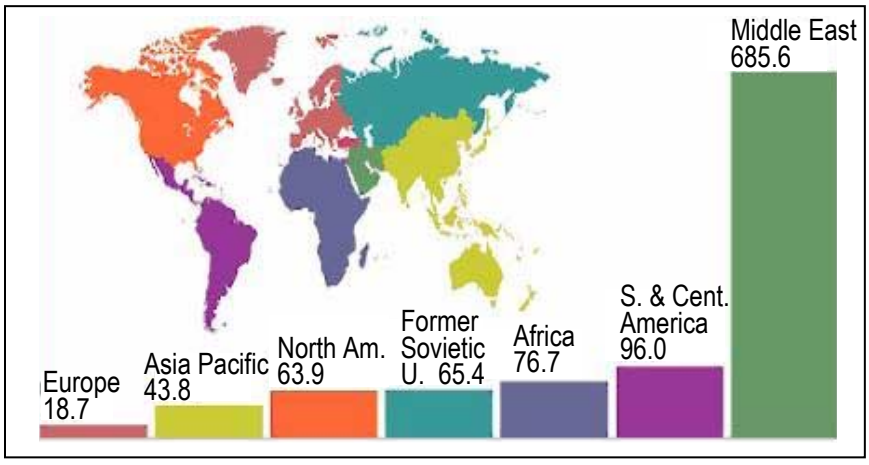

Figure II-4 Reserves oil at 2001 (thousand millions barrels) [94]

In addition, as a consequence of the great demand for crude oil, the resources are depleting. For that reason a replacement for crude oil is needed. Figure II.5 depicts the discovery vs. the consumption of oil in the last years.

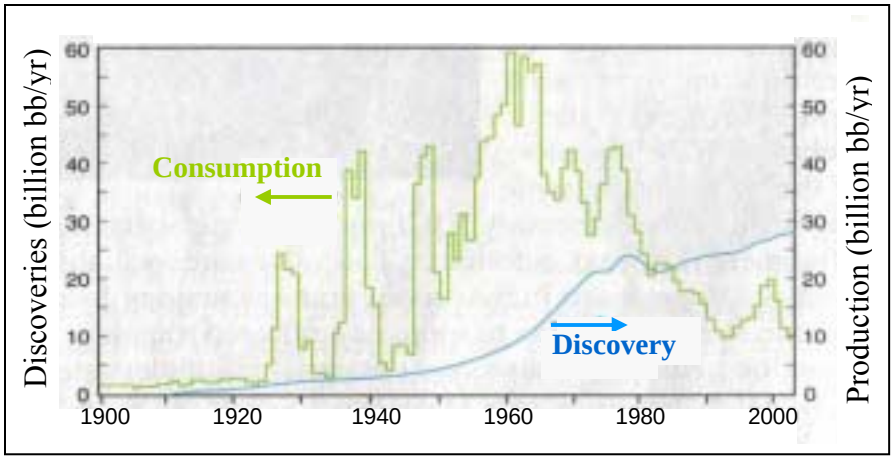

Figure II-5 Rate of discovery and use of conventional crude oil vs. time [93]

One of the proposed alternatives for such replacement is hydrogen. Actually an assessment of the options available for the transport fuels supports the idea of a hydrogen based economy. Between the alternatives for future transport fuels are: greenhouse gas free fuels conversion of shale oil, coal and tar sands to liquid fuels; and hydrogen. Each option is very different to each other. However, they all need hydrogen to produce the fuels. Hydrogen can be produced by solar, nuclear and traditional fossil fuel steam reforming as described in figure II.6.

Table II.1 Near and long term transport fuel options [93]

Product	Feedstock	Greenhouse
Liquid fuels	Crude Oil	Yes
	Heavy oil	Yes
	Tar sands	Yes
	Oil shale	Yes
	Coal	Yes
CO_2 - Neutral fuels	Air	No
	Biomass	No
	H_2 Carrier	No
H2	H_2O	No

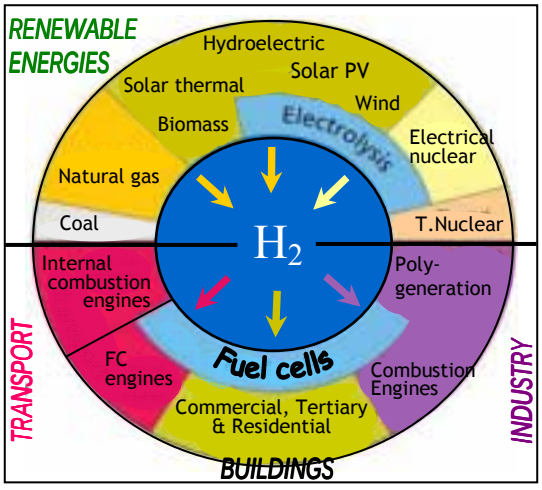

Figure II.6 Supply and demand of H_2

Another important component in the future of transportation is electric cars. If they were successful there is no need for liquid fuels. However they have two key limitations: vehicle range and battery recharging. Although hybrid vehicles are now being tested and used it is not a complete replacement of the liquid fuels (see appendix C).

As a consequence hydrogen is still proposed as the future transportation fuel. However, from an economic point of view this technology has its limits. The cost of using hydrogen directly as a transport fuel is higher than the cost of using liquid fuels. Its production cost is less than others, but not the distribution and storage costs. Different approaches including hydrogen can provide the fuel for the transport systems without increasing the concentration of atmospheric greenhouse gases (Table II.1). Economy factors are going to be the determinant consideration.

II.2 Reforming Systems

The generic term most often applied to the process of converting liquid or gaseous hydrocarbon fuels to hydrogen is “reforming”. Fuel reforming processing is a bridging technology to assist the commercialization and enhancement of FC systems in the absence of a hydrogen infrastructure. During the last decades, numerous studies have been carried out on oxidation, reforming and autothermal reforming of different fuels. Indeed, numerous studies have been carried out with a single fuel such as methane, methanol, ethanol, gasoline, diesel, isooctane, n-heptane, and bio-fuels. Also, mixtures of two single components, specially n-heptane and isooctane have been studied as fuels for reforming processes [14, 16, 18, 23].

In reforming systems there are different characteristics that must be evaluated, such as: fuel composition, reforming processes, catalyst, W/C and O_2/C ratios, coke formation, temperature reaction and NOx and CO pollutants. It is required to accelerate the implementation of FC in the transportation sector to eliminate the dependence in petroleum systems and begin to minimize the level of toxic emissions. In the economic perspective, Wheeler [62], used a financial model in order to recommend the design with

high reformer outlet temperature, low S/C ratio and high recovery in the PSA unit for a given operating pressure to obtain the lowest cost in H_2 production.

To achieve good fuel cell functionality it is essential for reforming systems to provide acceptable ranges in the quality of the feed stream. Some authors proposed ranges between (10- 50) ppm in CO and 10-200 ppb in other poisons [12, 20, 64]. Whatever the nature of the fuel to be used in reforming, the fact that petroleum contains sulfur, which is a well know poison to the FC catalyst, a preliminary desulphurization and gas-cleaning step, is necessary to guarantee that FC stacks are exposed to very low levels of sulfur and carbon monoxide. However, it is worth mentioning that biofuels have very low levels of sulfur and should be considered for reforming processes [5, 26, 27, 28]. A group of authors considered the cleaning of CO and sulfur of the reformate product key for the good performance of FC systems. Some of them suggested doing more investigations in the mentioned processes to identify mass transport limitations and examine the effect of water-fuel-oxygen mixture [3, 14].

Hadidi *et al.*[38], Sirignano[39] and Liu *et al.*[40] in order to improve the feed mixtures in reforming processes, identified theoretical and experimental considerations of fuel droplet vaporization. In conjunction with that, Borup *et al* [2,30] examined the effects of fuel on hydrogen devices. They found that to obtain proper conversion of HC's and avoid hot/cold spots, the mixture preparation is critical. Similarly, Kopasz *et al.*[79] concluded that to obtain high efficiencies and avoid hot spots and areas of non-uniform W/C and O/C ratios it is needed to have proper delivery and mixing of reactants.

Whereas ANL, to address the poison problem, is optimizing sulfur scrubbers for compact systems like ATR's, developing more robust water gas shift catalysts that will work better under transient operating conditions than current catalyst [16], and testing catalysts for preferential oxidation of CO and CO sorbents to treat the product stream.

Thermodynamic calculations are essential for the evaluation of POx, SR and ATR of hydrocarbons to calculate the reaction conditions at equilibrium. Palm *et al.*[50] suggested to make these simulations under adiabatic conditions. Computer software such as CHEMKIN II, EXGAS, ASPEN, KINGAS and THERGAS has been used to generate detailed chemical kinetic models [14, 41 and 42] in several reforming process.

The reaction heat is calculated by the Gibbs free energy minimization method, describing the system temperature and product composition [51]. PROII, HYSYS, AspenPlus or others commercially available software also can be used for this purpose.

Docter *et al.*[20], in their thermodynamic predictions, defined the relation between the reformer reactor with preheat temperatures, pressure inside of the reactor, chemical composition, heat loss of the reactor and fuel/air and fuel/water ratios. In the same group Rampe *et al.*[21], estimated the potential energy efficiency η_{ref}, as depicted in equations 1 and 2.

$$\eta_{ref} = (n\mathrm{CO} + n\mathrm{H_2})\ \mathrm{LHV_{H2}} / n_{fuel}\ \mathrm{LHV}_{fuel} \quad \text{(II.1)}$$

$$\eta_{ref} = (n\mathrm{CO} + n\mathrm{H_2})\ \mathrm{HHV_{H2}} / n_{fuel}\ \mathrm{HHV}_{fuel} \quad \text{(II.2)}$$

Where *n* is the number of moles of CO, H_2 and the fuel, LHV is the lower heating value and HHV the higher heating value. In addition, they stated from a thermodynamic point of view, the formation of solid carbon (coke or soot), that depends on the ratio of C/H in the fuel as well as on the O_2/Fuel and W/C ratio plus the reactor temperature. Hartmann *et al.*[68], described that the reforming efficiency, generally, increase with decreasing air ratios while sufficient water takes place in the reforming reaction.

Another important parameter in reforming is the space velocity (SV). It is defined as the proportion between the standard volumetric flow of the ducts and the volume of the catalyst material [21]. Similarly, Fogler [93] defined the SV as equation II.4, where υ_o is the volumetric flow rate and V is the reactor volume. The two space velocity commonly used in the industry are the liquid hourly and gas hourly space velocities, LHSV and GHSV respectively. The υ_o in the GHSV is normally measured at standard temperature and pressure.

$$\mathrm{SV} = V_{\mathrm{duts}}/V_{\mathrm{catalyst}} \quad \text{(II.3)}$$

$$\mathrm{SV} = \upsilon_o / \mathrm{V} \quad \text{(II.4)}$$

Bae *et al.*[3], established thermodynamic equilibrium with ATR of iso-octane. In this study, they found 700°C as the preferred operating temperature, stability to convert various fuels to H_2 and excellent resistance to sulfur and coking.

II.2.1 Brief history of Reforming

In the 1930s, the first unit of Steam Reforming (SR) was implemented to convert steam and HC's to hydrogen for the production of ammonia [70]. Actually, SR catalysts and technology are now used worldwide to produce most of the hydrogen used for ammonia/methanol and refinery operation [1]. H_2 as a fuel is interesting because the insufficiency of petroleum and greenhouse gas and since the 90's decades several studies have assessed the cost and feasibility of building a H_2-refueling infrastructure for vehicles.

At the beginning, CH_4 was the first choice to obtained H_2. However, other HC's such as alcohols, propane, heavy and light compounds even biomass are now considered. These processes can be done by catalytic or non-catalytic routes. The former, improves the temperature range, enhances the performance and could favor a specific mechanism. Also, experiments of reforming without catalyst have been evaluated. In addition, it has been recommended to study additional combinations of fuels, catalysts, feed ratios and temperatures to obtain better performance. The trend has been to develop more compact, simpler and therefore lower cost reformers. In fact, the FC developers moved toward systems where each plate in the reformers has a double function (the reforming reaction take place in the 1^{st} and the 2^{nd} drives the catalytic heating in the reaction). POx systems and ATR's involve more complex purification systems that are being developed for these reformers. Membrane reactors, ion and oxygen transport has been a growing interest in these processes. In 1998, Daimler-Benz Company in Frankfurt on the automotive fair presented the first vehicle with FC propulsion and gas processing system based on methanol as fuel (NECAR III) [20]. Moreover, oil and manufacturing cars companies such as British Petroleum, Amoco, Shell, GM and DuPont are involved in joint ventures to develop fuel processors and hydrogen infrastructure demonstrations.

At the present time the government sector in the U.S have 2010 year where the technical target for startup in less than 30 seconds and achieve $2.90/Kg for purified hydrogen. The FASTER project goal led by ANL is to design and test an experimental fuel processor to demonstrate concepts for rapid startup [35]. DOE targets toward year 2015 as the limit for hydrogen technology to be competitive with gasoline [82].

II.2.2 Oxidation (Ox)

Ox is a commercially available method for producing H_2 from HC's. $C_nH_mO_p$ or C_nH_m type compounds are oxidized to H_2, carbon oxides and water (H_2O). It is an exothermic reaction and no indirect heat exchange is needed. For alkanes (C_nH_m) the reaction is expressed by equation II.5 [6].

Similarly, Borup *et al.*[2] presented a reaction for a generic aliphatic HC's to CO as depicted in equation II.6. To minimize CO formation, his recommendation includes a water gas shit reaction (WGSR) as presented in equation.II.7.

$$C_nH_m + nO_2 \leftrightarrows nCO_2 + 0.5mH_2 \qquad \Delta H < 0 \qquad \text{(II.5)}$$

$$C_nH_{(2n+2)} + 0.5mO_2 \Rightarrow mCO + C_{(n-m)}H_{2(n-m)} + H_2 \qquad \Delta H < 0 \qquad \text{(II.6)}$$

$$CO + H_2O \leftrightarrows CO_2 + H_2 \qquad \Delta H = -41 kJ/gmole \qquad \text{(II.7)}$$

Oxidation processes have large heat production that can complement the endothermic reactions via heat compensation. The Partial Oxidation (POx) of higher alkanes could result n operational problems, such as flames during vaporization and mixing, soot formation associated with combustion of fuel-rich gases and coke formation on reactor walls and on the catalysts [23]. Those processes can lead to an easy start ups on ignition even without the presence of a catalyst. However, the H_2 yield per mole of fuel input can be significantly enhanced by the use of catalysts [5, 7, 14 and 15].

Large scale POx systems have been used commercially to produce H_2 from HC's such as residual oil, for applications such as refineries. Besides, companies and government laboratories such as Epyx, Nuvera, Hydrogen Burner Technology (HBT) and ANL are involved in developing small-scale POx systems, but are still undergoing intensive R&D with various fuels and catalysts. POx can utilize a wide range of HC's feed stocks, is more compact than a SR, in which heat must be added indirectly via a heat exchanger.

Nevertheless, oxidation systems have high energy consumption and less suitable H_2/N_2-ratios in the produced synthesis gas and the energy in the PSA purge gas can not be fully recovered. POx is favored for economic reasons especially by availability of

cheap refinery residues. Pereira *et al.*[16], suggested the supply of oxygen in the feed according with the type fuel to have efficient oxidations. According to ANL the partial oxidation results in simple designs, fast response but coke formation is observed.

During the previous decades, n-heptane gained a major attention because it is found relatively large amounts in commercial fuel like gasoline. Currently, alternatives fuels and new catalysts are studied with this process.

II.2.3 Steam Reforming (SR):

SR is an endothermic process leading to hydrogen, carbon monoxide and carbon dioxide. SR is the most common method for hydrogen production. SR method converts any oxygenated organic compound $C_nH_mO_p$ as well as C_nH_m to H_2. The generic formulation for SR is shown in equation II.8 [5]. According to other authors to avoid the presence of CO in the gas product, SR can be followed by WGSR (Equation II 7).

$$C_nH_mO_p + (n\text{-}p)\ H_2O \leftrightarrows\ CO\ + (n{+}0.5m\text{-}p)\ H_2\ \ \Delta H{>}0 \qquad \text{(II.8)}$$

Therefore, the overall process can be represented as follows [15]:

$$C_nH_mO_p + (2n\text{-}p)\ H_2O \leftrightarrows nCO_2\ + (2n{+}0.5m\text{-}p)\ H_2 \qquad \text{(II.9)}$$

Likewise, Springmann *et al.*[57] considered the following two main reactions and WGSR to describe SR reaction (See Eq. 10 and 11). They described that methane can be formed as a side product. Suggesting that at low temperature methane-formation is thermodynamically favored, but may be kinetically suppressed with appropriate catalysts.

$$C_nH_m + nH_2O\ \rightarrow\ nCO\ + (n{+}0.5m)\ H_2 \qquad \text{(II.10)}$$

$$C_nH_m + 2nH_2O\ \rightarrow\ nCO_2\ + (2n{+}0.5m)\ H_2 \qquad \text{(II.11)}$$

The main process step involves the reaction of steam with HC's over a catalyst at high temperatures. However, it is a thermally inefficient process with slow response at start-up and during transients. The efficiency could be improved if it is combined with Ox, since the reaction absorbs thermal energy from the surroundings, promising to have a much better dynamic response. Methane reforming is the most common and cheapest process to produce H_2. Krumplet *et al.*[15] proposed for saturated HC's the following reactions. They describe SR as an endothermic process with complicated design, heat transfer limited and high H_2 concentrations.

$$C_nH_{2n+2} + nH_2O \rightarrow nCO + (2n+1)\,H_2 \qquad \Delta H > 0 \text{ overall reaction} \qquad \text{(II.12)}$$

$$CO + 3H_2 \leftrightarrows CH_4 + H_2O \qquad \Delta H = -206 \text{ kJ/gmole methanation} \qquad \text{(II.13)}$$

Pietro *et al*. [44] established that the main role of SR is to push the equilibrium toward H_2, CO or CO_2 formation. Similarly, Wheeler [62], who focused on operating costs to product hydrogen, mentioned that a higher S/C ratio drives the reaction closer to the equilibrium and increases the H_2 yield.

II.2.4 Autothermal Reforming (ATR)

ATR is a combination of SR and Ox reaction. Both reactions occur simultaneously. This combination is considered one of the most attractive options for on-board reforming of kerosene type fuels [72]. Its purpose is to enhance SR reaction by including Ox reaction heat compensation. Combining Ox and SR equations, the overall equation yields the idealized ATR reaction as shown by the following equation [15]:

$$\text{Fuel } (C_nH_mO_p) + H_2O + O_2 \rightarrow \text{Carbon Oxides} + H_2, \qquad \Delta H < 0 \qquad \text{(II.14)}$$

Liu *et al.*[6] and Moon *et al.*[22] presented equations II.15 and II.16 respectively to describe the overall process in ATR, *x* represents the molar ratio of O_2 to fuel (O_2/C=x/n)

in the feed mixture. The molar ratio of H_2O to fuel are represented by y and $(2n\text{-}2x)$ respectively.

$$C_nH_m + xO_2 + yH_2O \rightarrow nCO_2 + (y+2x-2n)\ H_2O + (2n-2x+0.5m)\ H_2 \qquad \text{(II.15)}$$

$$C_nH_m + xO_2 + (2n-2x)\ H_2O \rightarrow nCO_2 + (2n-2x+0.5m)\ H_2 \qquad \text{(II.16)}$$

ATR, an alternative reforming method, has been used since 1950s in small scale as an energy efficient process [61]. Its main characteristics are: low energy requirement (due to the complementary SR and Ox reactions), low energy consumption, High Gas Space Velocity (HGSV) at least one order of magnitude relative to traditional SR and preset H_2/CO ratio easily regulated by inlet $CH_4/O_2/H_2O$ ratios and CO_2 recycling [4].

Relevant investigations by ANL [3, 6, 12, and 15] suggested that ATR could have a simple design and fast response. Typically ratios used in reactions of ATR are 0.2 – 0.6 for oxygen-to-carbon (O_2/C) and 1.0 – 3.0 to steam to carbon ratios (W/C) [2, 6].

As in the reactions of SR and Ox, the use of catalyst in ATR process could be used to improve the selectivity and operation at low temperatures. Autothermal reformers, fuels and catalysts have been studied with the support of DOE by several laboratories and companies such as ANL, NREL, Alamos, Idatech, General Motors and others.

In order to enhance ATR technology the research and academic sectors has been developing the following aspects. Borup *et al.*[30] examined the effect of fuel on hydrogen devices, discovering that the mixture preparation of feed is a critical step to obtain proper conversion of HC's and avoid hot/cold spots. According to this, Hartmann *et al.*[68] appreciated that the mixture generation for diesel reforming, constitutes a key factor in terms of the quality of a reforming reaction. If the components are not homogeneous, the tendency for soot to be formed or hot spots in the catalysts will increase. Pereira *et al.*[16] in ATR of diesel recommended the use of pure oxygen to improve the detection of the hydrocarbons present in the product.

Docter *et al.*[20] and Ersoz *et al.*[51] performed thermodynamic calculations. The first one, found that ATR, theoretically, yields higher reforming efficiencies than partial oxidation. Meanwhile, the second one worked with HYSYS software to established differences in ATR process with one lower molecular weight HC and other higher

molecular weight HC. They concluded that the selection of the right operation parameters is very important in terms of the ATR efficiency and hydrogen production.

Rampe *et al.*[21] designed a reactor for ATR with propane. They found that a variation in S/C does not represent a great influence on the characteristic performance data. The best result was reach with an S/C ratio of 1.0. Also, the process was tested with and without air preheating. In preheated condition, the H_2 and CO mole content rises up to about 34%, this is 1.3% as in the no preheated mode. Equally, Ayabe *et al.*[7] investigated ATR of methane and propane, observing coke formation only with propane.

Suzuki *et al.*[10] performed experiments to develop high efficiency hydrogen through reforming of naphtha to kerosene fractions. They confirmed that as the reaction temperature rises, increases the yields and production volume of hydrogen, approaching the equilibrium value gradually. Also, they developed catalysts to study activity and coking resistance.

Deluga *et al.*[24] worked with ethanol, and found O_2 and ethanol conversion to be >99% and >95% respectively. They do not have evidence of deactivation or carbon buildup on its catalyst. Its Autothermal reactor systems have extremely short startup times (< than 5 s) and wide flow ranges, presuming that it is possible to manufacture small portable fuel reformers.

Kumar *et al.*[65] patented an Autothermal Cyclic Reformer (ACR) process. Among its benefits are: reduces the internal heat generation, increases efficiency, high purity H_2, fuel flexibility (sulfur tolerance) and coke burnt off during regeneration. It is a technology that can be applied for the production of H_2 or syngas from many fuels, including natural gas, diesel, coal and renewable feed-stocks. The ACR process operates in a three-step cycle that involves SR of fuel on Ni catalyst (reforming), heating the reactor through the oxidation Ni catalyst (air regeneration) and the reduction of the catalyst to its original state (fuel regeneration).

In addition, Aasberg *et al.*[67], developed experiments with ATR and pre-reforming to synthesize methane into liquid fuels (Gas-to-Liquids fuels or GTL). They concluded that plants based on oxygen-blown ATR at low H_2O/C ratios are the preferred option for large-scale and economic production of synthetic gas for GTL plants.

Finally, ANL has favored catalytic ATR developing new catalysts for the reforming and shift reactors. They suggest that ATR systems can be very productive, fast starting and compact. In their studies, they had used several fuels as alcohols, bio-fuels, gasoline and methane. Ahmed *et al.*[1] and Springman *et al.* [57] depicts an idealized series of equations for ATR reaction of hydrocarbons.

$$C_nH_mO_p + (n\text{-}p)\,H_2O \leftrightarrows n\,CO + (n+0.5m\text{-}p)\,H_2 \quad \text{(II.17)}$$

$$C_nH_mO_p + (n+0.25m\text{-}0.5p)\,O_2 \leftrightarrows n\,CO_2 + 0.5m\,H_2O \quad \text{(II.18)}$$

$$n\,CO + n\,H_2O \leftrightarrows n\,CO_2 + n\,H_2 \quad \text{(II.19)}$$

$$C_nH_mO_p \leftrightarrows n\,CO + 0.5m\,H_2 + 0.5(p\text{-}n)\,O_2 \quad \text{(II.20)}$$

Combining the equations II.17 to II.20, the overall reaction for ATR (including alcohols) is:

$$C_nH_mO_p + xO_2 + (2n\text{-}2x\text{-}p)\,H_2O \rightarrow n\,CO_2 + (2n\text{-}2x\text{-}p + 0.5m)\,H_2 \quad \text{(II.21)}$$

As was mentioned before, x is the oxygen to fuel molar ratio. This ratio determines the amount of water required to convert the carbon to carbon dioxide, the hydrogen yield (moles), the concentration (mol %) of hydrogen in the product and the heat of reaction. When x = 0, equation II.21 reduces to the endothermic steam reforming. Complete combustion is obtained when x = 12.5. They suggested operating the reactor at a low value of x, where higher hydrogen yields and concentrations are favored.

II.2.4.1 Development, commercialization status of ATR

The incorporation of fuel processors into vehicles is the key to successful near-term commercialization of low temperature fuel cells. The technology is at the demonstration phase of development in the whole world and it is expected to be fully deployed in the year 2010. The target regions are USA and European Union (EU). In EU today, there are over 100 FC and hydrogen related organizations. Denmark & Finland have around 20 and Norway & Sweden around 30 organizations [73 and 74]. In figure II.7, the technology distribution in these countries is presented.

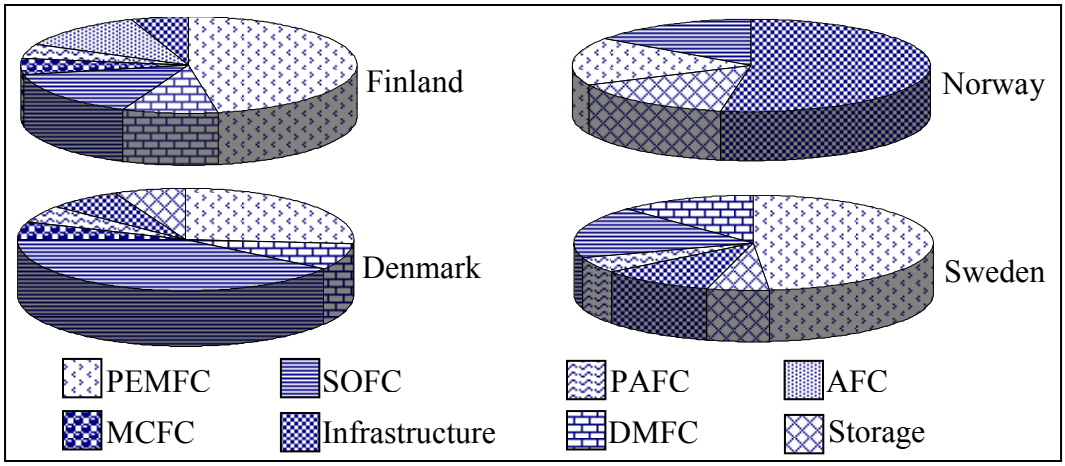

Figure II.7 Organization by technology focus in Europe [74]

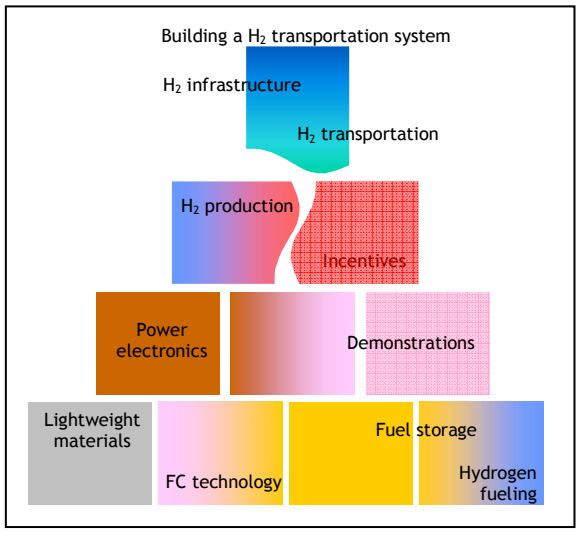

Figure II.8 DOE Targets to reforming technology [75]

The European Union and Japan are the currently preferred regions of deployment, but the technology is applicable all over the world. Equally, Johnson Matthey has been working in fuel processors, catalysts, and membranes. Also, is developing HotSpotTM a series of autothermal reformers to process fuels such as natural gas, LPG, methanol and higher hydrocarbons, including gasoline.

The first and second one are reformed in a dual fuel processor since year 2000 [69]. Reforming technologies are being developed by a number of firms, mostly for fuel processors of gasoline, diesel and logistic fuels, and for natural gas fueled PEMFC cogeneration systems as depicted the table II.2.

At the same time, DOE focuses today on the development of advanced reforming technologies that will make it possible to meet the DOE targets (cost equivalent to gasoline / 70% energy efficiency) [75]. An outline of targets is shown in figure II.8.

Table II.2 Ogden J. Review of small stationary reformers for hydrogen production [31]

Firms, Organizations	Technology testing
ANL	Checking of ATR systems and catalysts
International Fuel Cells	ATR that runs on logistics fuels
BWX and McDermott technology	Naval distillate for shipboard fuel cells
Fraunhofer Solar Energy Institute	ATR for LPG and diesel fuel
Honeywell and energy partners	Developing a 50 kW PEMFC system for buildings cogeneration
Daimler-Chrysler	ATR for gasoline reforming
IdaTech	Multi-fuel reformer from methane

II.2.4.2 ATR and reforming of biomass, Glycerol and Biodiesel

Liquid bio-fuels are an energy resource derived from organic matter. These include wood, agricultural waste and other living-cell material that can be burned to produce heat energy [78] as well are transport fuels, primarily biodiesel and bio-ethanol or ETBE processed from agricultural crops and other renewable feed stocks.

Reforming experiments including ATR has been performed with biomass-derived hydrocarbons. Cortright *et* al.[80] converted sugars and alcohols at temperatures near 440 °F in a single reactor in an aqueous phase reforming process using a Pt-based catalyst. Figure II.9 presents a schematic of the reaction pathways for production of H_2 and alkanes from oxygenated hydrocarbons over a metal catalyst that they proposed.

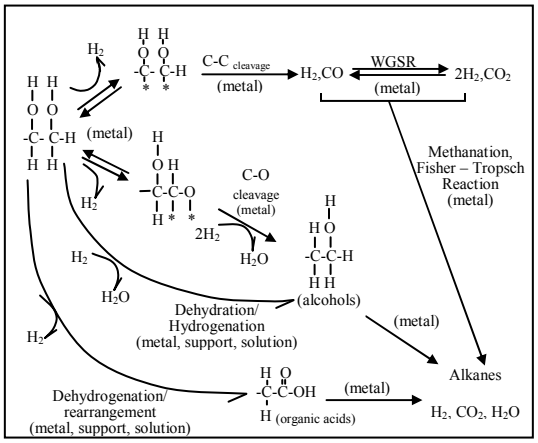

Figure II.9 Reaction pathways for production of H_2 by reactions of oxygenated HC's with water (Asterisk represents a surface site) [80]

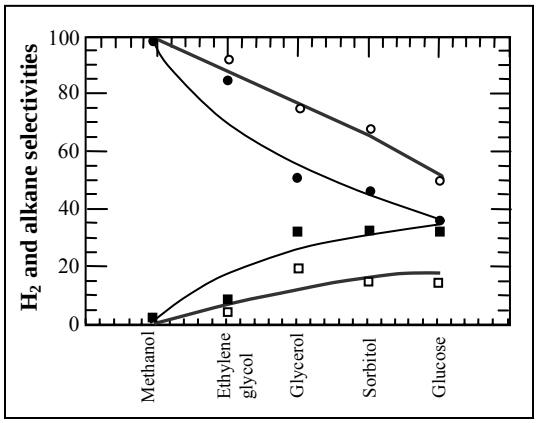

Figure II.10 Selectivity (%) vs. oxygenated HC.
H_2 selectivity (circles) and alkane selectivity (squares) from aqueous-phase reforming of 1wt% oxygenated HC's over 3wt% Pt/Al_2O_3 at 498ºK (open symbols) and 538K (filled symbols) [80]

Additionally, in this work, they suggested that the energy required for the aqueous-phase reforming of oxygenated hydrocarbons may be produced internally, by allowing a fraction of the oxygenated compound to alkanes through exothermic reaction pathways. In their experiments, alcohols and organic acids were presented in the gas effluent, but only at trace levels (300 ppm and about 5 ppm, respectively). Figure II.10 illustrates that the selectivity for H_2 production improves in the order glucose < sorbitol < glycerol < ethylene glycol < methanol. As well, they observed that lower reaction temperatures result in higher H_2 selectivities. For glycerin the composition of H_2 was between 57-65 mole%.

Biodiesel is also of interest to Argonne National Laboratory. Biodiesel is produced by the reaction of vegetable oil or animal fat with methanol or ethanol catalyzed by either acid or base to produce methyl esters of fatty acids as depicted in figure II.11. Other possible materials in Biodiesel transesterification include residual alcohol, moisture, unreacted feedstock (triacylglycerides), incompletely reacted mono- and diglycerides and free fatty acids [92]. The separation of biodiesel and glycerol is normally carried out by gravity. Anderson *et al*. [27] developed some methods for the separation of biodiesel

from the glycerol byproduct and they concluded that it could be generally accomplished by gravity.

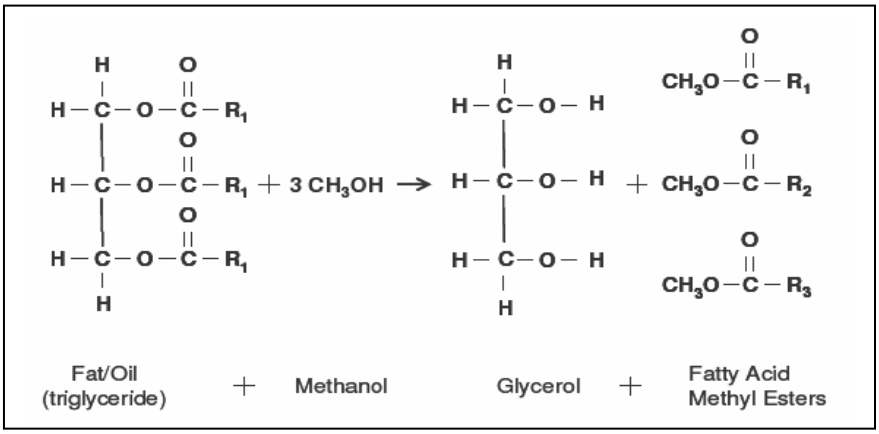

Figure II.11 Schematic of the transesterification process to produce biodiesel [26]

Glycerol is an interesting oxygenated sub-product that could be used to produce H_2 gas. Some studies have been conducted with glycerol to investigate the technical and economic feasibility of generating hydrogen [5, 26, 80].

According to Virents Lab. [26], presently USA requires nearly 61 billion gallons of diesel fuel. It is estimated that Biodiesel can easily penetrate at least 3% of the diesel market. This represents over 1.8 billion pounds of glycerol. This would greatly exceed the current demand of 0.5 billion pounds of glycerol. Therefore, future biodiesel production is expected to greatly reduce the chemical value of glycerol.

In other areas Czernik *et al*.[82] proposed that biomass has the potential for producing 40 Mt/year (or more) of hydrogen, enough to fuel 150 million FC vehicles. Also, Virents and NREL laboratories [5, 26, 28] developed a reforming process from glycerin and biomass. Both concluded that glycerin can be a valuable resource for producing hydrogen. They suggested continuing these investigations. Particularly, Virents Laboratory, found that the selectivity to H_2 in aqueous-phase reforming depends on the nature of the reactant (ethylene glycol > glycerol > sorbitol > glucose) similar to the studies of Cortright *et* al. [80].

In other reforming studies, NREL recommended that to facilitate pumping and atomizing the crude glycerin had to be preheated (60-80 °C). They noticed an increment

in methane production and observed hydrogen yields around 77% that could be improved to 90% with the combination of WGSR.

Wang *et al.*[43] studied reforming of complex oxygenates. They concluded that it is chemically possible to have reforming if Ni-based catalysts and high W/C ratios are used. The condition of W/C is considered because oxygenates rapidly dehydroxylate, which results in the formation of aromatics on the surface of the catalyst.

Naidja *et al.* [14] agreed with the hypothesis of Wang *et al.*[43]. Both mentioned that the reaction products of cool flame treated fuels, which are predominately formed by oxygenates, have potential for reforming. Suggesting that bio-fuels, which contain a significant proportion of oxygenates, could be good candidates for reforming processes.

Furthermore, Wang *et al*.[43] and Czernik *et al*.[12,28] proposed a method that combines fast pyrolysis of biomass to generate bio-oil or catalytic steam reforming of the bio-oil to hydrogen and carbon dioxide. In renewable fuels, Argonne initiated the Autothermal reforming of Biodiesel in 2004 to accomplish their targets [79].

II.2.5 Coke formation

All hydrocarbons will decompose spontaneously at reforming temperatures in the absence of steam to form carbon and hydrogen according to the following reactions [67]:

$$C_nH_m \leftrightarrows nC + 0.5\,mH_2 \qquad \text{(II.22)}$$

$$CH_4 \leftrightarrows C + 2H_2 \qquad (\Delta H_{298K}) = 75 \text{ kJ/mol} \qquad \text{(II.23)}$$

During normal operation, carbon deposition during methane cracking can be originated from either methane decomposition (Eq.23), CO disproportionation (Boudouard reaction Eq. II.24) which is thermodynamically favorable below 1173K [83] or by reduction reactions (Eq. II.25) [15] that in some cases favor carbon removal.

CO disproportionation: $2CO \leftrightarrows C + CO_2$ $(\Delta H_{25°C}) = -172$ kJ/mol (II.24)

CO reduction: $CO + H_2 \leftrightarrows C + H_2O$ (II.25)

In reforming systems such as SR, gas synthesis or catalytic reforming the formation or accumulation of carbon is a permanent problem. Chevron web page [11], illustrates a typical reforming cracking diagram, which is shown in figure II.12.

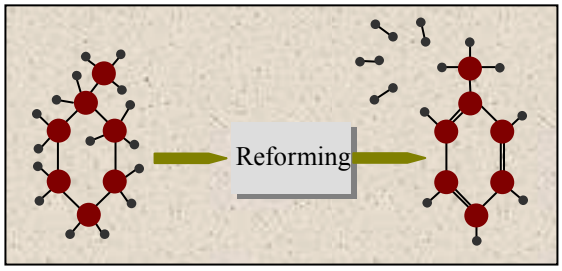

Figure II.12 Reforming Cracking Diagram [11]

Similarly, ATR processes also result in carbon deposition. For example, Asberg *et al.*[67], related soot formation in an ATR reactor on feed gas compositions, temperatures, pressures and, especially burner designs. They mentioned that the design of the burner, catalyst and reactor is essential in order to ensure that the precursors are destroyed by the catalyst bed to avoid soot formation.

Susuki *et al.*[10], also studied carbon formation using ATR. They presented comparisons of relative reforming activities for normal paraffin due to differences in carbon numbers (Figure II.13). It can be seen that as carbon number increases the activity declines. Equally, they suggest that when the carbon chain becomes larger, even though it decomposes midway, unreformed hydrocarbon increases (Figure II.14).

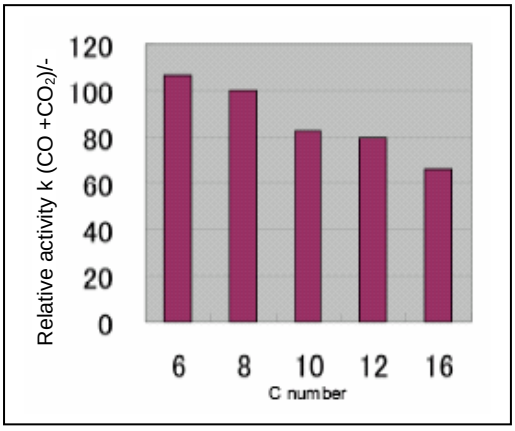

Figure II.13 Comparison of ATR reactivity of normal paraffin due to differences in carbon number [10]

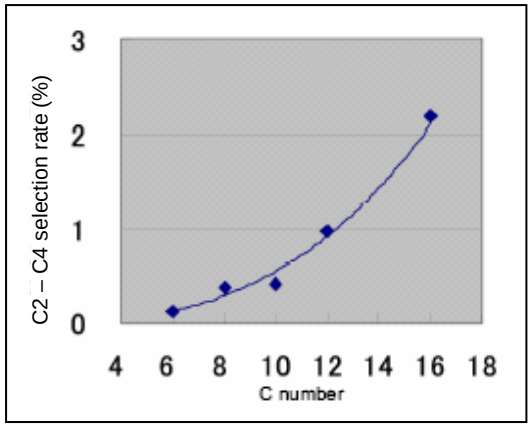

Figure II.14 Selection rate of C2-C4 hydrocarbon in normal paraffin due to differences in carbon number [10]

In a related study Borup *et al.*[30] compared the carbon formation of fuels vs. pure hydrocarbons in the vaporization process. In this research, it was possible to establish that the S/C ratio not always minimize the carbon formed. The fuel composition is also important. They recognized that carbon formation is a key variable for ATR processor durability. They performed equilibrium calculations to identify the proper operating zones to prevent carbon formation. It was concluded that it is difficult to avoid non-zero carbon equilibrium. In addition, they recommended fuel vaporization before the injection into the autothermal reformer.

Similarly, Krumplet *et al*[1,15] and others mentioned that the temperature could affect the reaction in relation with coke formation. They observed that at higher temperatures, there are more possibilities to crack the fuel and obtain coke. Freni *et al*[4] found similar conclusions and additionally, suggested a preliminary pre-reforming in ATR of heavy hydrocarbons to avoid C_3-compounds that are precursors to soot formation.

Borup *et al.*[2] in figure II.15 depicts the behavior of carbon formation with respect to reaction temperature and S/C ratio.

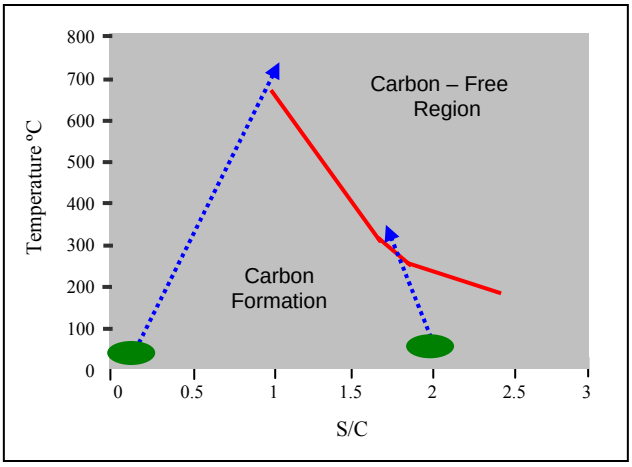

Figure II.15 Carbon formation zones [2]

In summary, coke composition depends on the structure of the catalyst used, reaction temperature, its acid characteristics and the nature of the reactants. In reforming reactions, soluble and insoluble coke could exist. Their formation depends on combinations of temperatures and S/C ratios. Several publications, confirmed that at

temperatures lower than 530 °F, soluble coke predominates. Borup *et al*.[2] quantified the carbon formation with water availability and temperatures changes in different rates of S/C, to predict the behavior of carbon formation. They recognized coke growth as a major challenge in ATR and concluded that equilibrium calculations can identify proper conditions to avoid the coke formation during the start up of the fuel processor. Likewise, Freni *et al*.[4] found that carbon deposition can be avoided controlling the gas composition, reducing catalyst particle size, using basic catalyst support, depositing a inert layer on hardware stainless steel walls and improving the burner design and operations set-up. It is also accepted that carbon deposition can occurred by either decomposition of CO and hydrocarbons and by thermal cracking.

Parallel, Chen *et al.*[63] studied reforming of heptane. They observed that carbon mass flow rate in the bed increased when steam-to-carbon feed ratio decreased. In other studies, Suzuki *et al.*[10] presented a comparison of relative reforming activities for normal HC's due to differences in carbon number, suggesting that when the carbon chain becomes larger, even though it decomposes midway, unreformed hydrocarbon increases. They presented carbon deposition from 0.05 mass% (6 C number) to 0.30 mass % (16 C number).

Typical carbon forming reactions, reported in the reforming systems, are carbon oxides and methane discomposed or reacted with hydrogen to produce carbon, water and carbon dioxide. Another related study was by Pereira *et al*.[16] who reformed diesel with ATR. They found coke formation and deactivation of its catalysts when using low H:C ratio and high molecular weight of diesel. Also, they identified an increase in soot formation, when the pressure drop across the reactor is increased or with over liquid water injection. Further, Krishna *et al.*[32] observed that soot production is critically dependent on the drop size. They suggested developing burners based on low pressure, air atomization, low firing rates, low excess air/high efficiency, two stage firing rates, low NOx emissions systems and low electric power consumption.

CHAPTER III

Experimental Methods and Equipments

Materials and Methods

Two propriety catalyst of Argonne's National Laboratory (ANL) were used in reforming processes to establish their feasibility to produce H_2 minimizing coke formation. Three fuels were studied; two reactors and two operational systems were used. Gas chromatographs were used to detect heavy and lighter hydrocarbons. Supplies, equipments and methods used will be discussed in this chapter.

III.1 Supplies and Reagents

Glycerol, biodiesel and methanol were used in the ATR experiments as fuels. Also, oxygen, hydrogen, carbon monoxide, carbon dioxide and methane gases were used to prepare the respective calibration curves. Helium at ultra high purity (99.99%) was the gas carrier in the analytical equipments. Platinum (Pt) and Rhodium (Rh) based catalyst supplied by ANL were used as the catalytic agent. Figure III.1 and III.2 depicts images of Rh and Pt based catalyst, respectively.

Figure III.1 Rh-based catalyst. (a) powder & (b) thin spherical pellets

Figure III.2 Pt-based catalyst and basket

The former illustrates the powder (original) and palletized catalysts and the second one the reactor basket that was used.

The catalysts are supported in alumina which promotes the dehydrogenation of fuel and the oxidation of carbon. In addition, Rh-based catalysts are made from a dark powder that are ball-milled resulting in particle sizes between 5 -50 microns. Chemical and physical characteristics of both catalysts are of confidential nature.

III.2 Equipment for ATR experiments

Two gas chromatographs with mass spectrophotometer (HP5973 as mass selective detector and HP6890 as GC system) and thermal conductivity detector (HP5890 series II) as analytical instrument were used. Also, scanning electron microscopy (SEM) field emission (Philips XL30S) was used for surface analysis. The operational system used two reactors, a Basket Stirred Tank Reactor (BSTR) model 4575 and a Plug Flow Reactor (PFR), combination of quartz tube with an oven model 21100. The procedure will be described in this section.

III.2.1 Basket Stirred Tank Reactor (BSTR)

A stainless steel basket stirred tank reactor (BSTR) Model 4575 with a total volume of 500 mL was used. It has inside a perforated metal case which contains a self-insulating vestibule molded of lightweight ceramic fiber that minimized the heat losses and improved the safety of the operation. Figure III.3 shows a photograph of the BSTR, whose maximum operating temperature is 1000ºF. A pressure gauge was used to monitor the pressure drop across the BSTR reactor to determine if the flow in the reactor is blocked, which indicates coking formation. This Reactor was used in two different modes. In the first one, an active carbon bed is set below the reactor with two gas

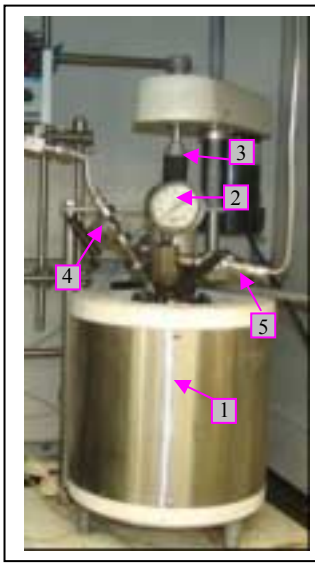

Figure III.3 BSTR: (1) Insulation Jacket, (2) pressure gauge, (3) Stirrer, (4) Inlet feed and (5) Outlet product gases

flow meters, a thermo par selector, rheostats, coil heating tapes, a condenser, and flash drum and a cooling system (using ethylene glycol as the refrigerant), connected to the reactor as described in figure III.4. A second system uses the BSTR reactor as a pre-reforming step connected to a Plug Flow Reactor (PFR) as can be illustrated in figure III.5. Two master-flex L/S peristaltic pumps # 7524-50 were used for the fuel and water feed. A temperature measurement board was used to control reactor input and output conditions. The temperature fluctuation in the reactor are shown in appendix A.1

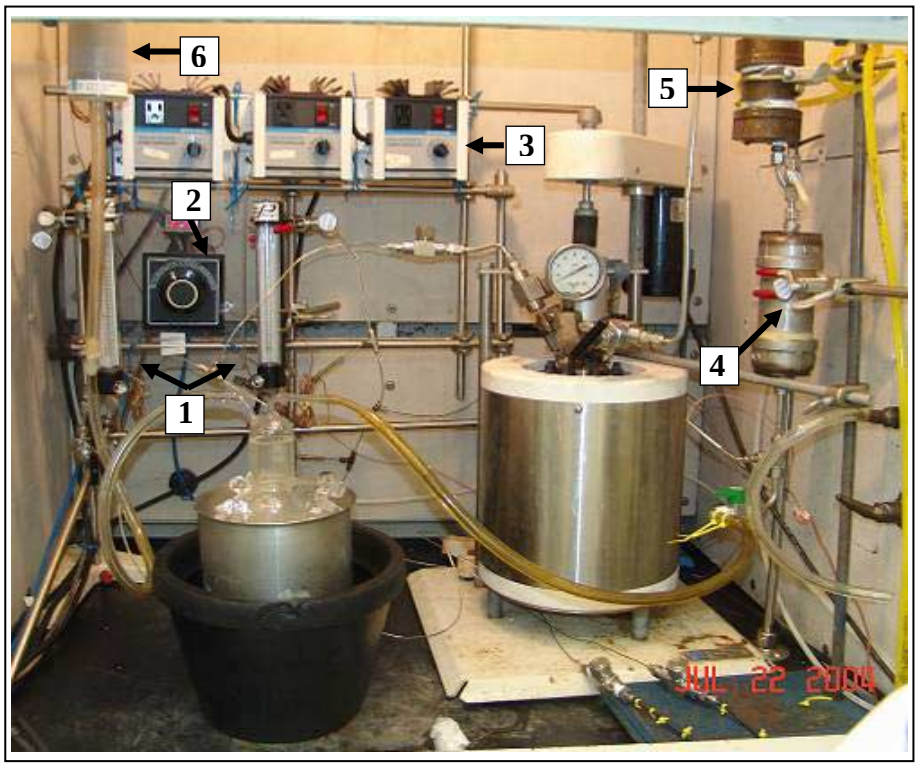

Figure III.4 BSTR in the system I.: (1) Flowmeters, (2) Thermo par selector, (3) Rheostats, (4) Flash Drum, (5) Condenser and (6) Active carbon

Figure III.5 summarizes the two systems used. The first system does not use the BFR, as shown in Figure III.4; the exit gas is connected directly to the condensation step. The second system, however, runs with the BFR, installed between the BSTR and the condenser according with the mentioned figure.

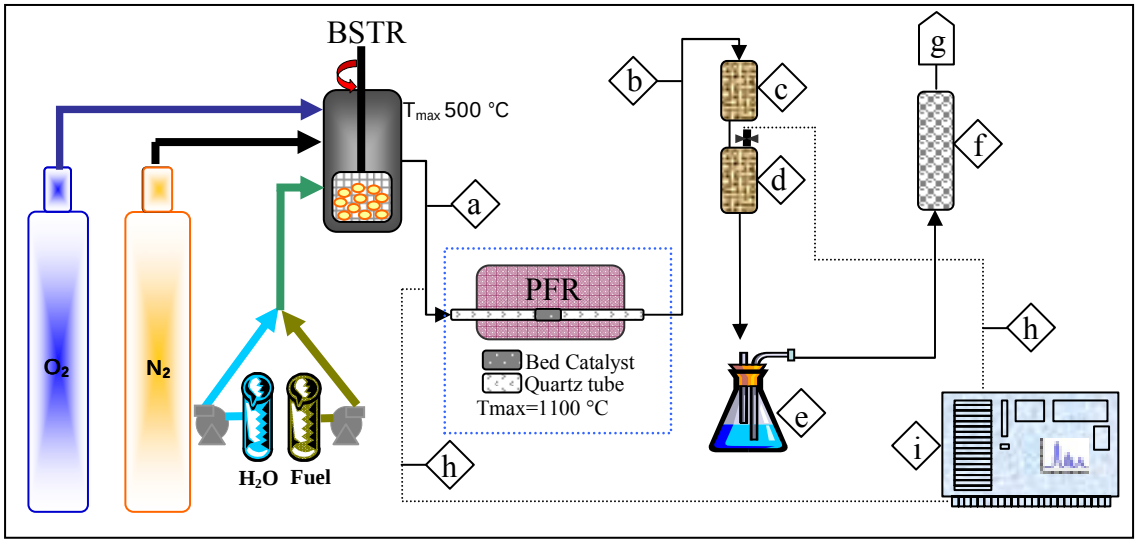

Figure III.5 Diagram of reforming experimental system schematic. 2nd system. (a) Exit gas 1, (b) Exit gas 2, (c) Condenser, (d) Flash drum, (e) Condensable products, (f) Active carbon, (g) final exit gas, (h) Gas sample to be analyzed and (i) GCMS & GCTCD

The outlet of pre-reformate gases in the second systems is shown in Figure III.6 this figure illustrates the pre-reforming step.

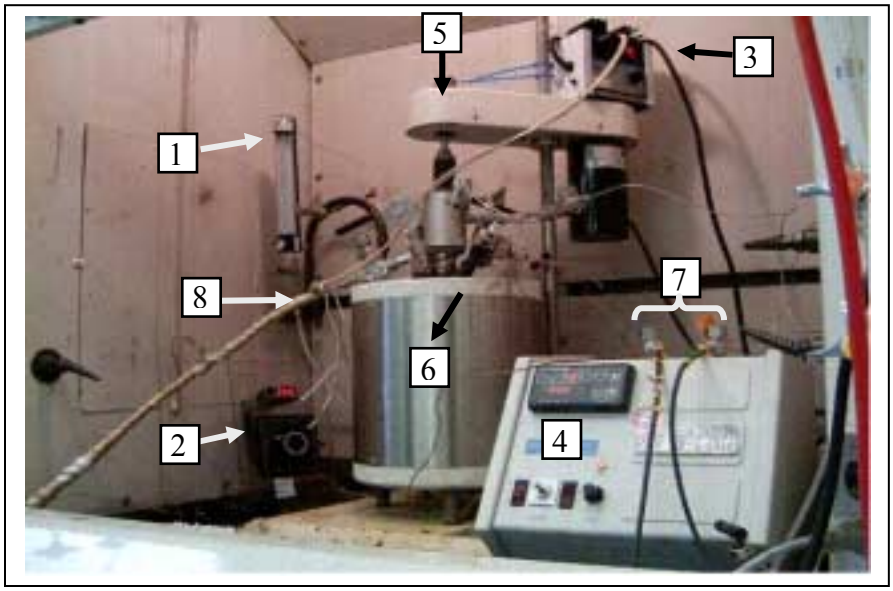

Figure III.6 Pre-reforming Step. 2nd system (1) Flow meter N_2, (2) Thermo par selector, (3) Rheostat, (4) Control panel, (5) reactor stirrer, (6) Insulated jacket, (7) Inlet fuel and water and (8) Exit gas pre-reformed

III.2.2 Plug Flow Reactor (PFR)

PFR is the combination of a quartz tube reactor with an isolate oven model 21100 tube furnace thermoline, with a total temperature capacity of up to 2000 ºF and with availability of to be used with tubes of diameter of 1 and 2 in. The quartz tube has two openings at the top and bottom, one fixed inside the reactor and one Mobile disc to attach the catalysts, 1.00 in inner diameter (ID) and 0.91 m of length. The figure III.7 schematizes the characteristics of quartz tube. A photograph of the reactor is shown in figure III.8a.

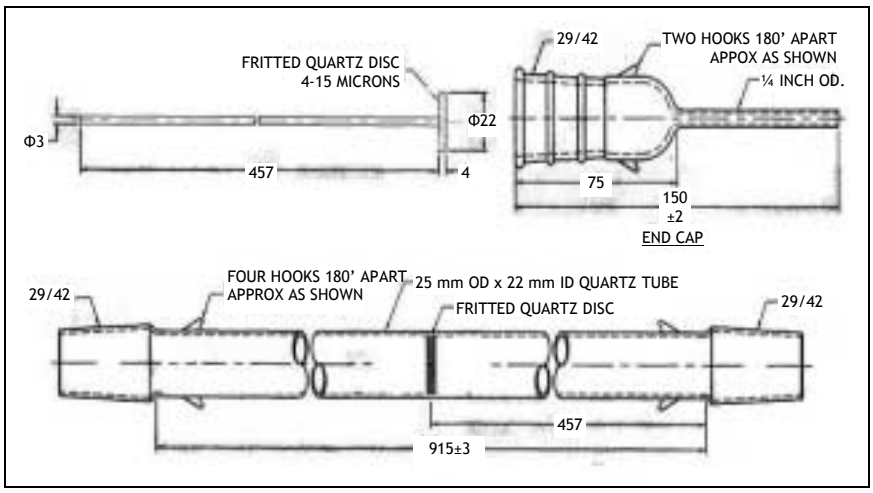

Figure III.7 Schematic of the Quartz tube design

The 21100 tube furnace has an outside shell thermally insulated and one analog control to read the catalyst bed temperature in the half of the reactor. Ten levels or cycles of heating are available, 10 is the maximum (>2000 ºF) and 1 is the minimum (~400F). The temperature is measured with one thermocouple (type K) placed inside of the center of the oven. The PFR was used in the 2nd system for reforming, but also can be used independently without the BSTR. An overall picture of the final reformate step is shown figure III.8b.

To guarantee the operating temperature conditions of the second system, a series of experiments to characterize the PFR, quartz tube and oven behavior were performed. It was carried out with the oven, oven with quartz tube and oven plus quartz tube with Pt-based catalyst combinations. (See appendix A.2).

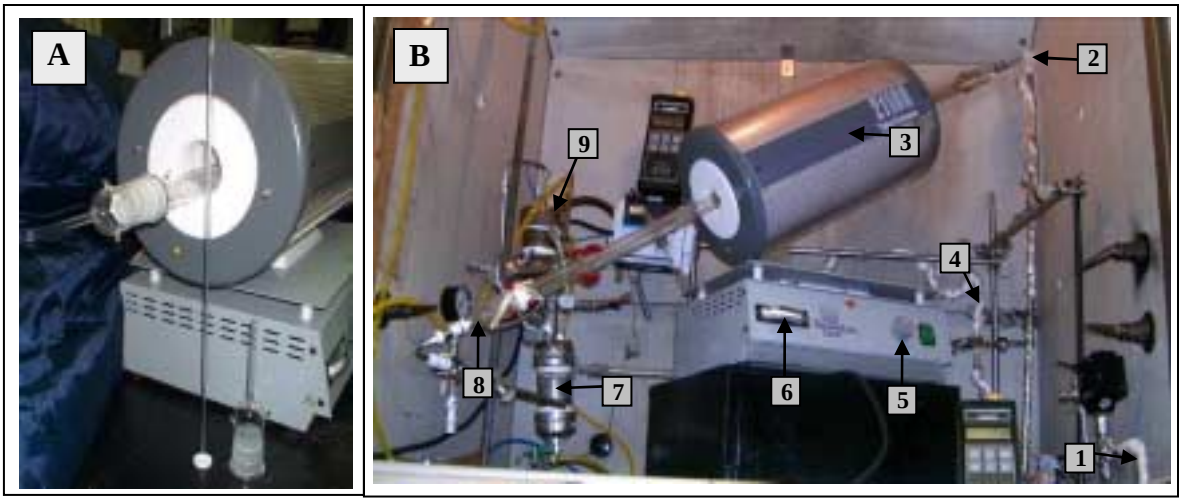

Figure III.8 PFR reactor and its assembly. (A)Oven and Quartz tube, (B) Continuation of system II. Catalytic reforming step: (1) Exit gases of BSTR (pre-reforming step), (2) inlet gases. (3) Oven connection, (4) oxygen stream, (5) temperature control, (6) temperature display, (7) flash drum, (8) exit gases and (9) Condenser

A series of pictures of the characterization process, shape of the quartz tube, oven and catalyst packed into the reactor are shown in figure III.9.

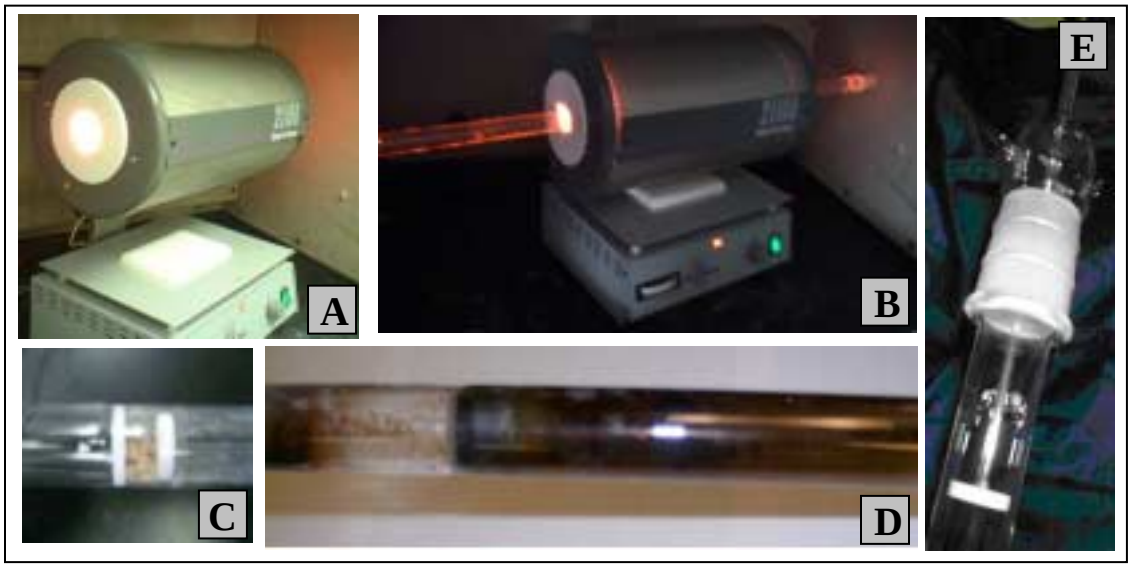

Figure III.9 Quartz tube and oven process characterization. (A) Oven at 600 °F, (B) Oven with Quartz at 1700 °F, (C) Quartz with Pt-based catalyst after temperature exposure - Coke formation was not observed, (D) Quartz after reforming reaction – coke formation observed and (E) End cap connection with a quartz tube and mobile disc clean.

III.3 Analytical section

III.3.1 Gas Chromatography

Gas chromatography (GC) was used to estimate the composition in the product gases collected from the ATR reaction. GC's with thermal conductivity (TCD) and mass selective (MS) detectors were used. Specifically, the GC-TCD was used to evaluate H_2, O_2, N_2, CH_4, CO and CO_2; the GC-MS was used to analyze heavy HC's as biodiesel, hexane, iso-octane, benzene, heptane, toluene, *i*-xylenes, and light alcohols.

The light analysis was performed in a Hewlett Packard 5890 series II Gas Chromatograph (TCD) coupled with a HP 3396 Series II integrator. The capillary column used was a ViCi GC Valcobond with a solid phase of (5A) sieve molecular, 30 m length, a film thickness of 15 μm, 0.53 mm internal diameter (ID) and a temperature limit of 350 °C[2].

Similarly, the heavy analyses were achieved with a HP 6890 Series GC system coupled with a 5973 mass selective detector and a capillary column with 100m length, 0.5 μm film thickness, 0.25 mm internal diameter (ID) and a temperature limit of 320 °C. For the GC-TCD method, the injector and detector temperatures were 155 and 200 °C, respectively. The oven temperature was held at 100 °C (5 min), then increased from 100 to 200°C at 20°C/min, and then was held at 200°C (15 min). The total analysis time was 25 min. Then, after the end of the experiments, the oven temperature was raised to 300°C for 15 minutes. The injector and detector were set to a temperature of 290 °C. The oven temperature was held at 98 °C (20 min) initially, and then increased at 65°C/min to 290°C (30 min).

Ultra high pure helium was used as the carrier gas in both chromatographs and standards gases and liquids were used for the calibrations curves. Figure III.10 and III.11 show photographs of the GC-TCD and GC-MS, respectively.

---

[2] ºF =1.8*(ºC)+32

Figure III.10 Gas Chromatograph-TCD

Figure III.11 Gas Chromatograph-MS

III.3.2 Scanning Electron Microscopy (SEM)

The combination of scanning electron microscopy (SEM) and energy dispersive X-ray spectroscopy analysis (EDS), permit performing map elements on a surface. It was used to analyze Pt-based catalysts surface. The objective of this analysis was to observe if existed uniformity, heterogeneity or homogeneity of coke accumulation in each pill surface. The magnifications were between 30X – 1000X and the input voltage was 2.5 kV. The input voltage for the elemental analysis (EDS) was 30kV.

For every run in the ATR experiments, it was necessary to use nineteen pills which correspond to approximately 2 grams of catalyst. For every run, two pills were selected and about five images of each one were taken. Table III.1 describes the different images type taken in the SEM.

Table III.1 Images type taken in the SEM and EDS technique

Images type taken in the SEM	**Picture capture**	
	Surface	**Inside**
Panoramic view	X	
Fracture spots	X	
Black point on the fracture spots		X
Black point	X	
White point	X	

III.4 Experimental procedure

The Autothermal reforming process was studied with three types of fuels at atmospheric pressure and at different temperatures; glycerol (700, 800 and 900 °F), biodiesel (900 °F) and methanol (300, 400, 500, 600, 700 and 800 °F). The temperature ranges studied were selected according with the gas phase of each fuel used, as well as in combination with the fed ratios coke formation could be appeared.

Three oxygen to carbon ratio and one water to carbon ratio were selected. The fuel reforming (both Ox and SR) reactions were performed over noble metal based catalysts (platinum and rhodium) supplied by ANL. For glycerol ATR experiments, Pt-based catalyst was used and the fuel, water and oxygen was mixed and reacted in the BSTR. For Biodiesel ATR experiments, Rh and Pt-based catalyst and two experimental systems were used; the first one experimental systems uses only a BSTR similar with glycerol ATR; the second one, used the BSTR in combination with a PFR as shown in figure III.5.

The general procedure consisted in packing the catalyst into the basket or quartz tube (see figure III.1 and III.9), starting the reactor temperature controller and then setting it to the desired temperature condition. The nitrogen flow meter is turned on to purge the system during 15 minutes and after this time, it is turn off. The oxygen flow meters with the water and fuel pumps were turned on all together at the established conditions.

Each experiment approximately ran for 4.5 hours at the established temperatures and during this time. Every thirty minutes one reformate gas sample was injected into the GC-TCD to determine the concentrations of H_2, O_2, CH_4, CO and CO_2. Also, volumetric flow [mL/min] and density [g/mL] on liquids reformate products were tested as well as passed through the GC-MS for an assay.

III.4.1 System I – BSTR

In the first system, the three components reacted simultaneously inside the BSTR. Similarly with the procedure describes in section III.4. Only one reactor was used. In the experiments with catalyst, the basket was filled with 2.0 g of the respective catalyst. The exit gas products passed through a condensation step which has a refrigerant system, with

recirculated coolant ethylene glycol around 36 °F; then, the system is connected into a flash drum. The flash drum has double functionality; samples for light HC's analysis in the GC-TCD are taken in the top (see section III.4), meanwhile in the bottom, a mixture of not condensable gases and liquids are collected in an adsorbed flask and then the gases are connected into a carbon active device. The sample gases were injected every half hour for approximately 4.0 hours at the desired temperature with a variation range of ±10 °F. The stability temperature in the BSTR is depicts in appendix A. It is important to mention that the gas sampling was manual not online. One milliliter manual injections of gas sample were injected. For liquid products, the GC-MS were used to identify the heavy hydrocarbons present in the biodiesel ATR reactions and also, a volumetric flow and density reading was performed. In both GC analytical tests, calibration curves were performed injecting several known volume amounts of the standards. Each gas and liquids standards had a purity of almost 99.99%. The value of the integration value was plotted vs. its volume percent (i.e. (0.5mL/1.0mL)*100). Appendix B, contain the respective compound calibration curves. With the system I, methanol, glycerol and biodiesel ATR assays were tested.

III.4.2 System II – BSTR and PFR

The second system was used exclusively for biodiesel experiments. Fuel and water were mixed and vaporized in the BSTR at around 800 °F as the pre-reforming step, and then the mixture passed through an insolated and heating stream to be jointed with the oxygen flow before the inlet into the quartz tube plus oven system. This system did not used catalyst in the pre-reforming step. The basket was always empty. The catalyst bed was packed in the quartz tube as illustrated in figure III.9c. The reactant mixture passes through the catalytic bed where an ATR reaction takes place to produce hydrogen and by-products. The exit gas stream of PFR passes through the condensation step and then the following steps of the process to continue as the procedure described in section III.4.1

Again as was mentioned in the section III.4, two analytical and equipment methods were used. The exit gases were analyzed for H_2, CO, CO_2, H_2O, CH_4 in GCTCD and

heavy byproducts were studied in GCMS. In parallel experiments, the capacity of temperature control of PFR was successfully demonstrated. According with the temperature level selected, a stability time to start the reaction must be established. Generally, between 2 to 3 hours was necessary to stabilize this system. (Appendix A).

III.5 Experimental Design

The objective of our experimental plan was to study the effects of the reaction temperature, fuel type, water to carbon (W/C) and oxygen to carbon (O_2/C) ratios in catalytic reactions of methanol, glycerol and biodiesel. A quantitative analysis in the GC-TCD and GC-MS were performed on the outlet gases and condensable liquids. When biodiesel and glycerol experiments were performed all systems lines presented soot formation. In addition, a brief SEM study on Pt-based catalyst surface was made to determine the coke deposition. All catalysts used with the three fuels studied had coke evidence.

Initially, with the purpose of setup our operational system, different conditions of water, oxygen and low temperatures reaction were studied for glycerol and biodiesel experiments. Hydrogen presence was not observed. Then, three O_2/C and one H_2O/C ratios were chosen for both compounds because of suggested interests of ANL.

Methanol experiments were done in order to probe if the use of Pt-based catalyst enhances the hydrogen production. Experiments with and without catalyst were performed. Six different temperatures were selected: 300, 400, 500, 600, 700 and 800 °F. One ratio of H_2O/C and O_2/C were studied; 0.76 and 0.39 respectively (See Appendix D).

For biodiesel and glycerol, ATR experiments were performed at 0.4, 0.5 and 0.6 as the O_2/C ratios and 2.0 for the H_2O/C ratio. With glycerol as fuel a 3^2 experimental design were performed with and without catalyst using three temperatures: 700, 800 and 900 °F. With biodiesel an experimental design of 3^1 were performed at 900 °F with and without catalyst. Additionally, with biodiesel as fuel, one trial with 3.5 H_2O/C ratio and 900 °F with catalyst were performed and a triplicate at 0.4 O_2/C and 2.0 H_2O/C ratios at 900°F were completed.

CHAPTER IV

Results and Discussion

This chapter focuses on experimental procedure and presents a summary about the experimental design, analytical methods and constant values used during the project. Additionally, it contains a comparison of the results of the ATR runs of methanol, biodiesel and glycerol as fuel with Pt-based or Rh-based catalyst and without catalysts. In addition, SEM and EDS analysis were performed on catalyst pills used and will be discussed.

Results and Discussion

A series of ATR experiments varying fuels (methanol, glycerol and biodiesel), ratios of oxygen to carbon (O_2/C) and water to carbon (H_2O/C) as well as reaction temperatures were performed. Calibration curves relating injected quantities of standard compounds were prepared to analyze the exit gas and liquid reformate. Hydrogen, oxygen, methane and monoxide carbon were analyzed with the GC-TCD (see Appendix B). Solvents as Hexane, benzene, heptane, toluene, isooctane, o-xylene, m-xylene, p-xylene and biodiesel were examined in the GC-MS. Also, calibration curves of alcohols (such as methanol, ethanol, 1-propanol, 2-propanol and butanol) were constructed to study the composition of the liquid aqueous reformate in ATR runs. Appendix E.3 illustrates several chromatographs obtained in both equipments for liquid products of Glycerol and Biodiesel ATR. Typically, the fuels and water are injected with peristaltic pumps individually. However, for these experiments a mixture of water and glycerol was injected to compensate for glycerol's high viscosity. Furthermore, 3 mL aliquots of the mixture were used because it was the most stable condition in the pump system.

The fuel flow rates of glycerol, described in table IV.1, consisted of mixture of 400 mL of glycerol and 600 mL of water. The other feed flows are also reported below in the

same table. Examples of the calculations for water, fuel and oxygen flow are shown in Appendix E.1.

The level definitions in table IV.1 are represented by two numbers and one letter. To interpreted must be considered the following explanation: the first number are related with the fuel used; *1*, *2* and *3* (methanol, glycerol and Biodiesel respectively), the second number correspond at the level of oxygen to carbon to be studied; *1*, *2* and *3* (0.4 – 0.5 and 0.6 O_2/C ratios correspondingly) and the letter (*A* or *B*) correspond at the presence/absence of Pt-based catalyst.

Table IV.1 Feed flow rates used in the experiments realized

Fuel	Pt-based Catalyst presence	Level[3]	O_2/C	H_2O/C	Fuel flow (mL/min)	H_2O Flow (mL/min)	O_2 Flow (mL/min)
Methanol	☑	1.1.A	0.39	0.76	3.0	0.6	489
Methanol		1.1.B	0.39	0.76	3.0	0.6	489
Glycerol	☑	2.1.A	0.40	2.0	1.2	1.8	487
	☑	2.2.A	0.50	2.0	1.2	1.8	610
	☑	2.3.A	0.60	2.0	1.2	1.8	728
Glycerol		2.1.B	0.40	2.0	1.2	1.8	487
		2.2.B	0.50	2.0	1.2	1.8	610
		2.3.B	0.60	2.0	1.2	1.8	728
Biodiesel	☑	3.1.A	0.40	2.0	0.5	1.0	585
	☑	3.2.A	0.50	2.0	0.5	1.0	705
	☑	3.3.A	0.60	2.0	0.5	1.0	842
	☑	3.4.A	0.40	3.5	0.5	1.8	288
Biodiesel		3.1.B	0.40	2.0	0.5	1.0	585
		3.2.B	0.50	2.0	0.5	1.0	705
		3.3.B	0.60	2.0	0.5	1.0	842

A series of experiments with methanol were performed with the purpose of establishing that using Pt-based catalysts triggers hydrogen production at lower temperatures in ATR systems. It is important mention that methanol was studied in the range of 0.39 O_2/C and 0.76 H_2O/C ratios and between 300 to 800 °F, since according to

[3] [A: with catalyst , B: without catalyst presence]

Perez R.[26] this condition obtained the highest hydrogen production. Also, one bed of catalyst was used for all methanol runs. The ATR experiments carried out with glycerol were studied at (700, 800, 900 °F)[4] and with biodiesel at 900°F.

Additional experiments were performed with biodiesel and glycerol at low temperatures as well as other feed ratios. The idea behind these was to establish the conditions at which hydrogen production initiates. The appearance of carbon was remarkable in the experiments using biodiesel and glycerol and the operational system showed plugging problems around four hours after the operation began. Specifically, the exit gases reformate blocked the rupture disc (part of BSTR reactor, see Appendix G). Similarly, the reactor and its parts were opened and cleaned. This procedure, which takes approximately five hours, allowed us to use different catalytic bed between runs so that we could carry out SEM analysis on the catalytic surfaces.

The values of densities and molecular weight used for mass balances and other calculations performed in this document are shown in table IV.2. To calculate the oxygen flow, the standard conditions were established as 86 °F and 1.00675 atm (measured barometrically). Moreover the flowmeter has a relation between the locations of flow versus the total flow, appendix F displays the calibration curve given by the supplier. This data were used to calculate the flow rates in the system.

Table IV.2 Densities and molecular weight used in the calculations

Fuel	Density (g/cm^3)	Formula	Molecular weight (g/mole)
Methanol	0.791	CH_3OH	32
Glycerol	1.25495	$C_3H_5(OH)_3$	92
Biodiesel	0.878	$C_{19}H_{38}O_2$	298

The theoretical yield values for conditions studied were calculated using equation II.21 which, was defined as grams of hydrogen produced per gram of fuel fed. Table IV.3 reports the calculated values.

Table IV.3 Theoretical yields

[4] 371, 427 and 427 °C

Compound / O_2/Fuel ratio	$Y_{theoretical}$ (g H_2/g fuel)*100%		
	0.4	**0.5**	**0.6**
Methanol	13.9*	N.A	N.A
Glycerol	10	8.7	7.4
Biodiesel	35.3	34.9	34.5

* In methanol results, the exact oxygen to fuel ratio was 0.39.

Atomic balances for ATR experiments, with methanol, glycerol and biodiesel as fuels in absence and presence of Pt-based catalyst were calculated. The following equations were used to establish the amount of Carbon (C), Hydrogen (H) and Oxygen (O). Figure IV.1 depicts the overall mass balance from which these relations were developed

H:
$$n_{in-H_2O}\times 2 + n_{in-C_zH_mO_p}\times m \cong n_{out-H_2}\times 2 + n_{out-CH_4}\times 4 + n_{out-H_2O}\times 2 + n_{out-C_zH_mO_p}\times m$$

O:
$$n_{in-H_2O}\times 1 + n_{in-C_zH_mO_p}\times p + n_{in-O_2}\times 2 \cong n_{out-O_2}\times 2 + n_{out-CO}\times 1 + n_{out-CO_2}\times 2 + n_{out-H_2O}\times 1 + n_{out-C_zH_mO_p}\times p$$

C:
$$n_{in-C_zH_mO_p}\times z \cong n_{out-CO}\times 1 + n_{out-CO_2}\times 1 + n_{out-CH_4}\times 1 + n_{out-C_zH_mO_p}\times z$$

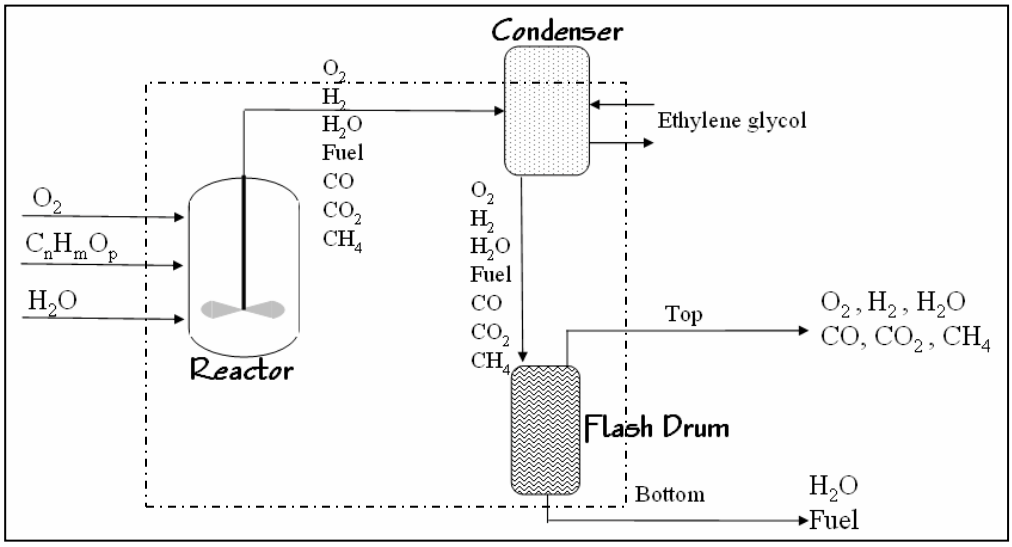

Figure IV.1 Process flow diagram with overall balance. Where $C_nH_mO_p$ represents the fuel used in the ATR assays.

IV.1 Methanol ATR experiments using Pt-based catalyst

The methanol experiments had the purpose of comparing the concentration of exit gases obtained with and without Pt-based catalysis. The temperature range was from 149 to 427 °C (300 to 900 °F). Figure IV.2 illustrates the production of hydrogen gas as a function of temperature in increments of 100°F for both types of experiments. The icon "+", represent the catalytic experiments and the icon "x" were performed without catalyst.

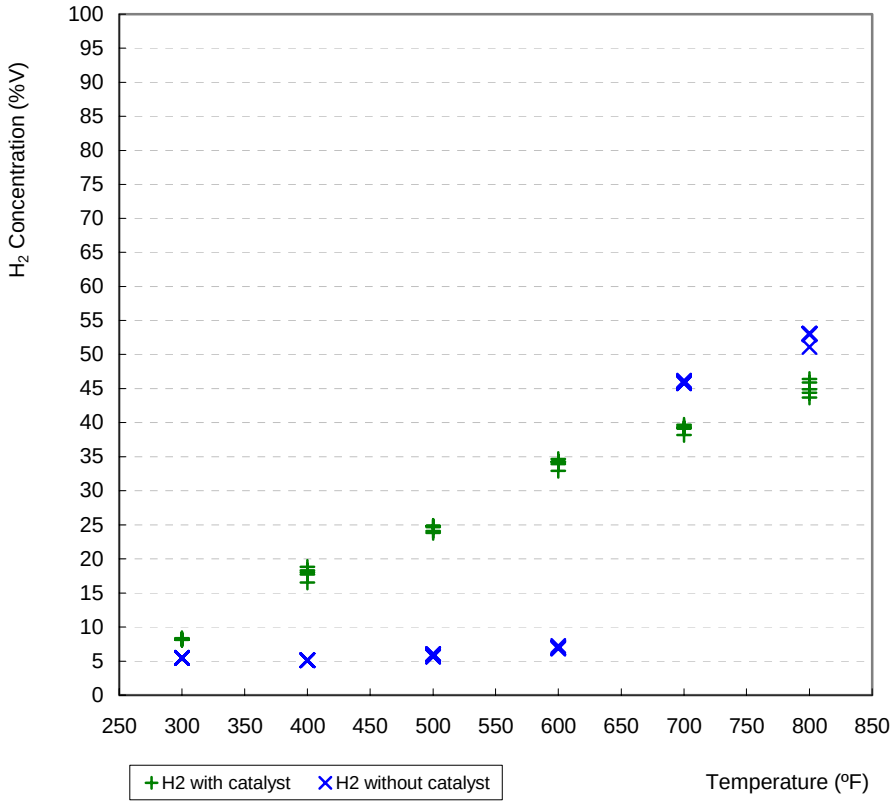

Figure IV.2 Hydrogen concentration of the exit gas with and without catalyst

An overview of the overall behavior in both experiments could be seen in Figures IV.3 and IV.4. The graphs illustrate the presence of exit gases throughout the temperature changes in the ATR experiments. At higher temperatures (≥ 700°F), the non-catalytic route resulted in 5% more hydrogen was than the catalytic one. Carbon monoxide generation during the non-catalytic experiment was less than 2%, except above 700 °F in

which it reached nearly 30%. In catalytic experiments a linear tendency of consumption of oxygen and hydrogen production was visible. Furthermore CH_4 presence was observed for temperatures above 500 °F. In the non catalytic experiments presence of CO_2 and CO as well as the formation of methane were established. The volume percent of H_2 up to 55% was achieved. Between 300 and 500 °F there is no evidence of H_2 formation.

The first indications of presence of hydrogen (≅ 6.0%) and consumption of oxygen in the non catalyst system were observed over 600 °F. Notice the sudden increase in hydrogen formation and the oxygen consumption at 700°F. The presence of CO, CO_2 and CH_4 observed during all experiments (catalytic and not catalytic) is illustrated in Figure IV.3 and Figure IV.4.

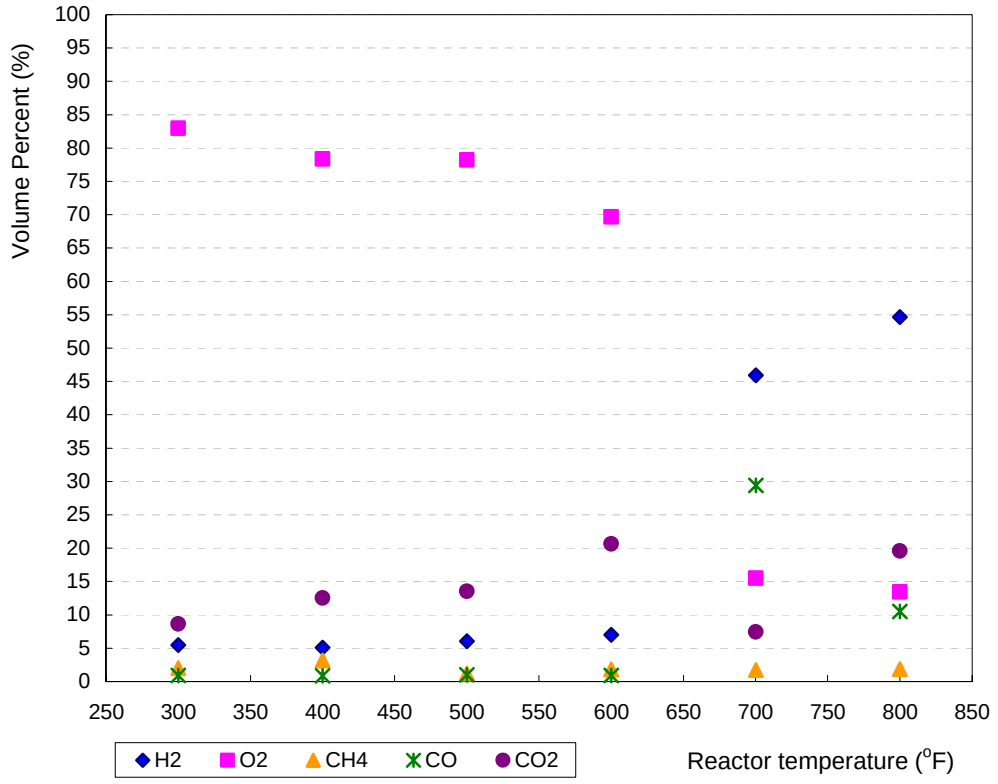

Figure IV.3 Exit gas concentrations of outlet gases at different temperatures with methanol as fuel without catalyst.

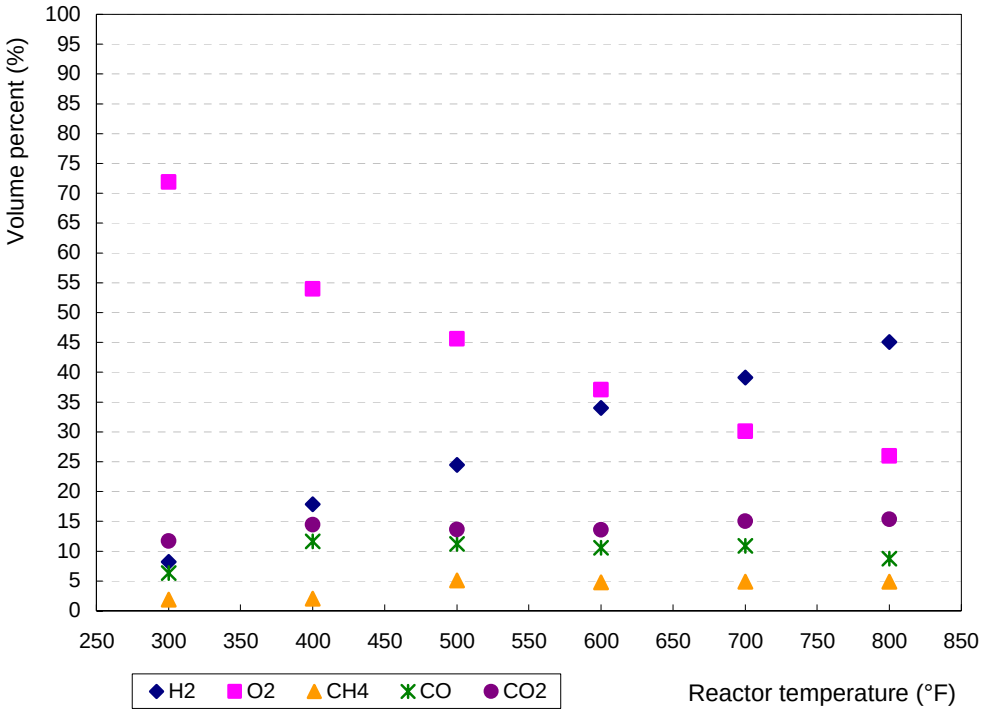

Figure IV.4 Exit gas concentrations of outlet gases at different temperatures with methanol as fuel with catalyst.

Hydrogen selectivity and methanol conversion in the ATR experiments was calculated with equations IV.1 and IV.2 described in [93]. These are illustrated in figure IV.5. The denominator in the following equation is obtained from the mass balance for the fuel in the whole system.

$$H_2 \text{ selectivity} = \text{moles of } H_2 \text{ produced/moles of methanol reacted} \quad \text{(IV.1)}$$

$$CH_3OH \text{ Conversion} = \text{moles of fuel reacted/moles of fuel fed} \quad \text{(IV.2)}$$

According to the overall ATR reaction (eq. II.21), the theoretical maximum hydrogen moles that can be produced for each mole of methanol reacted is 2.22 moles. The experimental results obtained were lower than this value as is illustrated in the next figure. The highest yield obtained was 2.1. This was accomplished in runs without catalysts. Both experiments portrayed advances in selectivities with increments in the

reactor temperature. The presence of catalyst improves the methanol conversion in 15% over the whole range studied.

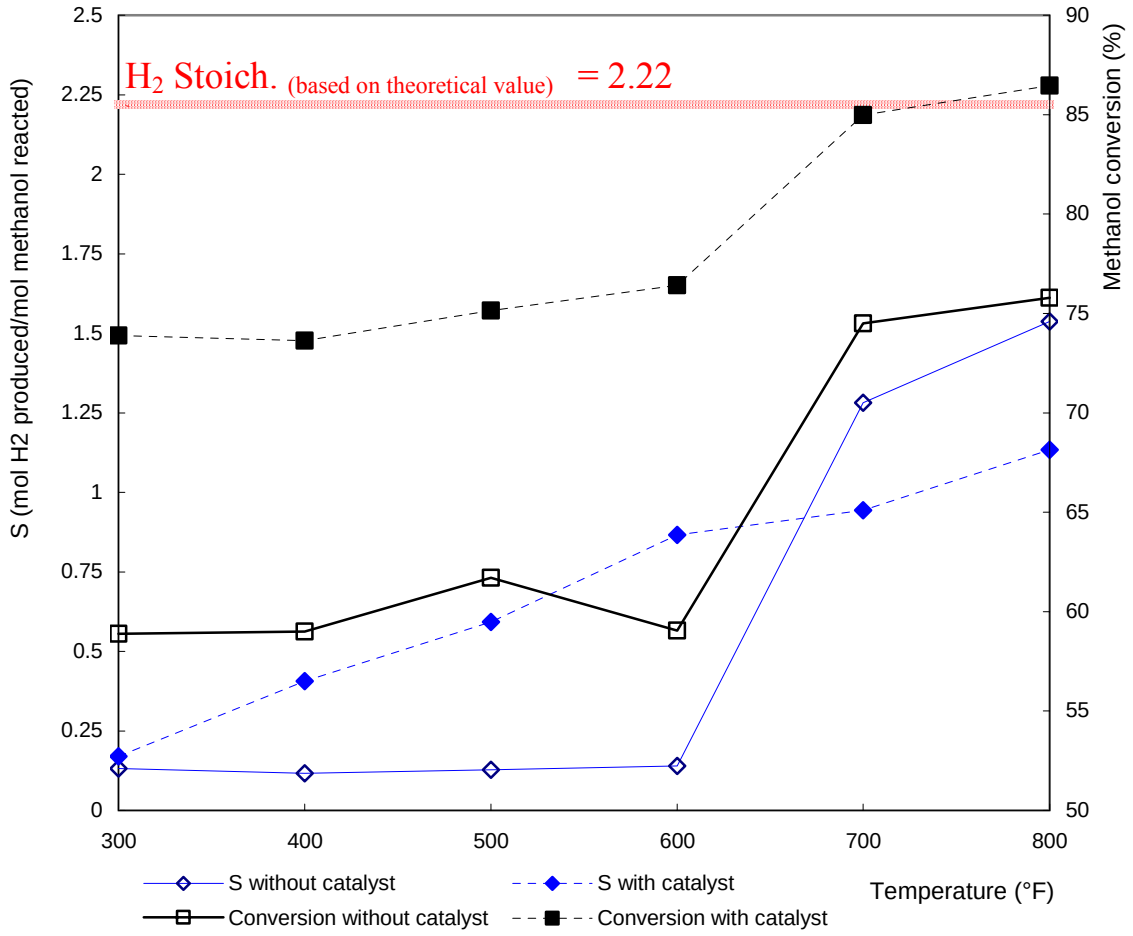

Figure IV.5 Hydrogen selectivity and methanol conversion with and without catalyst at different temperatures

Figure IV.5 shows that the selectivity in the experiments without catalyst was nearly zero for all temperatures less than 600°F. In contrast, selectivity increased in catalytic runs on the same range. At higher temperatures the value of selectivity for the non catalytic route was over 1.5. A possible explanation for this behavior is that at higher temperatures the SR reaction is favored and their effect is more significant than with catalyst presence.

Also, space velocity was calculated for both experiments. The highest values were found at the higher temperatures.

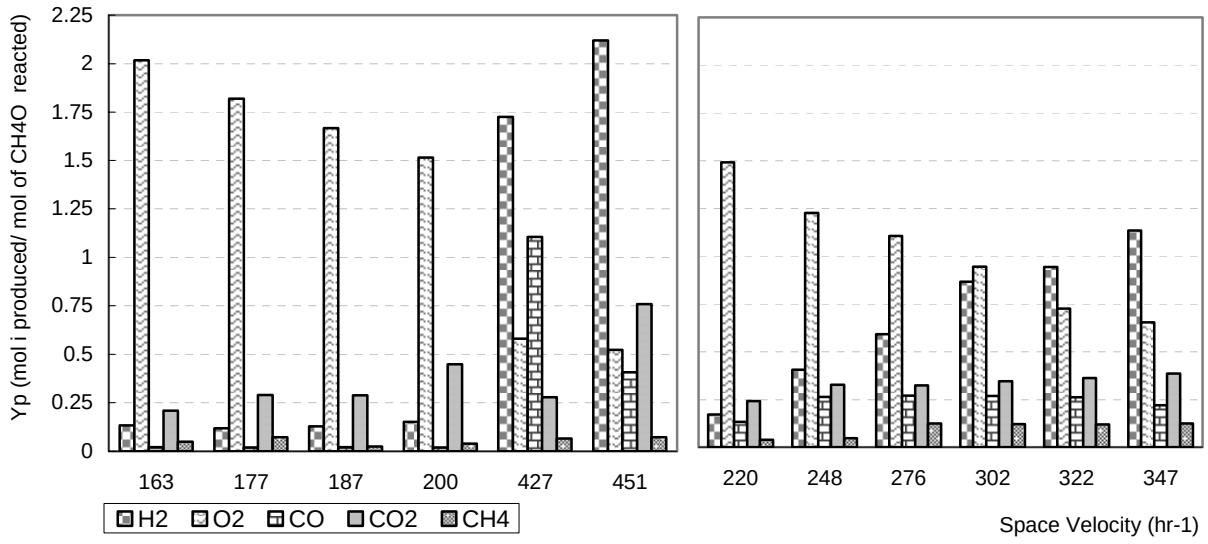

Figure IV.6 Products yield as a function of Space Velocity (SV) for Methanol ATR (left) without and (right) with Pt-based catalyst

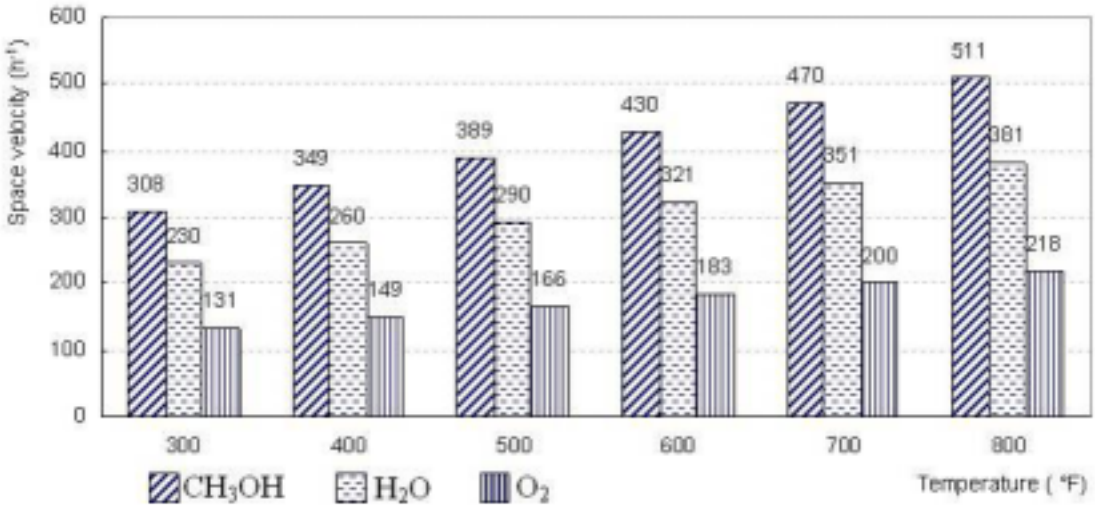

Figure IV.7 Space Velocity (SV) as a function of reactor temperature for Methanol, water and oxygen fed.

Atomic balances for methanol experiments with and without Pt-based catalysts are shown in the following tables. The best accountabilities for H and C atoms were observed at the higher temperatures. The opposite was observed for the O atoms. With the Pt-based catalysts the atoms accountabilities were more uniform.

Table IV.4 Atomic balance in Methanol ATR without Pt-based catalyst

T (ºF)	Inlet reactor (atom/min)			Outlet reactor (atom/min)			Mass Balance accountability (%)		
	H	C	O	H	C	O	H	C	O
300	0.407	0.074	0.193	0.277	0.047	0.202	*68.0*	*63.7*	*104.6*
400	0.407	0.074	0.193	0.289	0.060	0.197	*71.0*	*80.9*	*102.5*
500	0.407	0.074	0.193	0.302	0.056	0.202	*74.1*	*75.0*	*104.7*
600	0.407	0.074	0.193	0.308	0.053	0.227	*75.7*	*71.7*	*117.9*
700	0.407	0.074	0.193	0.310	0.064	0.182	*76.3*	*86.6*	*94.2*
800	0.407	0.074	0.193	0.347	0.065	0.187	*85.1*	*87.9*	*97.1*
						average	*75.1*	*78.5*	*103.5*

Table IV.5 Atomic balance in Methanol ATR with Pt-based catalyst

T (ºF)	Inlet reactor (atom/min)			Outlet reactor (atom/min)			Mass Balance accountability (%)		
	H	C	O	H	C	O	H	C	O
300	0.407	0.074	0.193	0.261	0.053	0.214	*63.9*	*71.7*	*111.3*
400	0.407	0.074	0.193	0.286	0.055	0.203	*70.2*	*73.9*	*105.2*
500	0.407	0.074	0.193	0.322	0.059	0.198	*79.1*	*79.5*	*102.7*
600	0.407	0.074	0.193	0.324	0.059	0.195	*79.5*	*80.5*	*101.3*
700	0.407	0.074	0.193	0.326	0.058	0.201	*80.1*	*78.9*	*104.2*
800	0.407	0.074	0.193	0.331	0.057	0.201	*81.3*	*77.4*	*104.1*
						average	*75.7*	*77.0*	*104.8*

IV.2 Glycerol ATR experiments using Pt-based catalyst

Glycerol experiments with and without presence of Pt-based catalyst were performed with an experimental design of 3^2. O_2/C ratio and temperatures were the variables. The values studied are described in table IV.1. Figures IV.8 shows the hydrogen content at the different temperature and oxygen to carbon ratio.

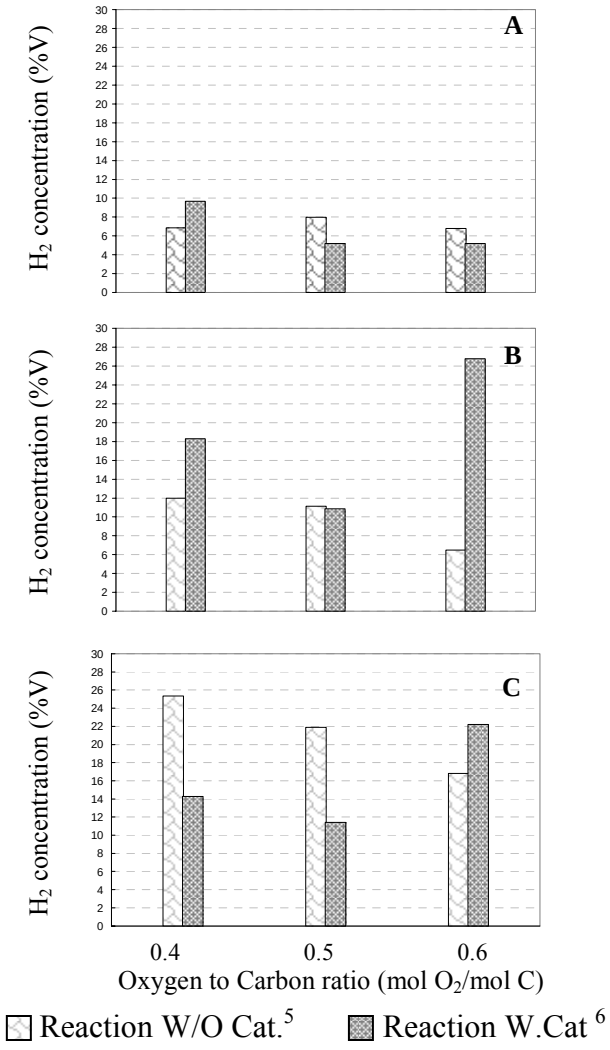

Figure IV.8. Exit gas concentration of Hydrogen at reactor temperature constant and presence or absence of Pt-based catalyst: (A) 700 °F, (B) 800 °F, and (C) 900 °F.

[5] W/O Cat. = without catalyst
[6] W.Cat = with catalyst presence

In experiments without catalyst (W/O Cat.), the hydrogen concentration in the three oxygen conditions studied increased when the temperature increased. The highest O_2/C corresponds to the least H_2 concentration in experiments without catalyst, except in 900°F. The use of catalyst in the ATR reaction improves four of the nine studied points. An inversely proportional relation was observed at constant temperature of 900 °F between the oxygen ratio and hydrogen concentration for the non catalyst system, which is depicted in figure IV.6C. The best condition was obtained at 800 °F and 0.6 O_2/C. A similar behavior was observed for the three oxygen conditions and 700°F.

Figure IV.9 shows the three-dimensional analysis of the oxygen to carbon ratio, temperature and process yield to determine more clearly the effect on the mentioned variables in the ATR process. The best process yield obtained in the ATR experiments was the non-catalytic route, almost 25%. With catalyst, a process yield of 20% was obtained. The process yield was calculated as grams of hydrogen produced per grams of glycerol fed.

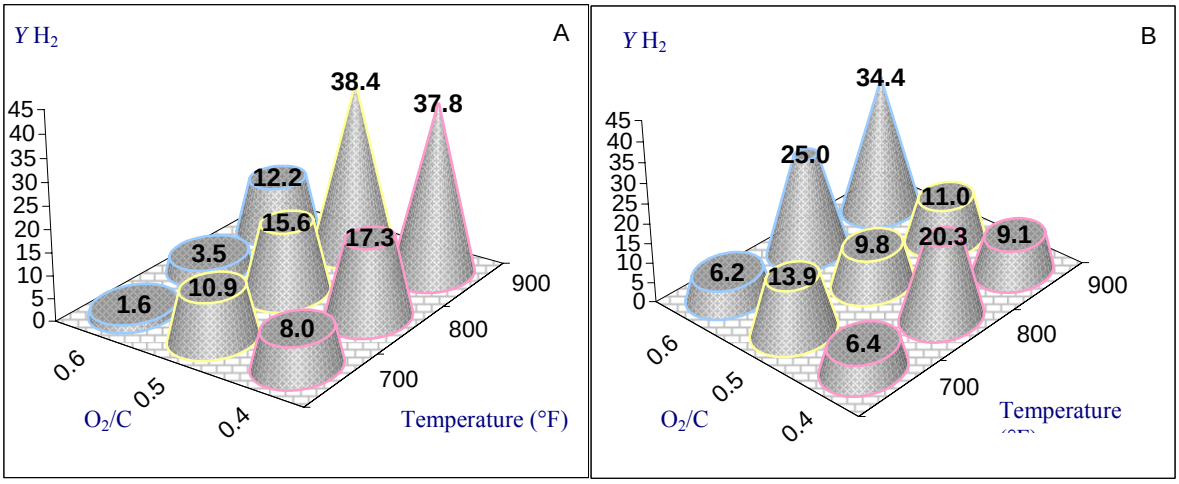

Figure IV.9. Hydrogen yields as function of reactor temperature, Oxygen to Carbon ratio and Pt-based catalyst presence. (A) W/O Cat and (B) W.Cat

All the glycerol experiments with catalyst (W.Cat.) were performed initially with one catalyst batch. An experimental design of 3^2 was studied and the system conditions are described in table IV.1. It was assumed that no poisoning or deactivation will occur. This assumption was based on the results of our methanol experiments as well as *Perez R.*

[26]. Hence only one bed of Pt-based catalyst was used. It was expected that our operational system will show a H_2 increase with catalyst presence but discrepancies with this hypothesis were found. Nine experiments with Pt-based catalyst in the order showed in table IV.6 at constant 2.0 W/C ratios were run (since 0.4 O_2/C and 700 °F to 0.6 O_2/C and 900 °F). Then, repetitions of the 0.5 O_2/C runs were performed without catalyst change. Table IV.6 displays the H_2 yield calculated for catalytic and non-catalytic runs. The H_2 yield without catalyst was higher than with catalytic route in seven levels. Only two conditions with catalyst in the first run showed increase in the H_2 production (0.6 O_2/C - 800 and 900 °F). And H_2 production obtained in the replicate of 0.5 O_2/C differed in all temperatures with the data collected in the first run.

Table IV. 6 Yield H_2 as function of reactor T, O_2/C ratio and catalyst used.

Day run	T (°F)	Y [W/O.	Y [W.Cat]
1	700	7.95	6.37
2	800	15.01	10.34
3	900	37.85	17.89
4	900	38.43	11.02
5	800	15.64	9.81
6	700	10.95	5.06
7	700	7.61	6.19
8	800	8.10	24.98
9	900	30.66	34.39
10	900	N.P.	21.96*
11	800	N.P.	48.73*
12	700	N.P.	11.66*

N.P: no performed - * repetition experiments

Therefore, activation/deactivation process may be occurring. This is opposite to what was originally expected and differs with behavior observed in the methanol experiences. Consequently, further experiments with biodiesel were carried on using a fresh catalyst in each run. It ought to be noted that a replication for 0.4 O_2/C was done and its result were the same as those of the original. Thus, it was assumed that the rest of the runs were as replicable as that particular one. The reproducibility of the experiments was corroborated

at 0.4 O_2/C, 2.0 W/C and 700 °F condition (see table IV.7). Figure IV.10 displays all glycerol experiments performed in three rows; first runs with one bed catalytic (columns with dashed border), its replicate at 700, 800 and 900°F with 0.5 O_2/C, (second row without dashed border) and W/O Cat (columns in the third row with horizontal background). The "*x*" and "*y*" axis correspond at oxygen to carbon ratio and experimental yield (g H_2 produced /g glycerol reacted) respectively.

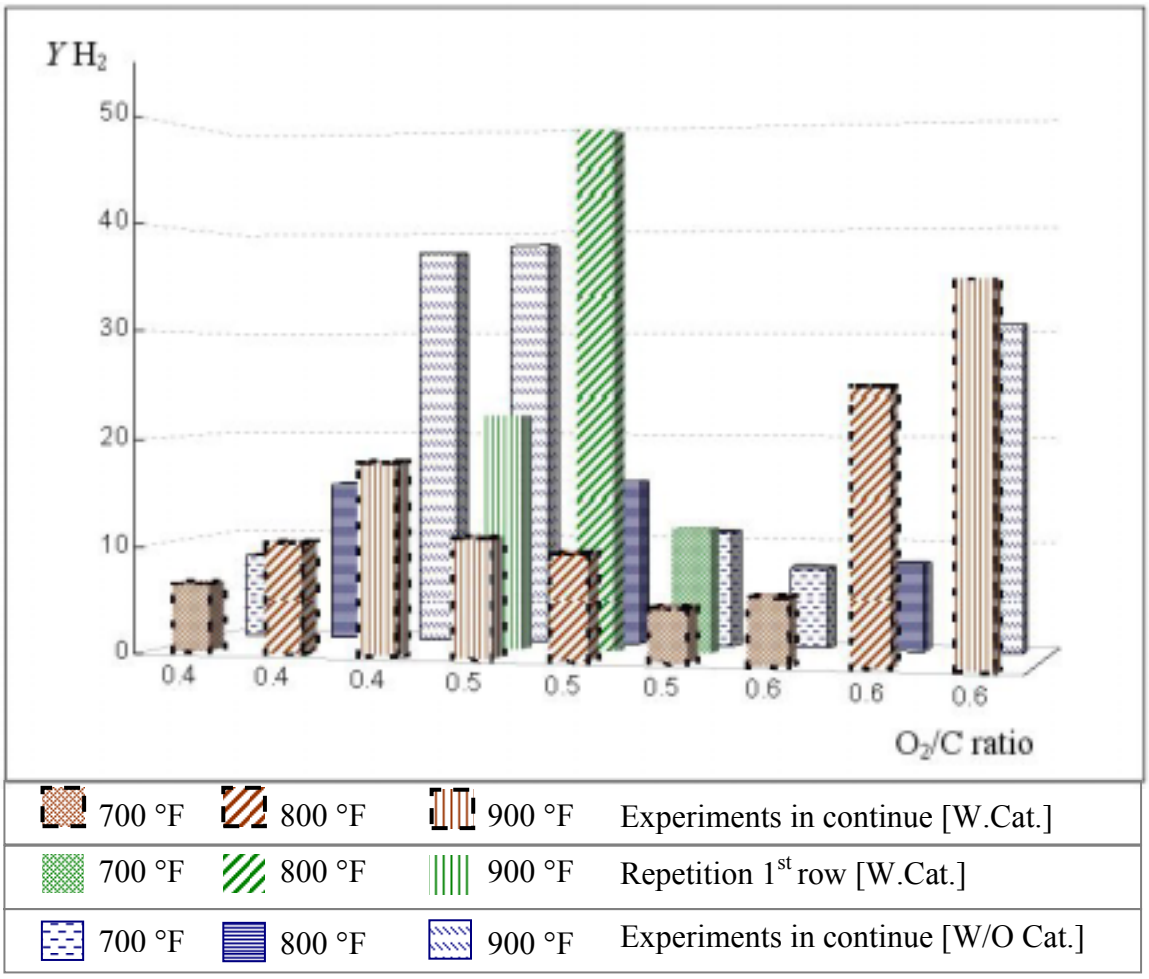

Figure IV.10 H_2 yields of glycerol ATR as function of reactor temperature and O_2/C ratio and presence or absence of Pt-based catalyst. 1st row: experiments W.Cat., 2nd row: repetition W.Cat. and the 3rd row: W/O Cat

Exit gases concentrations in glycerol experiments shown in Figure IV.9 displays a clear sign of different baseline in the system in each run day. Space velocities (SV) for every run were calculated. Figure IV.11 contain 6 graphs of ATR glycerol and each one have 3 SV values corresponding at 700, 800 and 900°F (left to the right) respectively.

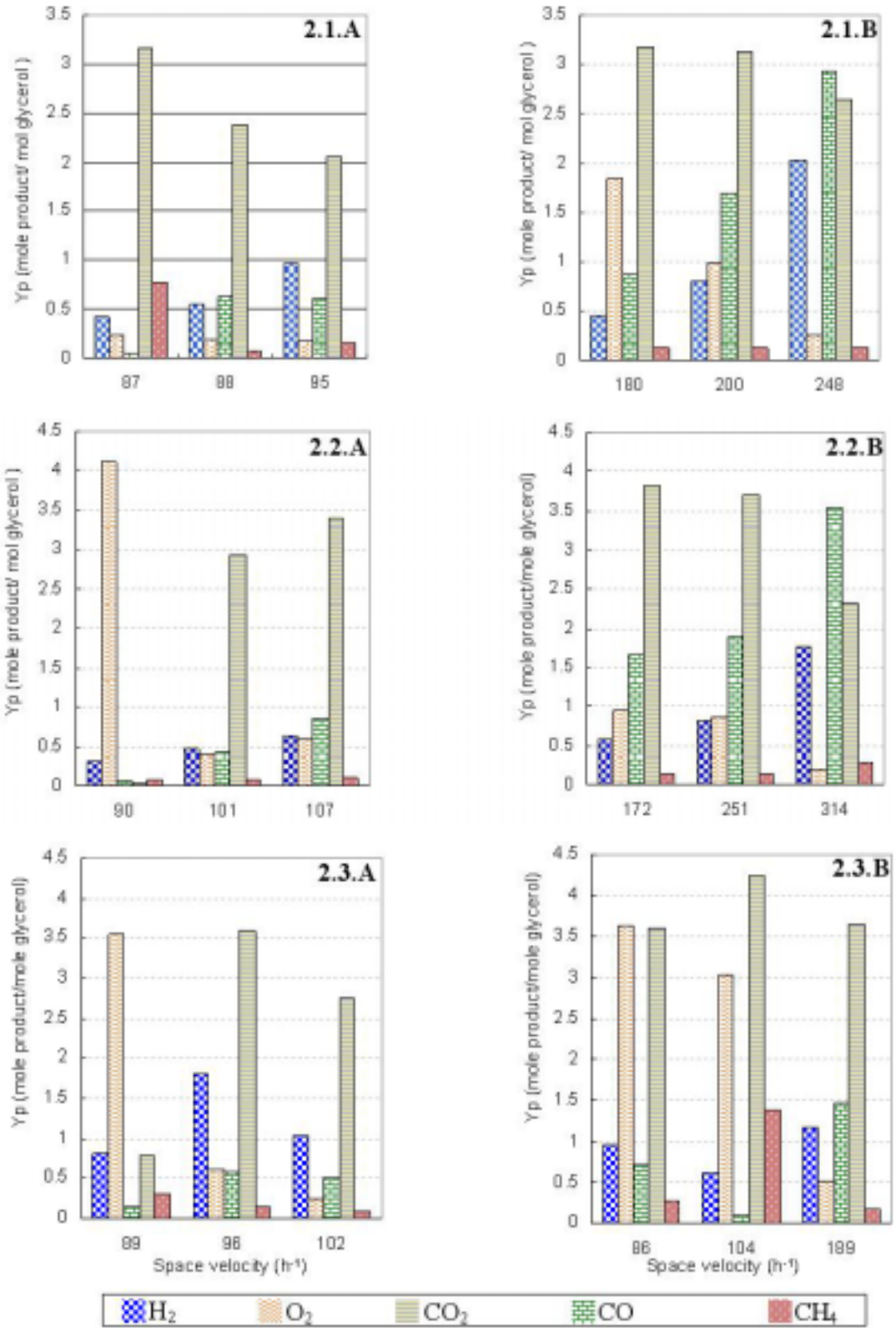

Figure IV.11 Products yield as a function of Space Velocity (SV) for gases product in ATR glycerol using Pt-based catalyst.

As was mentioned, the following table contained the replicate results for glycerol ATR experiments to establish the reproducibility in the level 2.1.A (according with table IV.1) at 700°F.

Table IV.7 Products concentrations (%V) in the triplicate of glycerol ATR at 0.4 O_2/C, 2.0 W/C and 700 °F

H_2			Average	St.Dev	CH_4			Average	St.Dev
9.34	8.86	8.93	*9.05*	**0.26**	16.86	17.05	17.11	*17.01*	**0.13**
9.39	8.84	9.21	*9.15*	**0.28**	16.86	17.06	16.86	*16.93*	**0.12**
9.06	8.89	8.52	*8.83*	**0.28**	16.90	17.04	16.62	*16.85*	**0.21**
9.27	8.98	9.01	*9.09*	**0.16**	16.84	17.00	16.72	*16.85*	**0.14**
8.94	8.82	9.37	*9.05*	**0.29**	16.95	17.07	16.50	*16.84*	**0.29**
8.93	8.86	9.31	*9.03*	**0.24**	16.94	17.05	16.39	*16.79*	**0.35**

CO_2			Average	St.Dev	CO			Average	St.Dev
67.06	67.36	67.50	*67.31*	**0.23**	1.28	1.29	0.95	*1.17*	**0.19**
66.99	67.36	67.88	*67.41*	**0.44**	1.30	1.30	0.95	*1.18*	**0.20**
67.25	67.36	68.60	*67.74*	**0.75**	1.31	1.29	0.94	*1.18*	**0.21**
67.15	67.35	67.75	*67.42*	**0.30**	1.30	1.28	0.97	*1.18*	**0.18**
67.33	67.37	68.17	*67.62*	**0.47**	1.28	1.30	0.94	*1.18*	**0.20**
67.37	67.36	67.98	*67.57*	**0.36**	1.26	1.29	0.96	*1.17*	**0.19**

Atomic balances are shown in tables IV.8 and IV.9 for each level studied. Similar to methanol experiments the atoms accountability was acceptable.

Table IV.8 Atomic balance in Glycerol ATR without Pt-based catalyst.

Level	**T (°F)**	**Inlet reactor (atom/min)**			**Outlet reactor (atom/min)**			**Mass Balance accountability (%)**		
		H	**C**	**O**	**H**	**C**	**O**	**H**	**C**	**O**
2.1.B	700	0.265	0.049	0.159	0.215	0.047	0.165	*65.0*	*96.3*	*103.2*
2.1.B	800	0.265	0.049	0.159	0.224	0.053	0.185	*67.9*	*107.9*	*115.9*
2.1.B	900	0.265	0.049	0.159	0.277	0.045	0.172	*83.9*	*92.4*	*108.5*
2.2.B	700	0.330	0.049	0.203	0.266	0.043	0.191	*80.5*	*86.9*	*93.9*
2.2.B	800	0.330	0.049	0.203	0.289	0.055	0.189	*87.5*	*111.2*	*93.2*
2.2.B	900	0.330	0.049	0.203	0.306	0.037	0.179	*92.7*	*76.1*	*87.9*
2.3.B	700	0.330	0.049	0.214	0.236	0.046	0.214	*71.4*	*114.8*	*100.2*
2.3.B	800	0.330	0.049	0.214	0.252	0.045	0.203	*76.3*	*92.2*	*94.9*
2.3.B	900	0.330	0.049	0.214	0.309	0.051	0.199	*93.8*	*104.2*	*93.1*
							Average	*79.9*	*98.0*	*98.9*

Table IV. 9 Atomic balance in Glycerol ATR with Pt-based catalyst.

Level	T(ºF)	Inlet reactor (atom/min)			Outlet reactor (atom/min)			Mass Balance accountability (%)		
		H	C	O	H	C	O	H	C	O
2.1.A	700	0.330	0.049	0.159	0.268	0.061	0.156	*81.4*	*123.4*	*97.9*
2.1.A	800	0.330	0.049	0.159	0.252	0.050	0.173	*76.4*	*102.4*	*108.7*
2.1.A	900	0.330	0.049	0.159	0.287	0.047	0.170	*87.1*	*95.2*	*106.5*
2.2.A	700	0.330	0.049	0.203	0.252	0.046	0.206	*76.4*	*93.5*	*101.4*
2.2.A	800	0.330	0.049	0.203	0.231	0.043	0.205	*70.0*	*87.7*	*100.8*
2.2.A	900	0.330	0.049	0.203	0.219	0.051	0.198	*66.5*	*104.6*	*97.6*
2.3.A	700	0.330	0.049	0.214	0.234	0.041	0.225	*71.0*	*84.2*	*105.5*
2.3.A	800	0.330	0.049	0.214	0.314	0.051	0.224	*95.2*	*103.2*	*104.9*
2.3.A	900	0.330	0.049	0.214	0.201	0.050	0.174	*60.8*	*101.6*	*81.5*
							Average	*76.1*	*99.5*	*100.5*

IV.3 Biodiesel ATR experiments using Rh and Pt-based catalysts

ATR experiments with biodiesel as fuel were performed amount 1000 °F. BSTR and PFR were used as reactors and two catalysts were studied. Also, experiments without catalysts at different feed conditions were completed and no hydrogen evidence was detected.

Experiments with Rh-based catalyst were carried out in the BSTR. The reactor basket was not adequate for the original shape of the catalyst. Fig III.2 illustrates the powder catalyst was transformed in slim pills to be contained inside the basket.

Hydrogen production was no observed. Exit gases concentrations of some runs performed with Rh are illustrated in figure IV.12. The exit gases concentrations obtained are similar with the results obtained in the non catalytic runs. Table IV.10 summarizes the settings/parameters used for the runs in either presence or absence of catalysts. Not hydrogen was observed.

Table IV.10 Conditions of water to carbon (W/C) and Oxygen to carbon (O_2/C) ratios studied in presence and absence of catalysts.

Observations	Catalyst type	W/C	O_2/C	Temperature(°F)
<6%	Pt[1]	2.98	0.38	700-900
No H_2	Pt NC[2] Rh[3]	5.97	0.75[1,2]	700-950
				1020-1040-1060
			1.42 [1,2]	700-980
			0.56 [1,2]	950-1000
			0.35	990-1025
No H_2	Pt, NC	4.97	0.35	940-980
No H_2	Rh, NC	2.48	0.18	940-980-1020-1040
No H_2	Rh, NC	2.48	0.28	950-1050-1100
No H_2	Rh, NC	2.0	0.4[2,3]	850-950-1050
			0.5[2,3]	
			0.6[2,3]	

[1] Pt-based catalyst - [2] Not catalyst presence and [3] Rh-based catalyst

The main results in the additional biodiesel experiments shown in table IV.10, were that no evidence of hydrogen production, small consumption of oxygen and no coke formation in the region studied

Figure IV.12 represents some of the mentioned runs in table IV.10. Hydrogen was not observed in these experiments, only oxygen (not reacted) and formation of carbon monoxide were detected. Organic condensable was identified as described in the section *biodiesel characterization*. Interested alcohols were no detected. It is important to mention that these experiments were performed in the BSTR system and that its maximum allowable temperature was about 1050 °F.

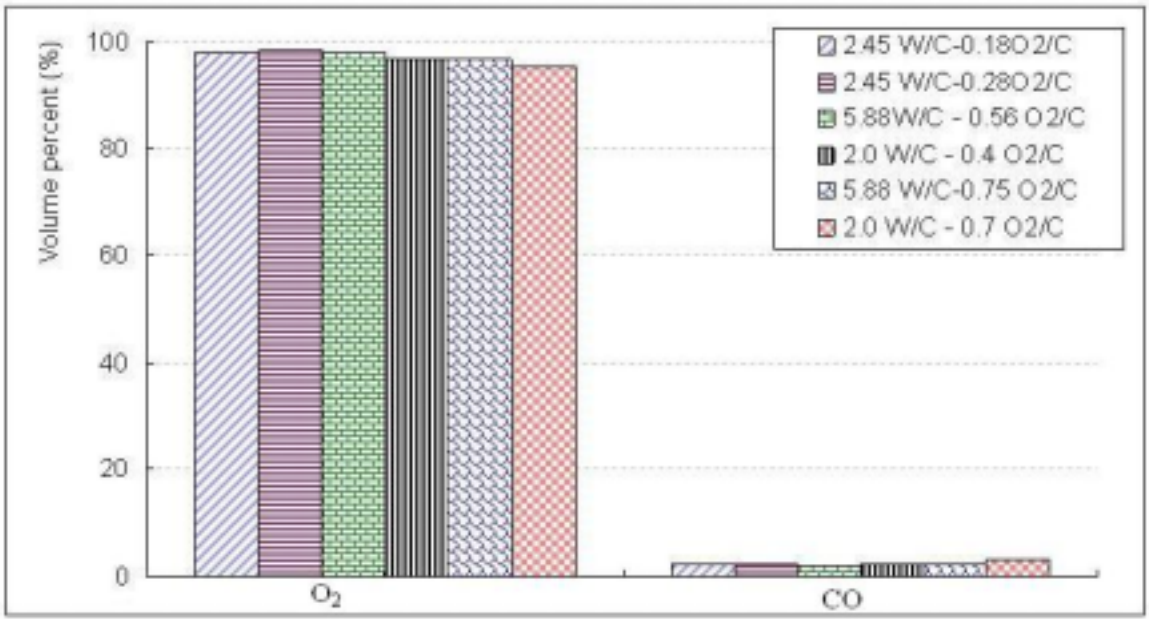

Figure IV.12 Exit gas concentrations of Biodiesel ATR as fuel and Rh-based catalyst

Experiments with Rh-based catalyst in Biodiesel ATR experiments also do not show evidence of hydrogen formation. We expected hydrogen evidence in accordance with previous results when using the Pt-based catalyst. We infer that this behavior could be related to the pellet pressing process. This process changes the surface of the catalyst and therefore damages the original characteristics. Nevertheless, it could be possible that for the ATR with Biodiesel given the system conditions the Rh-based catalyst does not enhance or improve the catalytic route despite the surface characteristics.

Likewise, powder Rh-based catalyst was used in the second system as is described in chapter III. Troubleshooting and inconveniencies in the assembly were noted in every trial run. This system was mounted two times because the quartz tube was fractured twice during the experimentation. No data could be collected, but carbon deposition was observed in fittings and tubing. Likewise, the organic waste was analyzed in the same way that in *biodiesel characterization* section. Figure IV.13 shows a brief overview for the PFR trials.

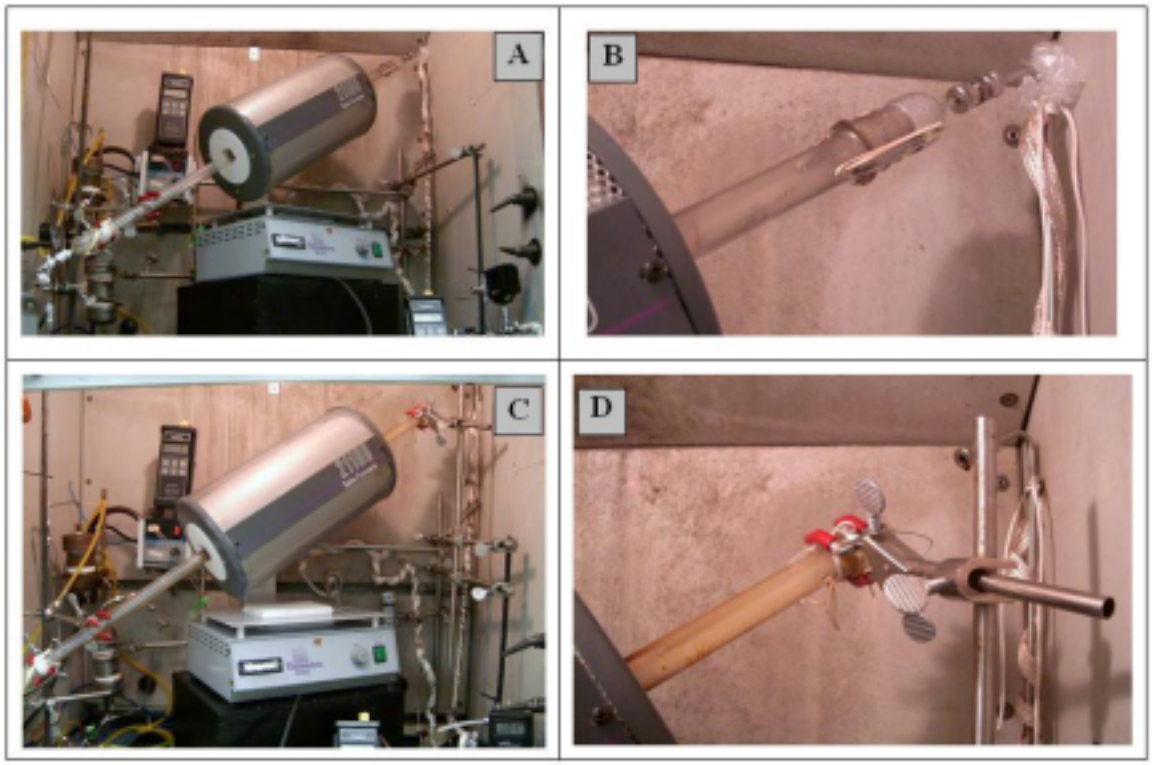

Figure IV.13. Experimental overview during PFR trials experiments. (A) PFR system starting, (B) inlet PFR reactor at initial time, (C) system general after cracking and (D) inlet PFR broken

Experiments with catalyst were performed with Pt-based catalyst using the system I, described in chapter III. Preliminary experiments out of the experimental design were practiced at different reactor temperatures and oxygen and water feeds. Evidence of hydrogen was detected above 1000 °F. Table IV.10 contained the most significant results obtained. Then, by ANL recommended other oxygen to carbon ratios. Four experiments at different ratios of O_2/C were performed as shown in table IV.1.

Using Pt-based catalyst, 25% H_2 was obtained. Furthermore, formation of CO_2, CO and CH_4 was also observed. An experiment with additional water content (3.5 water mole/carbon mole) was performed.

The ATR biodiesel system does not shows a significantly change in the hydrogen production. In the 3.5 W/C condition, minor changes in the CO (diminished 8 %) and O_2 (increased 10%) content were noted. Based on this CO behavior we could postulate that WGSR occurred. Figure IV.14 displays the results obtained.

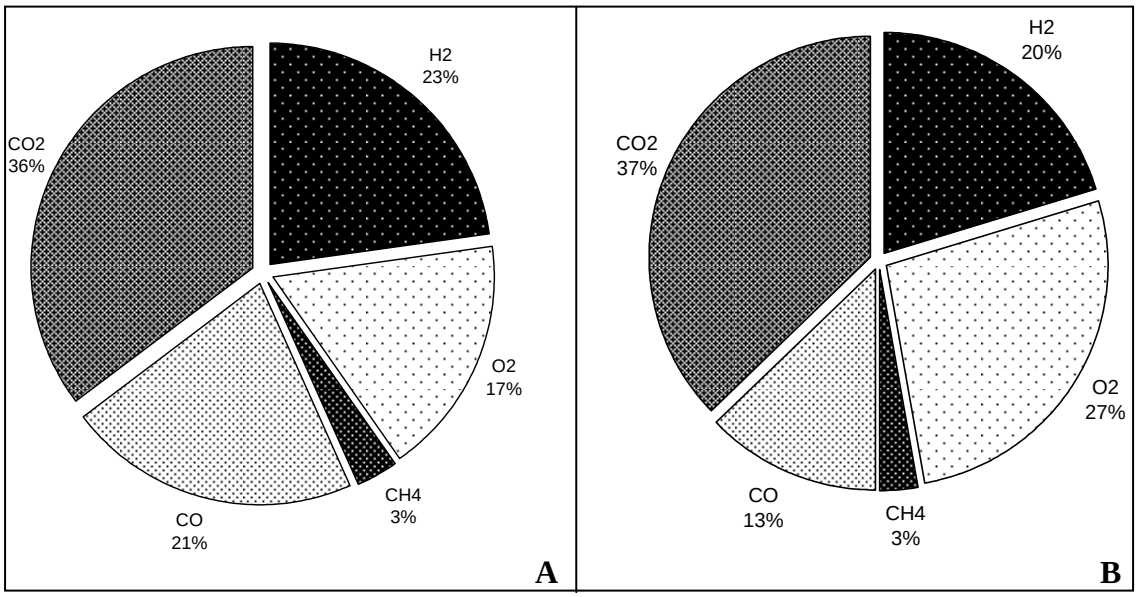

Figure IV.14 Exit gas concentrations of Biodiesel ATR with Pt-based catalyst at 900°F, constant oxygen to carbon (O_2/C) ratio and different water to carbon (W/Cat) conditions: (A) 2.0 and (B) 3.5

Although hydrogen concentration was similar in the three oxygen ratios studied, at 0.5 O_2/C maximum CO_2 formation with the lower CO presence (see figure IV.15) was observed also, hydrogen yields as function of feed ratios and temperature are shown in figure IV.16. The fed condition 0.6 O_2/C ratio obtained the highest hydrogen yield, though the other values are almost similar. Atomic balances were also performed for Biodiesel as shown in tables IV.11 and IV.12. Similar to methanol and glycerol the accountability were acceptable.

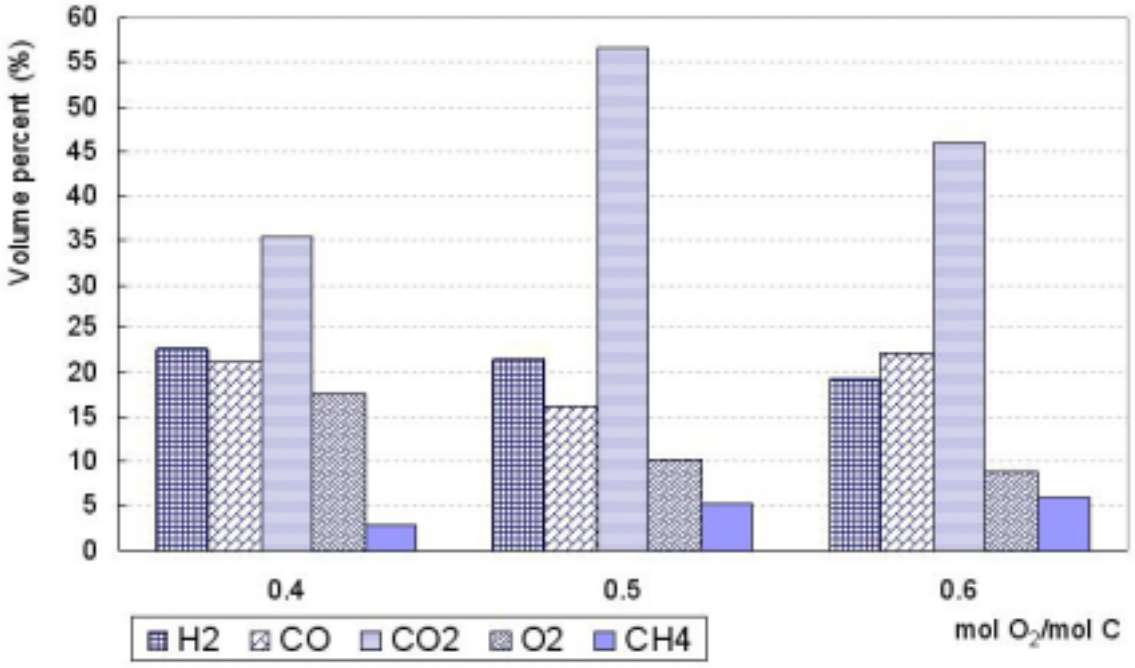

Figure IV.15 Exit gas concentrations of H_2, CO and CO_2 at 900°F using Pt-based catalyst at three different O_2/C ratios and constant W/C ratio

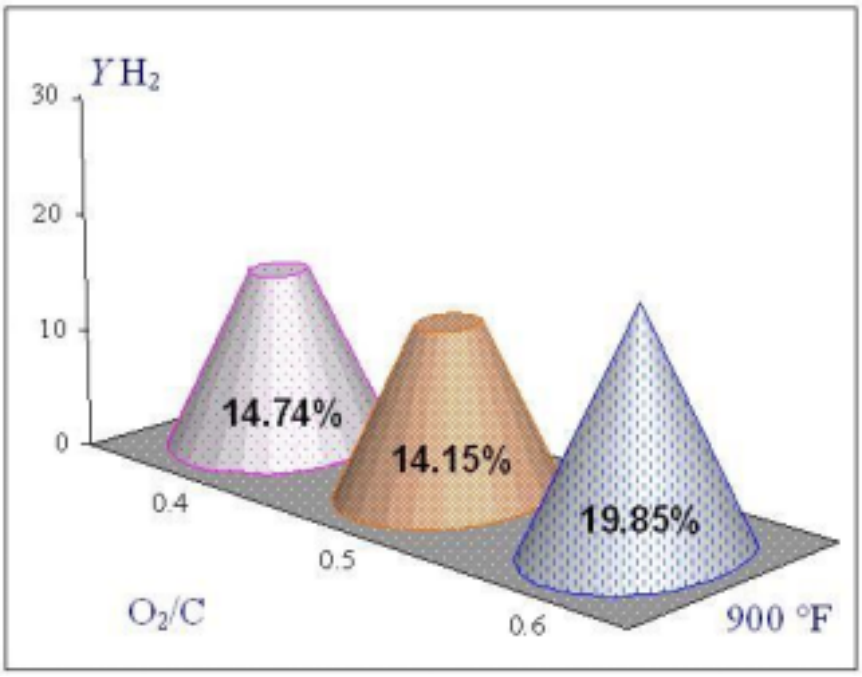

Figure IV.16 H_2 yields as function of O_2/C ratio with Pt-based catalyst at 900°F

Table IV.11 Atomic balance in Biodiesel ATR without Pt-based catalyst

Level	T (ºF)	Inlet reactor (atom/min)			Outlet reactor (atom/min)			Mass Balance accountability (%)		
		H	C	O	H	C	O	H	C	O
3.1.B	900	0.164	0.028	0.082	0.148	0.024	0.077	*90.1*	*85.7*	*104.5*
3.2.B	900	0.325	0.056	0.175	0.296	0.053	0.169	*91.1*	*94.9*	*108.0*
3.3.B	900	0.164	0.028	0.132	0.149	0.025	0.130	*91.3*	*89.3*	*106.1*
							Average	*90.9*	*89.9*	*106.2*

Table IV.12 Atomic balance in Biodiesel ATR with Pt-based catalyst.

Level	T(ºF)	Inlet reactor (atom/min)			Outlet reactor (atom/min)			Mass Balance accountability (%)		
		H	C	O	H	C	O	H	C	O
3.1.A	900	0.164	0.028	0.082	0.160	0.026	0.081	*97.8*	*91.8*	*98.7*
3.2.A	900	0.325	0.056	0.175	0.314	0.054	0.179	*96.8*	*96.0*	*102.1*
3.3.A	900	0.164	0.028	0.132	0.155	0.024	0.120	*94.8*	*86.8*	*91.4*
3.4.A	900	0.248	0.028	0.124	0.226	0.024	0.128	*91.4*	*86.6*	*102.6*
							Average	95.2	90.3	98.7

IV.3.1 Reproducibility of biodiesel ATR experiments

In order to verify the reproducibility of ATR experiments, triplicate runs of biodiesel and glycerol Autothermal reforming were performed. The feed conditions used are described in table IV.13.

Table IV.13 Feed conditions for reproducibility experiments with Pt-based catalyst

Fuel	Temperature (°F)	O_2/C ratio	W/C ratio
Biodiesel	900	0.4	2.0
Glycerol	700	0.4	2.0

For each reproducibility experiments, three runs were performed with catalyst change for every one. One gas reformate sample was taken every thirty minutes for four hours. Table IV.14 contains the standard deviations obtained in mentioned runs. Figure IV.17 illustrates the exit gases concentrations of hydrogen, oxygen, methane and carbon monoxide during the elapsed time in the triplicate group. The icon no filled represents the average gas concentration. The section IV.3.3 will discuss the triplicate results for liquids organic condensable (detection of 270, 294, 296 and 298 mass) in these experiments.

Table IV.14 Standard deviation for exit gases obtained in the triplicate runs

Stdev* / Sampling time	H_2	O_2	CH_4	CO
30	0.971	0.492	0.036	0.861
90	0.627	0.241	0.042	0.616
150	0.688	0.312	0.020	0.540
210	0.774	0.336	0.028	0.966
270	0.390	0.644	0.023	1.072
330	1.032	0.374	0.019	0.884

Stdev*: Standard deviation

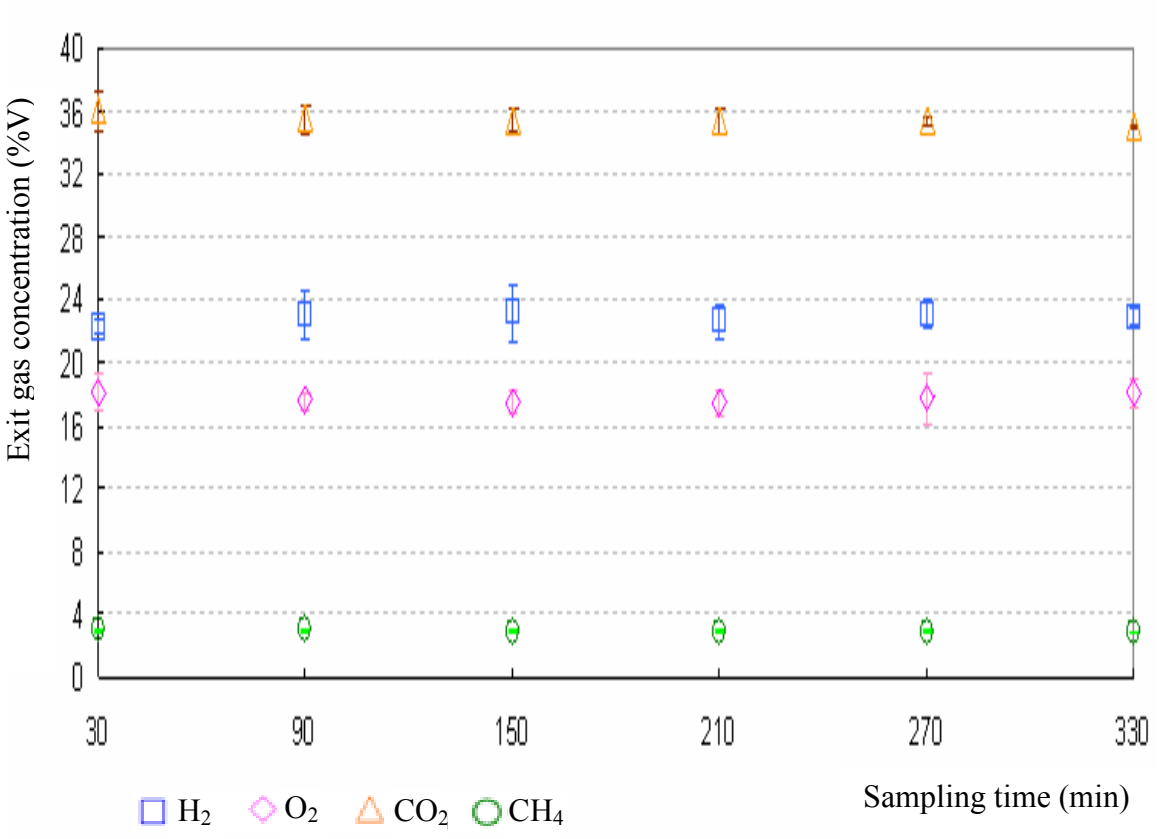

Figure IV.17 Exit gases concentrations reproducibility in biodiesel ATR experiments

IV.3.2 Heavy solvents evaluation on biodiesel samples

A qualitative analysis was performed to identify hexane, benzene, heptane, toluene, isooctane, o-xylene, m-xylene, p-xylene and Biodiesel in the condensed liquid steams. THF also was detected because it was the solvent used to determine the biodiesel composition in each experiment and for this reason was the selected control compound. Its respective retention time was determined for each one and table IV.14 shows the retention time of each species.

Liquid condensable reformate samples were analyzed in the GC-MS. Two sets of analytical experiments were carried out. The first one corresponded to injecting 0.5 μL of direct organic sample into the GC to determine the solvents' presence. The second one consisted of injections of the organic sample dissolved in tetrahydrofurane (THF) to determine the biodiesel peaks conversion. Appendix B contains the respective equations and calibration curves prepared for the mentioned analysis.

Table IV.14 Average retention time and Standard deviation of qualitative analysis for solvents and biodiesel compound.

Appearance order	**Name**	**Av. retention time (min)- deviation standard**			
1	Hexane	10.23 - 0.66			
2	THF	10.515 - 0.25			
3	Benzene	11.12 - 0.87			
4	Heptane	12.79 - 0.39			
5	Isooctane	12.91 - 0.39			
6	Toluene	15.10 - 0.41			
7	o-xylene	18.84 - 0.31			
8	m-xylene	18.91 - 0.29			
9	p-xylene	21.46 - 0.18			
10	Biodiesel	38.458	40.688-	40.758-	41.032-

* Those values could vary briefly depending on the used temperature, conditioned flow and mainly samples handling.

The performed qualitative analysis established that some of our solvents were present in the biodiesel samples in concentrations of less than 2000 ppm. Figure IV.18 displays three images of the same biodiesel run; the first one is the original chromatograph of 40 minutes. The 2nd and 3rd are a magnification between 9 and 20 minutes and a mass visualization of fragments present in the samples. This corresponds to hexane (86 m/z).

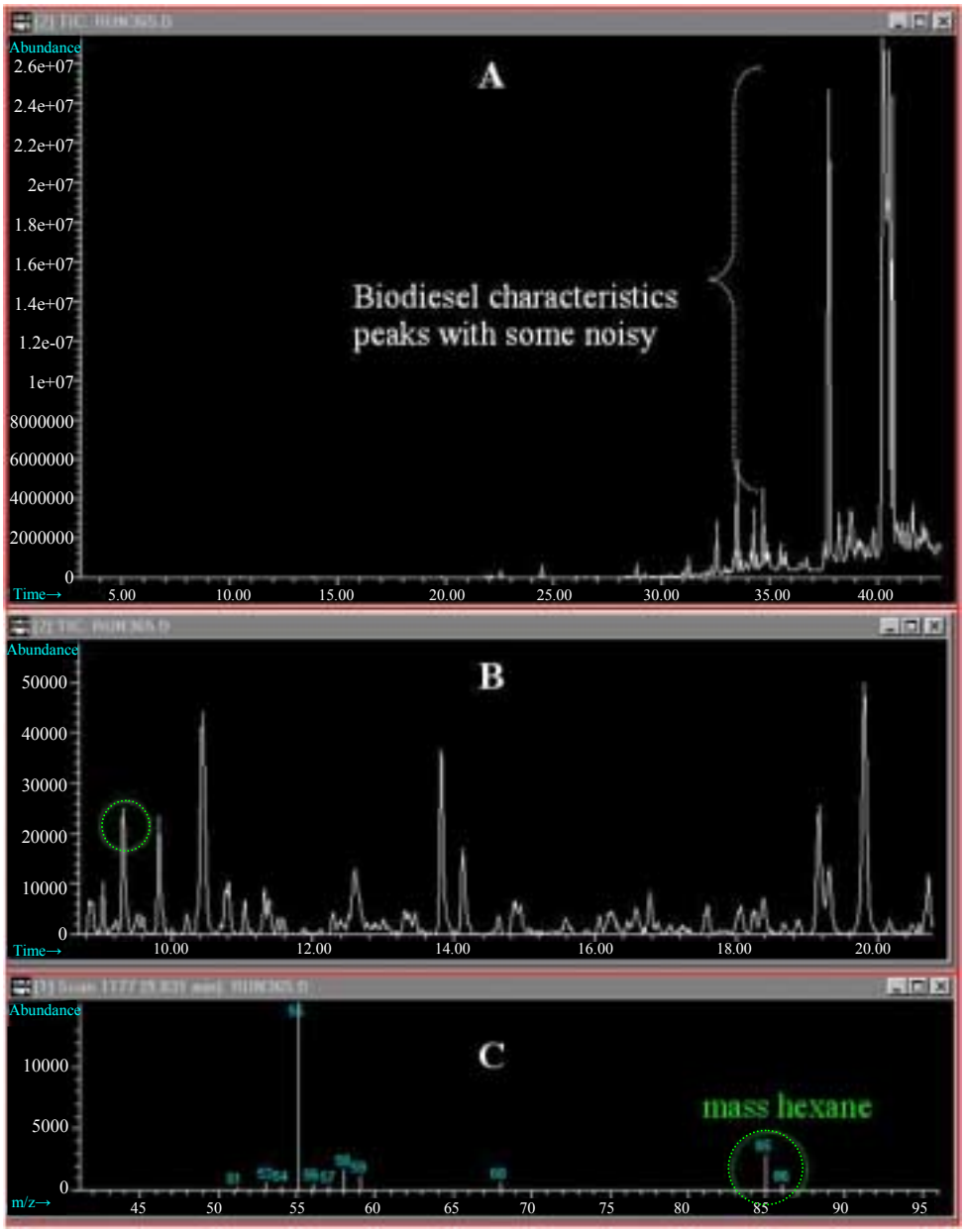

Figure IV.18 GCMS biodiesel analysis. (A) Original chromatogram (B) magnification on the original chromatogram and (C) scan on 9.831 minutes

Each of the compounds of interest (hexane, benzene, isooctane, heptane, toluene and xylene isomers) was evaluated accordingly and the results were recollected on the following table.

Table IV.15 Estimated solvents concentration in biodiesel samples

Solvents	**Concentration in ppm**						
Level	**3.1.A**	**3.2.A**	**3.3.A**	**3.4.A**	**3.1.B**	**3.2.B**	**3.3.B**
Hexane	1428	1683	358	841	57	77	355
Benzene	4382	650	253	490	222	210	20
Isooctane	1150	1541	50	665	74	54	17
Heptane	921	1540	71	221	31	108	24
Toluene	1996	3271	31	208	10	20	18
m-xylene	772	1507	15	266	n.d	14	28
o-xylene	408	788	17	88	n.d	27	20
p-xylene	2085	875	37	533	n.d	53	13

n.d = not detected

The feed condition 0.5 O_2/C (level 3.2, defined in table IV.1) presented the highest presence of heavy solvents in the liquid waste reformates. Levels 3.1.B, 3.2.B and 3.3.B where there is absence of catalysts obtained the less formation of the mentioned compounds. Apparently, the use of catalyst promotes solvents formation. 0.6 O_2/C, which was the highest yield, also shown minimal presence of these solvents.

IV.3.3 Quantitative GCMS analysis on characteristic peaks

All condensable organic samples runs recollected in biodiesel ATR were analyzed in the GCMS. Four characteristics peaks of 270, 294, 296 and 296 masses were found in all chromatograms. No other fatty acid compound formation was detected.

The fraction of each of the mentioned peaks versus the biodiesel was calculated with the relations obtained from the calibration curve (appendix B.14). Additionally, appendix G.3 contains the chromatographs of these biodiesel runs.

Table IV.16 Experimental average fatty acids composition in biodiesel samples

Level	270		294		296		298	
	Vol %	**Stdev**	**Vol %**	**Stdev**	**Vol %**	**Stdev**	**Vol %**	**Stdev**
3.1.A	*69.06*	0.0125	*35.03*	0.0017	*60.81*	0.0119	*59.56*	0.0011
3.2.A	*91.15*	0.0013	*44.76*	0.0002	*93.34*	0.0041	*78.71*	0.0026
3.3.A	*68.54*	0.0009	*36.13*	0.0008	*69.08*	0.0015	*60.79*	0.0011
3.4.A	*76.19*	0.0102	*48.37*	0.0018	*77.57*	0.0096	*63.55*	0.0012
3.1.B	*97.45*	0.0031	*59.48*	0.0053	*110.54*	0.0007	*86.35*	0.0016
3.2.B	*90.85*	0.0094	*60.24*	0.0070	*90.63*	0.0056	*80.67*	0.0008
3.3.B	*63.63*	0.0027	*42.72*	0.0044	*64.46*	0.0028	*57.32*	0.0045

Different volume percent for each peak were found. In theory they all should have the same percentages. This seems to indicate that these compounds have different reactivities. During the triplicate assay mentioned in the section IV.3.1, organic liquid samples were collected every thirty minutes by four hours to perform the accountability in the characteristics peaks. Every sample was injected in the GCMS and similarly with the biodiesel analysis as raw material, four principal peaks were detected. Formations of other compounds were no observed in the samples. To verify the abundance of every compound, mass ratios for each peak are reported in the following table.

Table IV.17 Ratios of fatty acids composition in triplicate biodiesel samples.

Characteristics peaks	270	294	296	298
Run 1	0.30	0.17	0.26	0.26
Run 2	0.29	0.18	0.29	0.24
Run 3	0.25	0.18	0.32	0.24
Stdev [Run 1- Run 3]	0.025	0.006	0.0295	0.0112

IV.4 H_2/ $CO+CO_2$ ratios

Perez R [26] presented the hydrogen to carbon monoxide and carbon dioxide ratio molar as indicators in determining the nature of the reaction pathways. These ratios are shown in table IV.18. They range from 1 to 3. Higher values slow tendencies of reforming, between 1 and 3, decomposition pathways could be occurring and values less than 1 neither of the reaction routes can be assigned.

Table IV.18 *H_2 /$CO+CO_2$* ratios at different level and temperatures studied.

T [°F] **Level**	**300**	**400**	**500**	**600**	**700**	**800**	**900**
1.1.A	0.46	0.68	1.0	1.40	1.50	1.87	----
1.2.B	0.57	0.38	0.42	0.32	1.24	1.81	----
2.1.A	----	----	----	----	0.13	0.18	0.36
2.2.A	----	----	----	----	3.18	0.14	0.15
2.3.A	----	----	----	----	0.87	0.437	0.317
2.1.B	----	----	----	----	0.11	0.17	0.36
2.2.B	----	----	----	----	0.11	0.15	0.305
2.3.B	----	----	----	----	0.22	0.14	0.23
3.1.B	----	----	----	----	----	----	0.4
3.2.B	----	----	----	----	----	----	0.27
3.3.B	----	----	----	----	----	----	0.28

Decomposition pathways could only be seen at higher temperatures (>500 °F) in methanol experiments. However in the other runs of heavy fuels such as glycerol and Biodiesel, one could not infer that reforming pathways occur. Only at the 2.2.A level (glycerol at 0.5 O2/C and 700°F) one can see a reforming tendency.

IV.5 SEM and EDS analysis

Scanning Electron Microscopy (SEM) and Energy dispersive X-ray spectroscopy (EDS) were performed on the Pt-based catalysts used in ATR experiments with biodiesel, methanol, isooctane and glycerol as fuels. At first, unused pills were analyzed to determine the initial conditions in the pellets without temperature and ATR reaction exposition. Then, the same pills were submitted to temperatures up to 2000 °F. Each experiment performed was purged for 15 minutes with nitrogen and the exposure time used was similar to our reaction experiment times. Thus, their wear should be equivalent to reforming experiments. Figure IV.19 describes the mentioned runs. The top and bottom images correspond to the original catalyst without any treatment and catalyst with temperature and nitrogen exposure effect. The magnifications selected to analyze the surfaces were from 30x up to 1000x. Each pill has approximately 5mm of diameter.

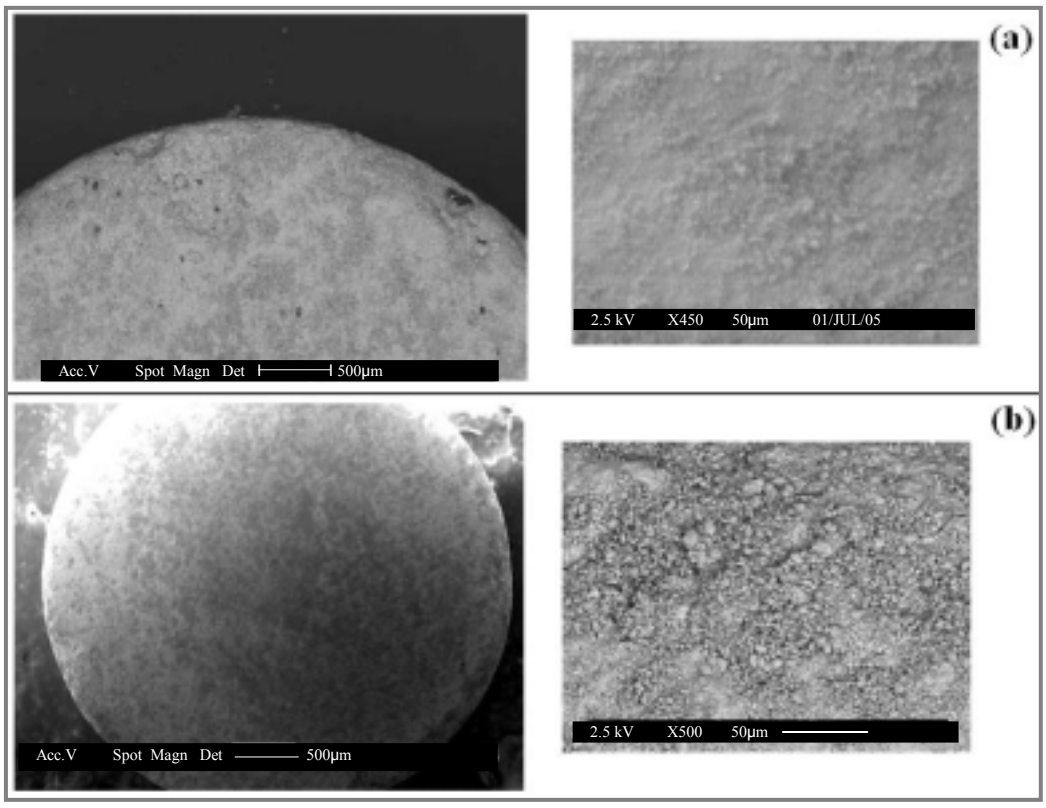

Figure IV.19 SEM of catalyst pills at 30X, 2.5 kV. (a) Original pill without any action and (b). Original pill with temperature treatment

Neither fractures nor carbon depositions were observed in the non-reforming temperature experiments. Their original yellow color remains unchanged and minimal wear down occurred. This implies that the input temperature reactor plus nitrogen purge do not generate ruptures on the Pt-based catalyst surface. Hence, their ruptures must be attributed to another reason.

On the other hand, the apparition of coke on the surface of the catalyst used in ATR experiments was notable. The surface color changed from yellow to black on all bed pills. Figure IV.20 presents an image of an initial and final catalyst. .

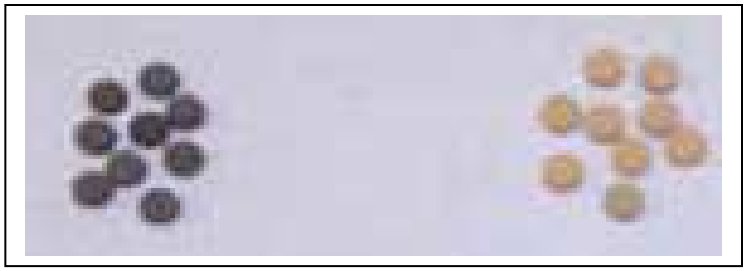

Figure IV.20 Pt-based catalyst images. Left (used catalyst) and right (new catalyst)

Additionally, fractured places were present in all bed catalysts studied. Figure IV.21 depicts a typical example of the catalyst appearance after an ATR reaction. Three different fuels were used.

Also, SEM analysis established that the intensity and depth of the fractures on the studied surfaces are related with the operational conditions sustained by each catalytic bed. The worse surface scenario corresponds to 3.5 W/C & 0.4 O_2/C ratios (where more water is added to benefit the steam reforming tendency) and 2.0 W/C & 0.5 O_2/C ratios (condition with the highest H_2 yield obtained).

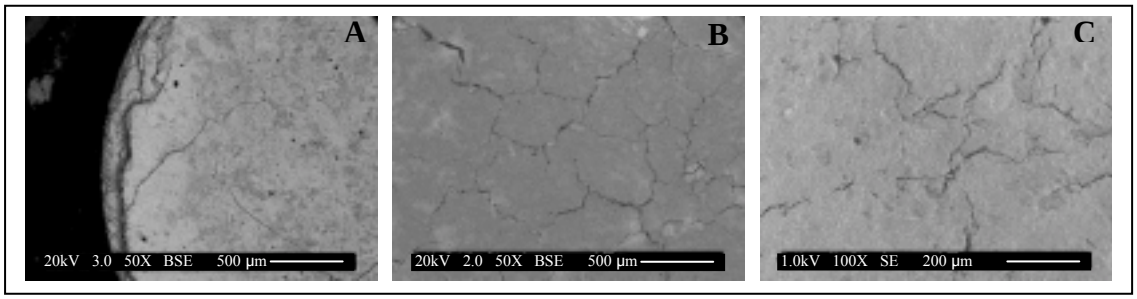

Figure IV.21 Pt-based catalyst SEM. Three bed catalytic and different fuels: (A) methanol (B) Isooctane and (C) biodiesel

SEM pictures of the catalyst used in glycerol experiments show more superfluous fractures. Figure IV.22 contains four pictures at two magnifications (50 and 503X). At 50 magnification fewer perceptible fractures are present in comparison to the behavior in other fuels as is shown in figure IV.21, where fracture places are vastly more notable at this particular magnification.

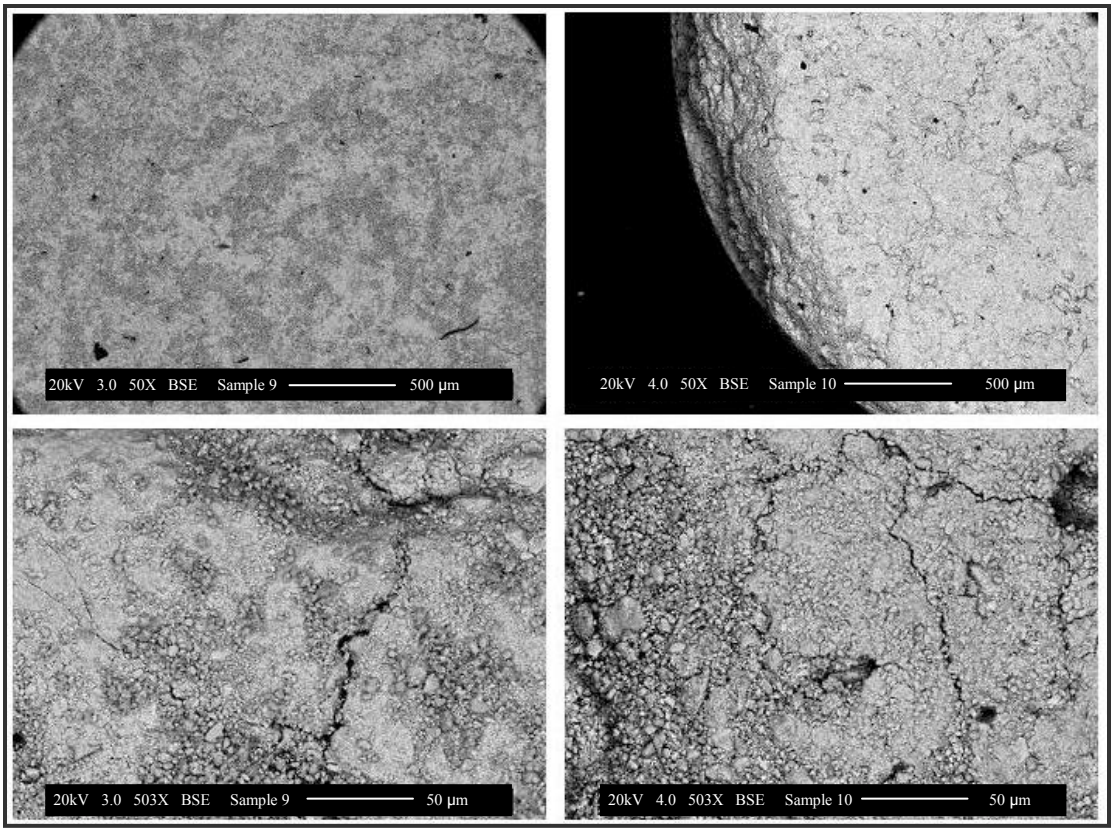

Figure IV.22 Photography of Pt-based catalyst used in glycerol ATR at two magnifications. Top (50X) and bottom (503 X)

EDS analysis was performed on all catalyst samples. Carbon, oxygen, fluoride, platinum, cesium, barium, gadolinium, platinum and nickel, among others elements, were detected in the mentioned analysis. A common EDS is represented by two axes; X and Y, which correspond to time (s) and abundance (A.U.) respectively. Figure IV.23 displays a typical EDS for unused pills with its typical compounds. A summary of various readings on the same pill are described in figure IV.24. Pill homogeneity was noted in the overlay of four EDS spectrums.

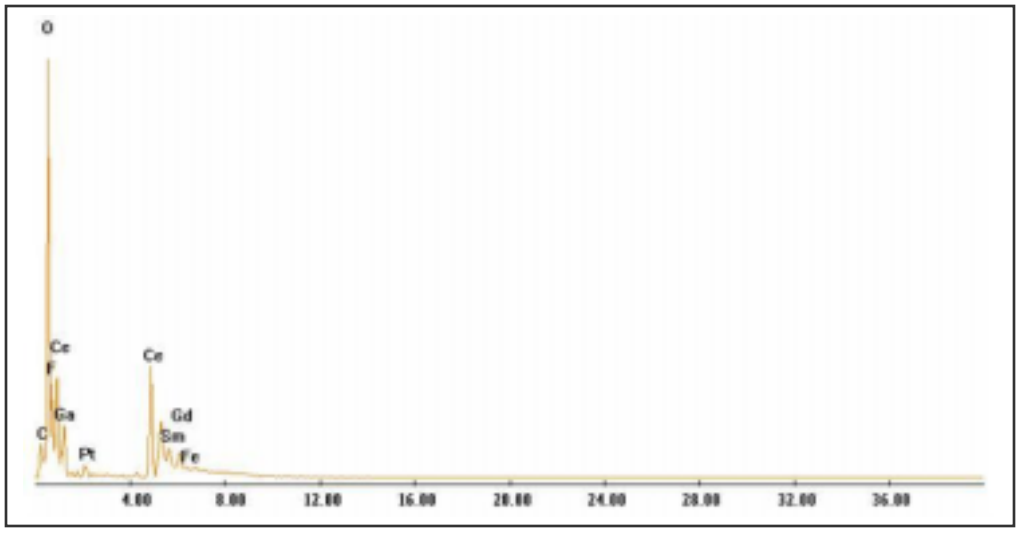

Figure IV.23 Unused pill EDS analysis. C, O, F, Ce, Pt among other compounds is present

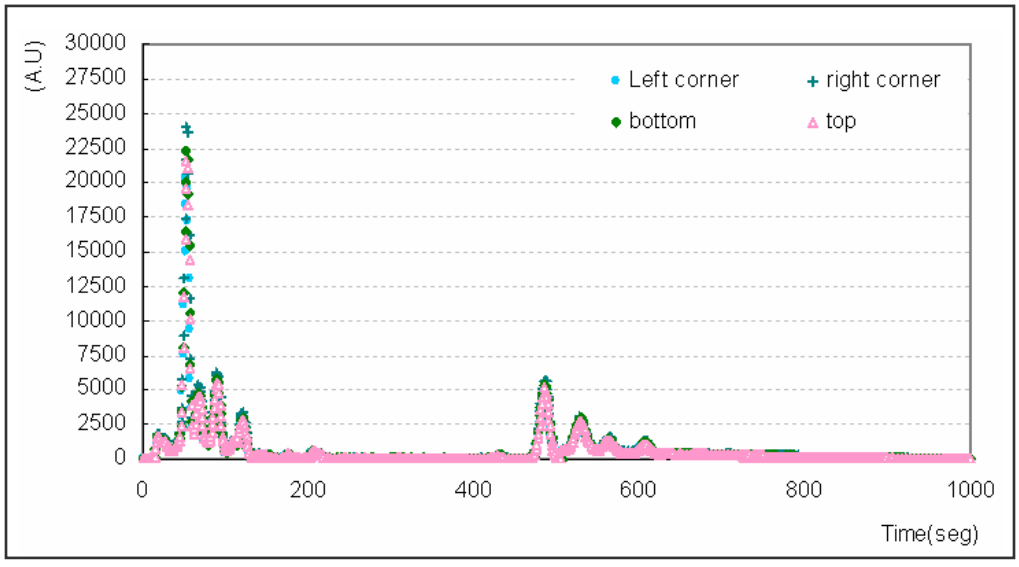

Figure IV.24 EDS Summary data on the surface of an unused catalyst

Also, superficially soot deposition was noted on all catalytic beds studied. Soft and rough areas were found in all samples. Various EDS analysis performed in the same used catalyst were compared. Heterogeneity in the carbon elemental presence and repeatability in the elemental analysis was noted. This suggests dissimilar soot deposition on the catalytic surface. Figure IV.25 contains two EDS performed on the same catalyst. Additionally, to verify the amounts in the others elements, ratios for each element of figure IV.25 were calculated. Table IV.19 shows the calculation.

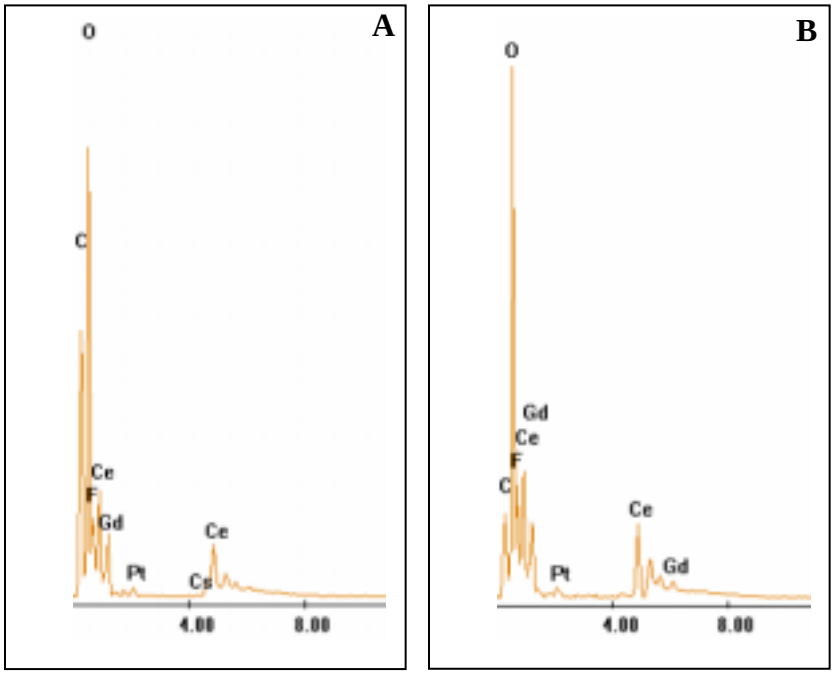

Figure IV.25 Comparison of two EDS analysis performed on the same pill. (A) Black point and (B) soft area

Table IV.19 Appearance ratios for EDS analysis on Pt-based catalyst

Ratios	C/Ce	O/Ce	F/Ce	Ce*/Ce	Gd*/Ce	Pt/Ce	Gd/Ce
A	6.67	11.32	1.70	2.15	1.18	0.17	0.27
B	1.31	10.58	1.66	1.94	1.14	0.16	0.28

* Reading of other transitions level

Moreover, deep and internal fractures were observed in almost all catalysts studied. Figure IV.26 contains an overview of the cracks present when biodiesel and isooctane

were used as fuels. The SEM magnifications were 500x and 1000x. Therefore, we could observe more contact surface in the ATR experiments performed.

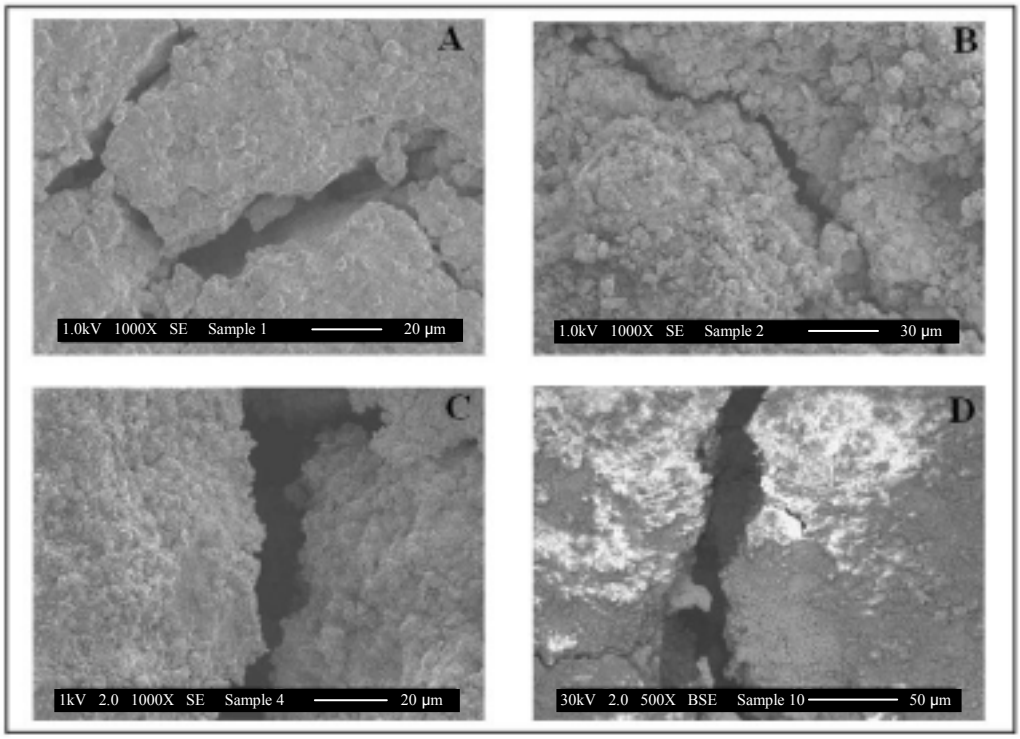

Figure IV.26 Internal and deep fractures. Replicates with biodiesel: (a) 0.4 O_2/C, (b) 0.4 O_2/C, (c) 0.5 O_2/C and (d) Isooctane*

Other SEM finding is related with the stress received by each pill in the same catalytic bed. The pills suffered different wear down. The degree of fractures was not uniform for the same conditions on a particular batch – some pills were more fractured than others-. All of this is evident in Figure IV.27.

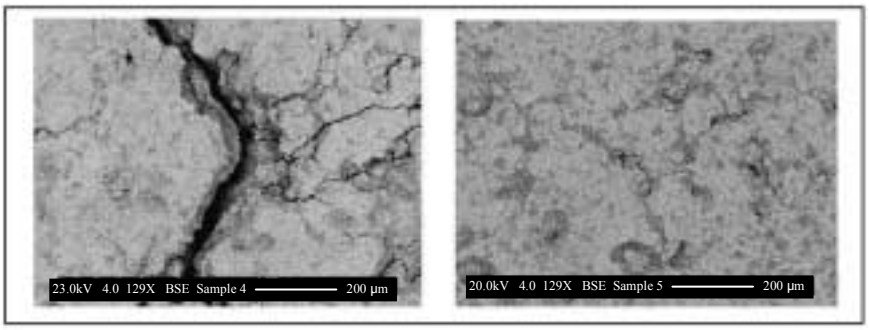

Figure IV.27 SEM of catalyst used in biodiesel ATR reactions. 0.5 O_2/C and 2.0 W/C, magnification of 129x.

CHAPTER V

Conclusions and Recommendations

V.I Conclusions

The experimental results presented here show that the reforming test bench is an operational, flexible device. Its operation appears satisfying at atmospheric pressure: wall temperatures acceptable, quick starts are realized and H_2 production takes place after only a few minutes.

The use of catalyst enhances the hydrogen production for autothermal reforming of methanol as fuel. Likewise, was established that at higher temperatures could be occurring reforming pathways in both experiments. The section IV.4 describes that in 4 of 6 temperature levels studied the predominant reforming pathways were not that obvious. Coke formation was not detected in the fittings system but, soot deposition on catalyst surface was perceived.

Hydrogen can be produced from vegetable oils (biodiesel) and glycerol by catalytic Autothermal reforming using Pt-based catalyst.

In glycerol runs without catalyst, it was observed that at 0.4 O_2/C and 0.5 O_2/C and 900 °F the highest hydrogen concentration was obtained. Experiments of glycerol ATR with one bed catalytic performed at all conditions proposed in table IV.1, resulted in discrepancies in the repeatability of 0.5 O_2/C at 700, 800 and 900°F. Thus, activation and deactivation could be occurring. Catalyst change daily was recommended for biodiesel experiments to obtain better performance. Additional catalyst triplicate experiments performed at 700°F, 2.0 W/C and 0.4 O_2/C ratios with three different beds catalytic showed system reproducibility. Coke formation was detected in all runs performed and catalyst soot deposition was noted.

Hydrogen was obtained from biodiesel at temperatures higher than 950 °F with Pt-based catalyst. Moreover, data reproducible was established and coke formation appears in the system and on the catalyst surface. Also, Rh-based catalysts did not increase

hydrogen production at the conditions studied. Heavy solvents were detected below 4500 ppm in the liquid organic waste. Also, methanol, ethanol, propanol, isopropanol and butanol were not detected in the aqueous phase of condensable products.

Additionally, the biodiesel used was characterized as a combination of four fatty acids, palmitic, linoleic, oleic and estearic. In the observed ratios were consistent with soybean and/or corn derived oils. In the analysis of organic condensable product, other compounds were not detected. Four peak in every sample analyzed were found. Additionally, the concentrations found in the mentioned peaks were different with the expected results. Thus, fatty acid may have different reactivities.

Homogeneity surface on unused and temperature attacked pill was established and carbon deposition on all catalyst pills was found. Carbon, Oxygen, Gadolinium, Platinum among others element were detected on the catalyst surface. The ATR reactions suggest fractures in catalyst pellets.

V.2 Recommendations

Future work in this area should concentrate on improving the simulation of the chemical reaction of typical ATR, SR and Ox processes, with different ratios of feed and several reaction temperatures.

Another recommendation is to perform a detailed surfaces catalyst analysis to better understand coking phenomena with daily monitoring that could be help to define the transformations of fuel to carbon deposition and its pathways.

It is also recommended to design and implement an automatic sampling system especially for the gases analysis. Additionally, improvements in the handling and the usage of the PFR system ought to be elaborated.

In order to improve the mass balance in the ATR experiments, additional analytical techniques must be used such as Total Organic Carbon (TOC) for liquid aqueous condensable, in situ laser scattering absorption for carbon formation monitoring and thermal gravimetric analysis (TGA) for detailed coke quantification.

APPENDIX

APPENDIX A: Reactor Temperature Control

A.1 Basket Stirred Tank Reactor (BSTR)

The temperature control of the BSTR was performed with the procedure developed by *Perez R.*[26]. Variations of 10°F were observed.

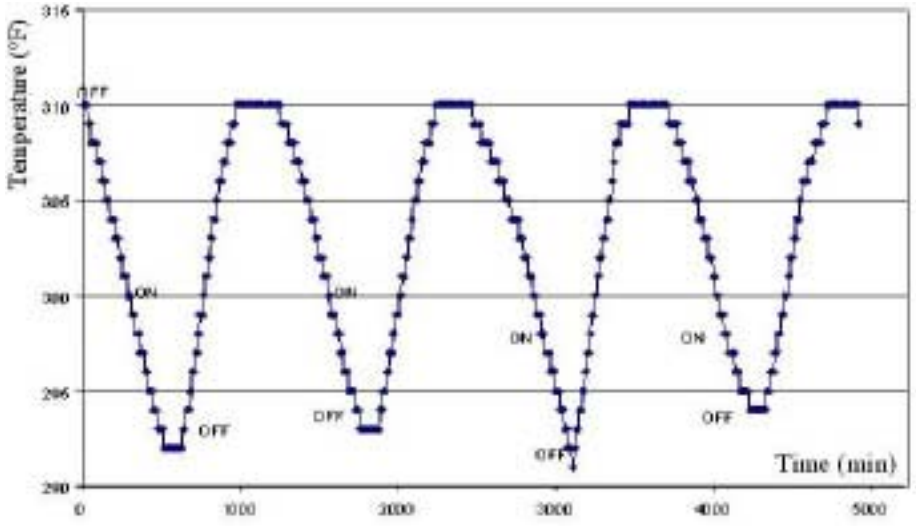

Figure A.1.1 Reactor Temperature Control Profile at 300 °F [26]

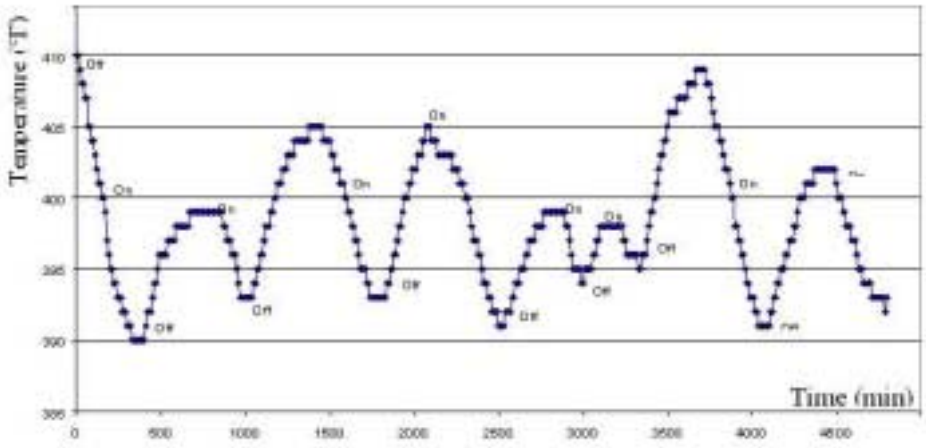

Figure A.1.2 Reactor Temperature Control Profile at 400 °F [26]

A.2. Plug Flow Reactor (PFR)

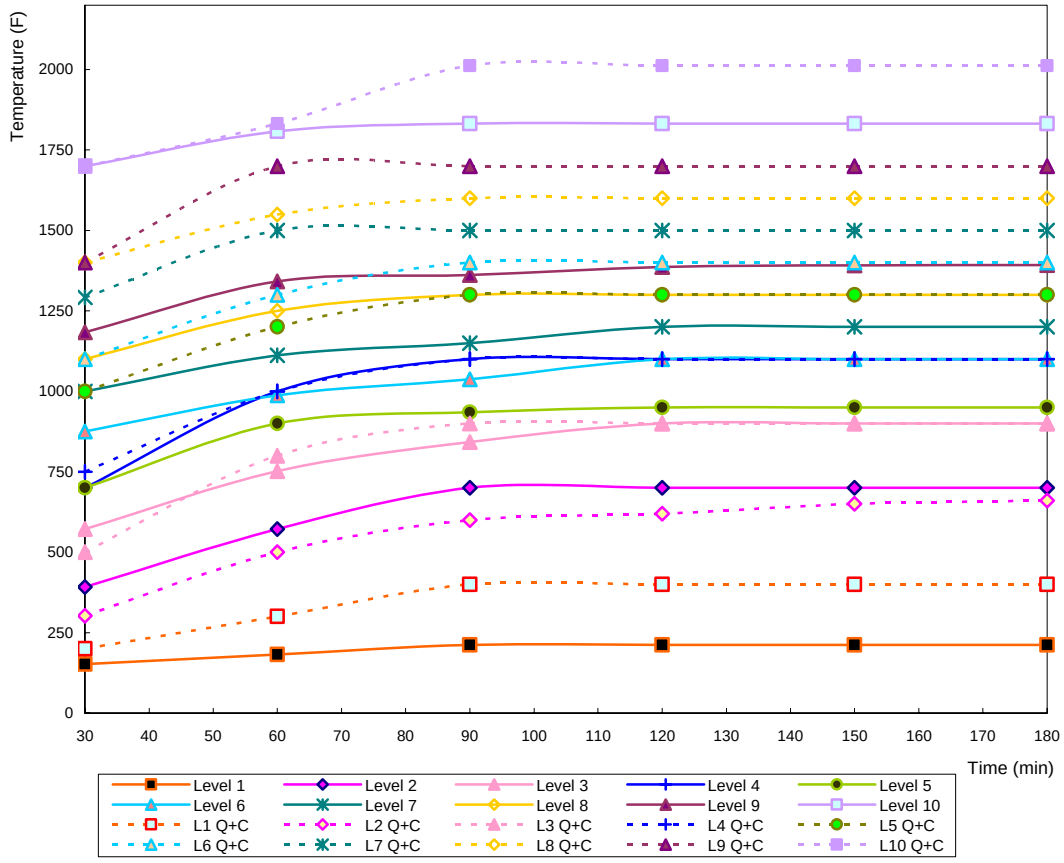

Figure A.2.1 Characterization of Oven with Quartz tube [Nomenclature: L=Level (1 to 10), Q=quartz and C=Catalyst

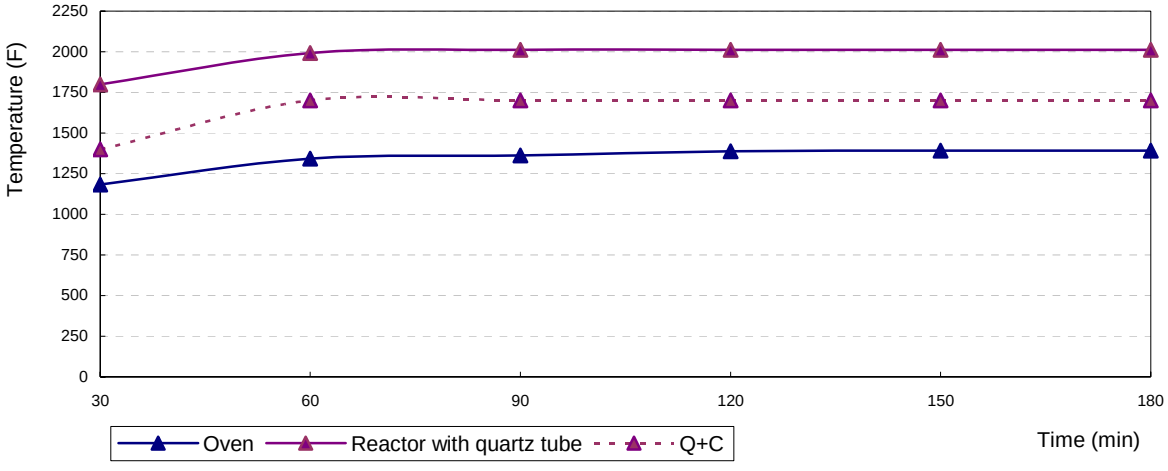

Figure A.2.2 Characterization of Oven, Quartz tube and Pt-based catalyst at IX level.

APPENDIX B: Calibration Plots

B.1. Calibration plots for GC-TCD analysis

The initial calibration plots were obtained from results of Perez [26]. Ongoing recalibration curves of H_2, O_2, CH_4 and CO were performed. The graphs were constructed at ten different levels; starting with 0.1 mL until 1.0 mL with increments of 0.10 mL in each level. The gases used have a purity of almost 99%. The TCD detected the pure gas at a certain retention time which was integrated by the HP 3396 Series II Integrator. The integration value was plotted versus its volume percent (i.e.,(0.50mL/1.0 mL)x 100). Each point in the curves represented an average of five injections. Furthermore, table B.1 show the typical retention times observed in the chromatographic system.

Table B.1. Compound gases and their range retention time

Compound	Range retention time
Hydrogen	0.5 – 0.6
Oxygen	0.8-0.9
Methane	1.4-1.9
Carbon monoxide	2.0 - 2.3
Carbon Dioxide	14.0 – 15.0

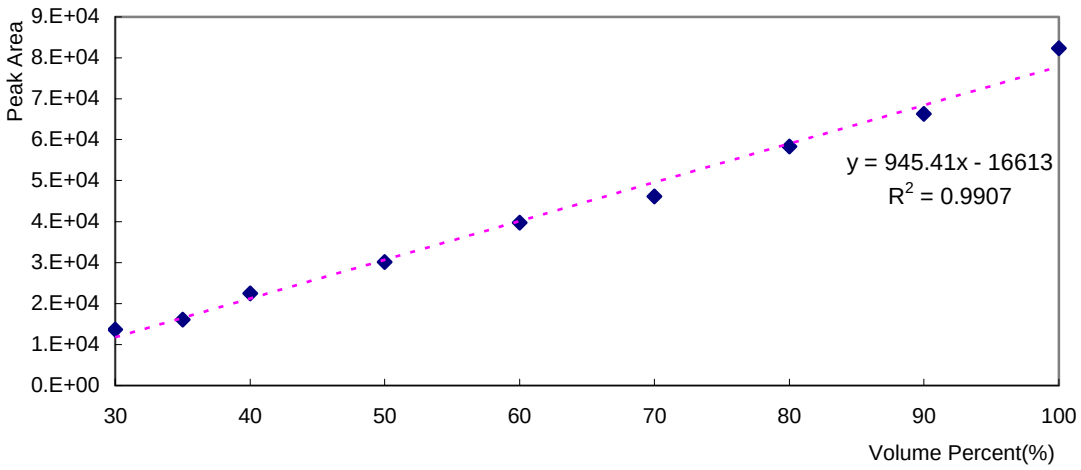

Figure B.1 Hydrogen calibration – High concentrations

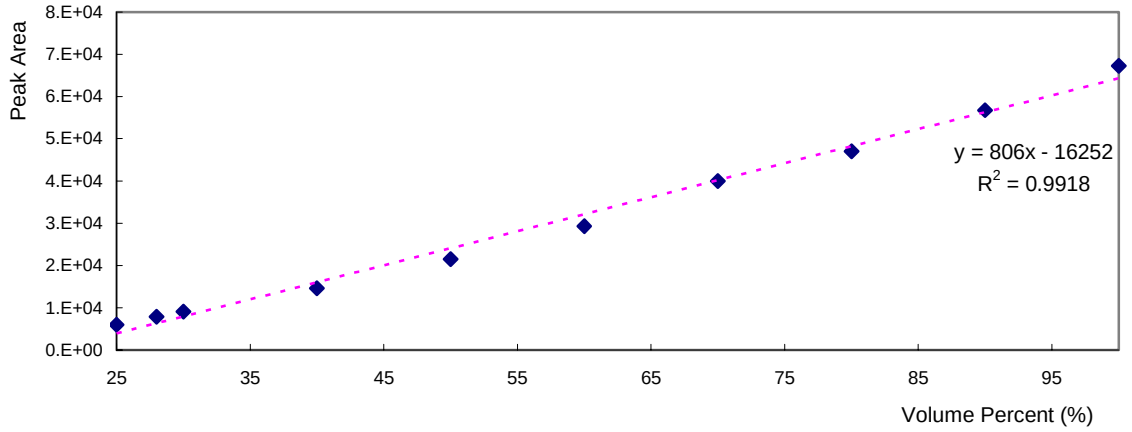

Figure B.2 Hydrogen calibration – High concentrations [26]

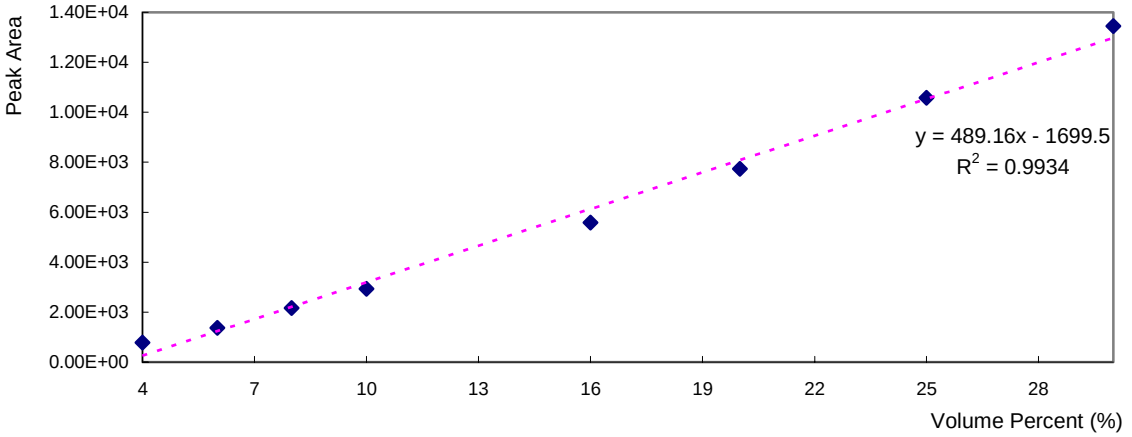

Figure B.3 Hydrogen calibration –Low concentrations.

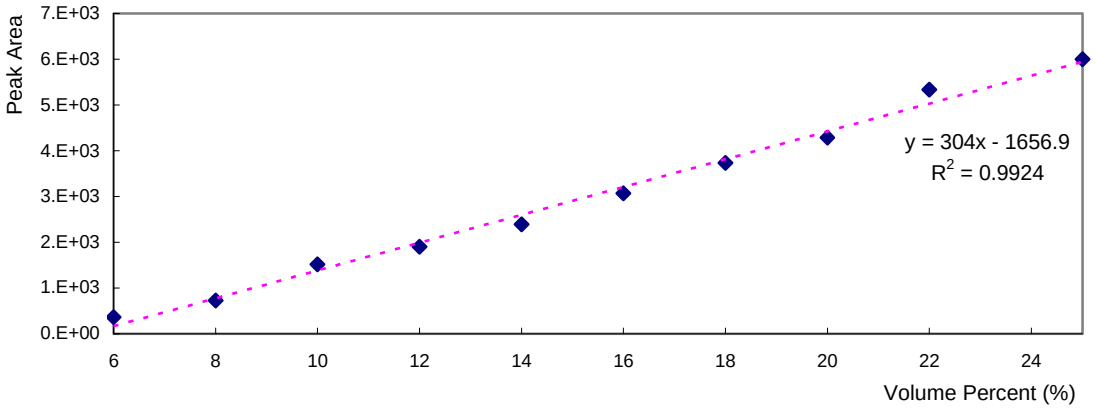

Figure B.4 Hydrogen calibration –Low concentrations [26]

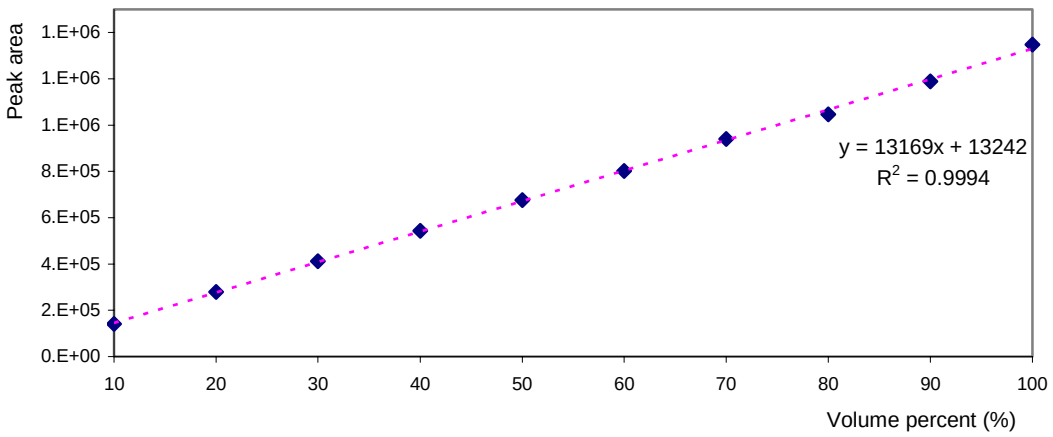

Figure B.5 Methane Calibration Curve

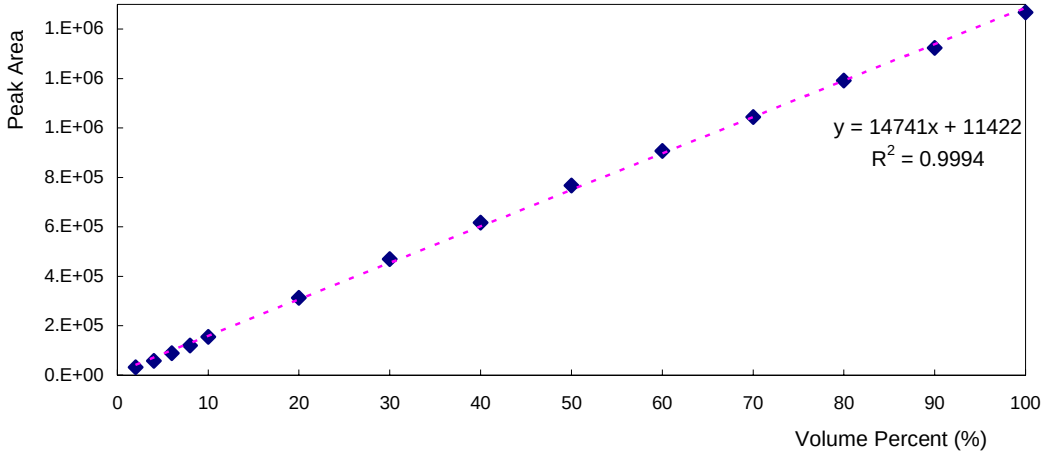

Figure B.6 Methane Calibration Curve [26]

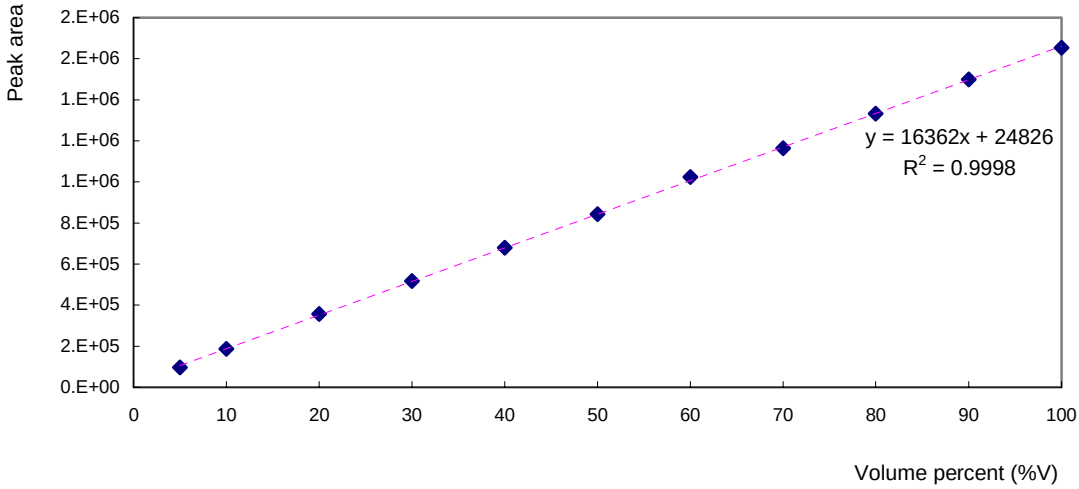

Figure B.7 Oxygen Calibration Curve

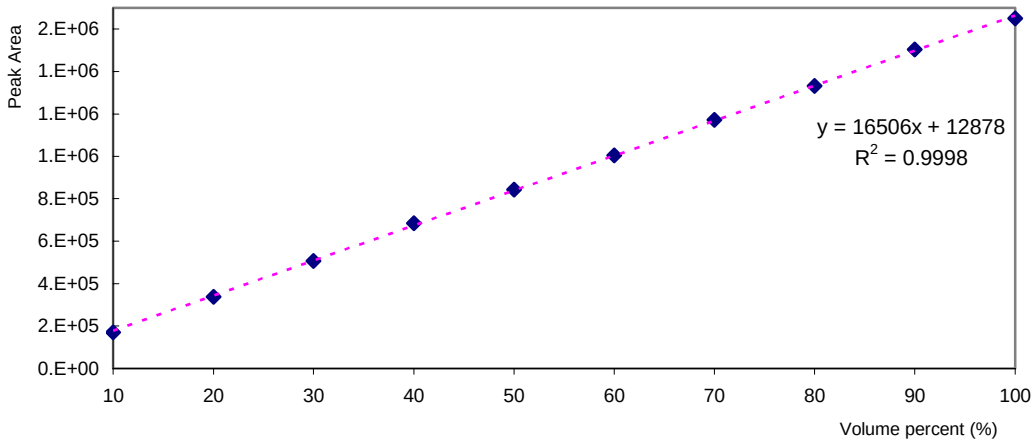

Figure B.8 Oxygen Calibration Curve [26]

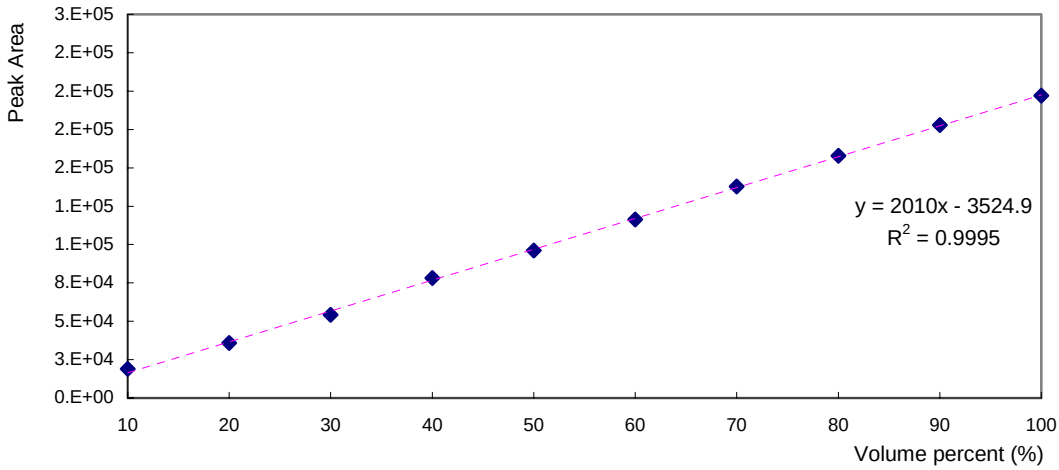

Figure B.9 Carbon monoxide Calibration Curve

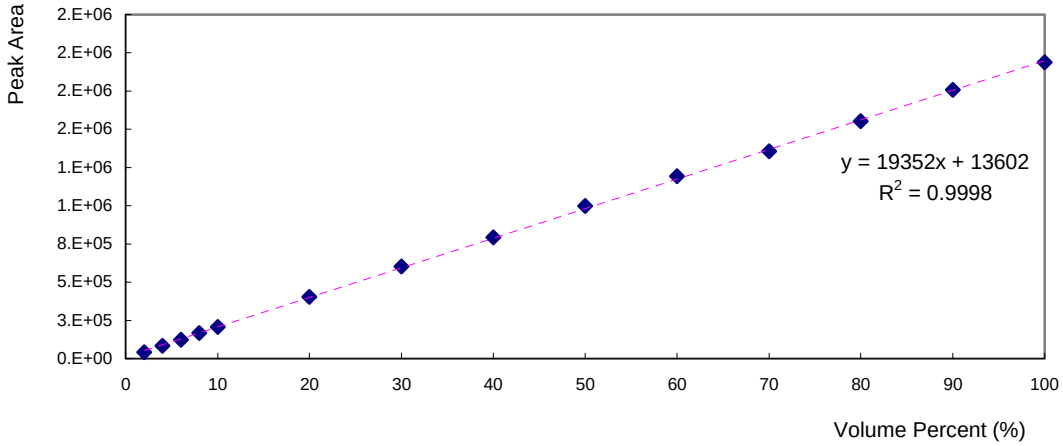

Figure B.10 Carbon monoxide calibration curve [26]

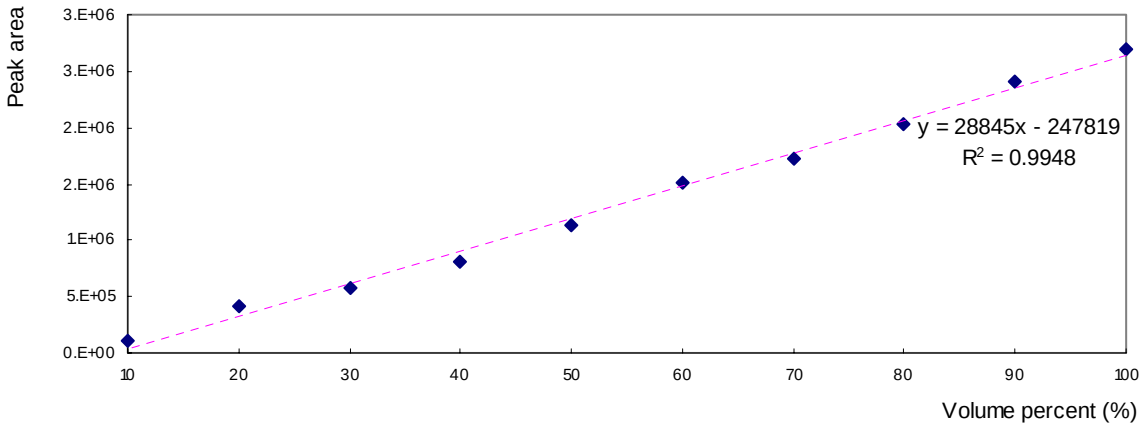

Figure B.11 Carbon dioxide Calibration Curve

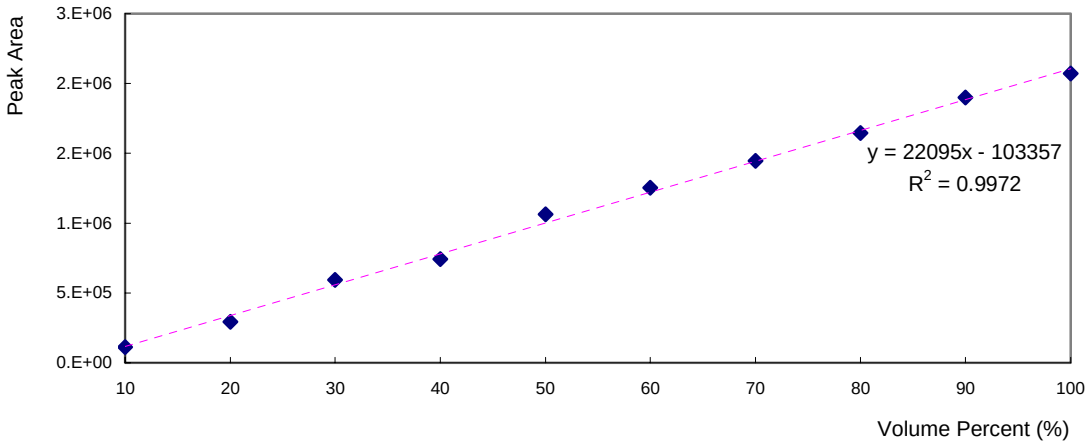

Figure B.12 Carbon dioxide Calibration Curve [26]

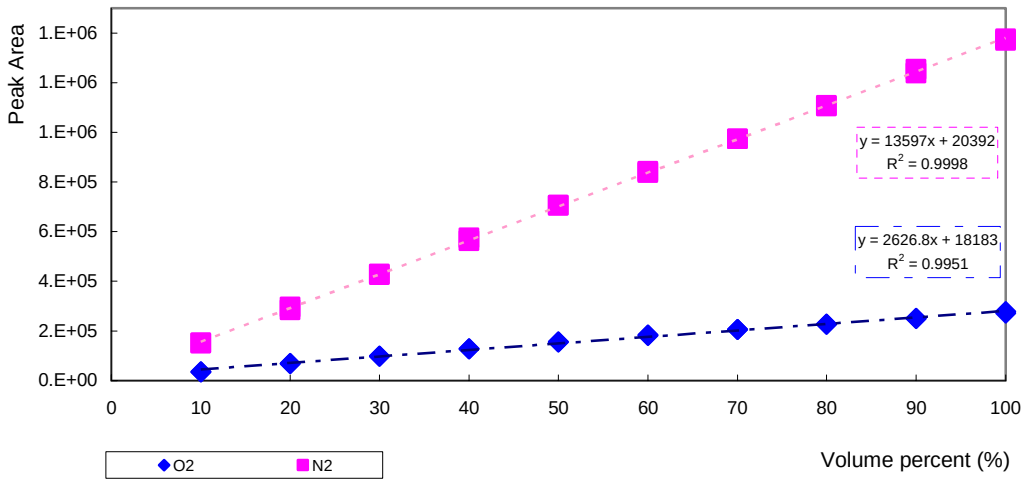

Figure B.13 Air Calibration Curve (O_2/ N_2 Separation)

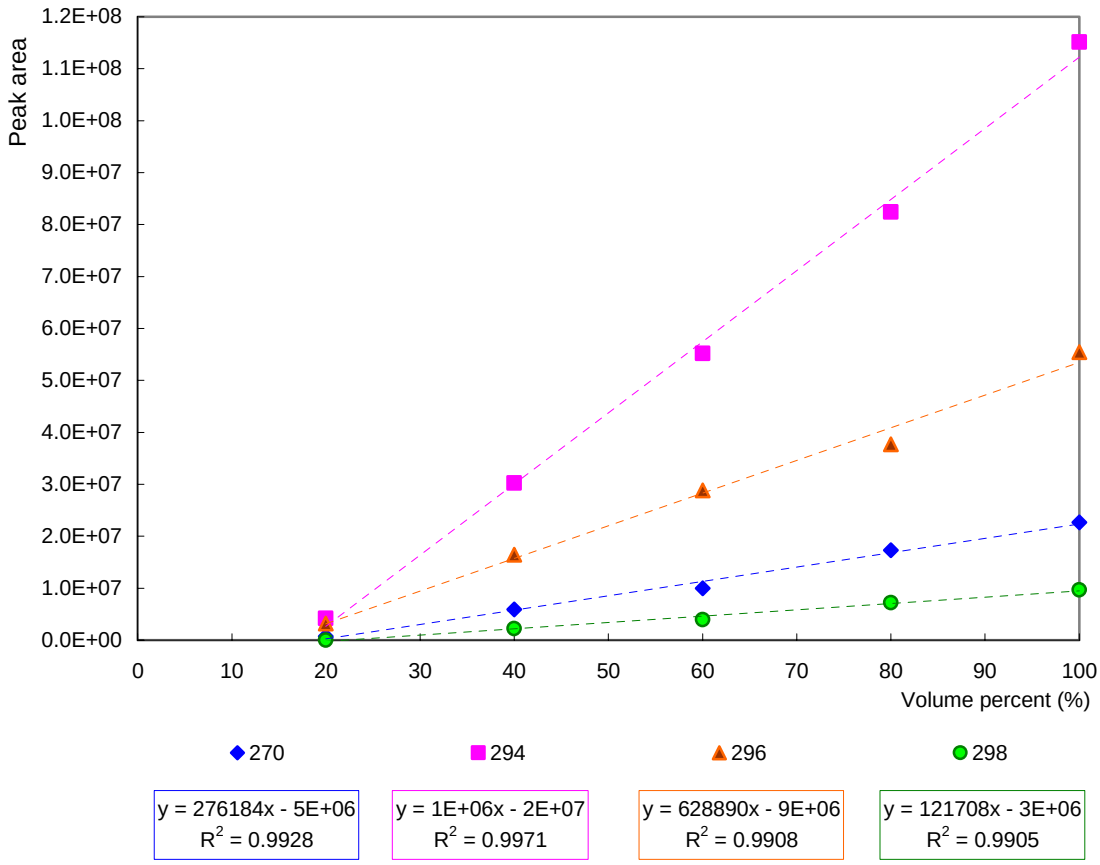

Figure B.14 Pure Biodiesel dissolved in THF

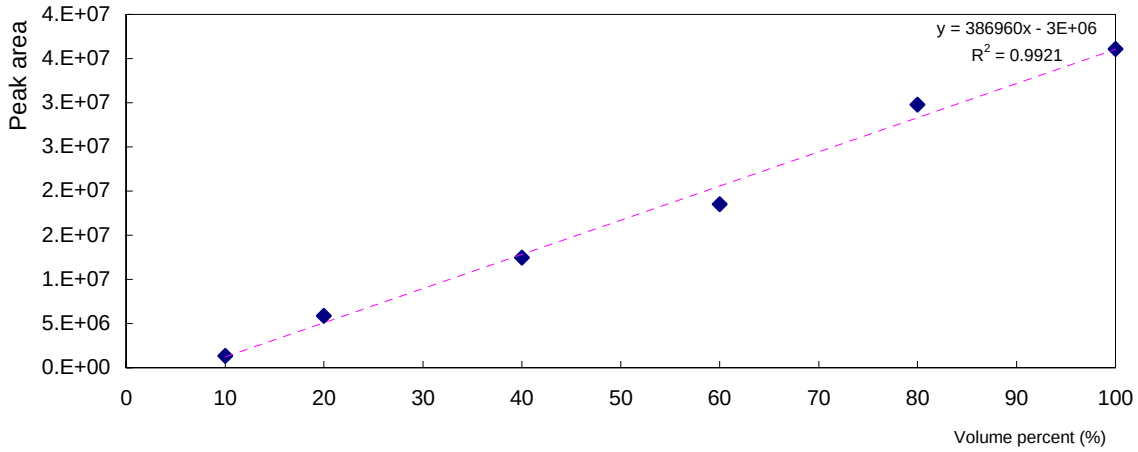

Figure B.15 Pure Hexane injected in the GCMS

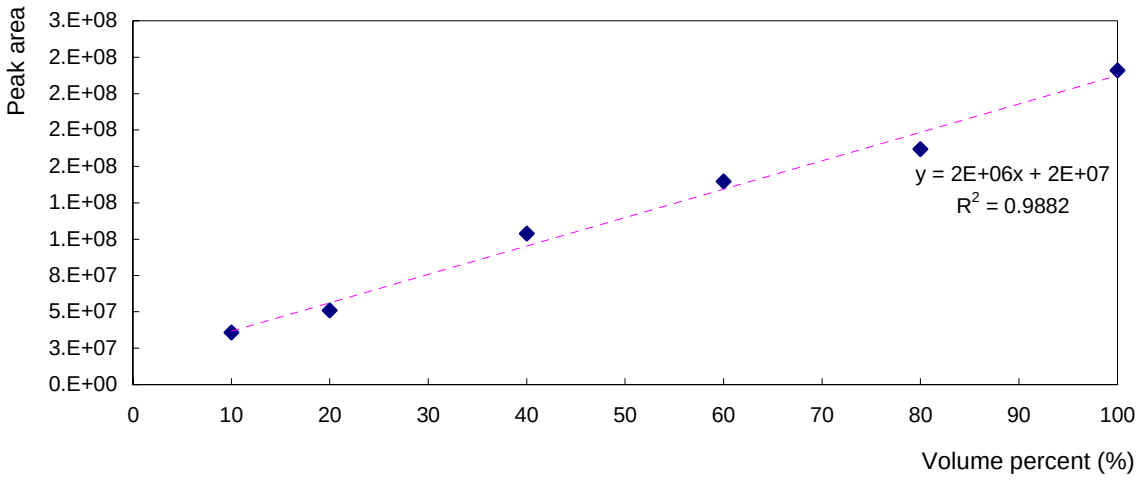

Figure B.16 THF pure injected in the GCMS

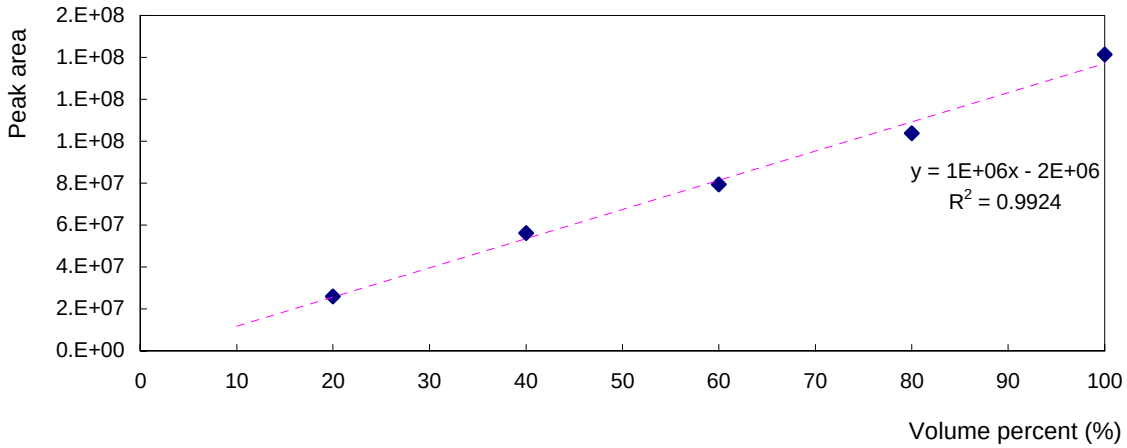

Figure B.17 Pure Benzene injected in the GCMS

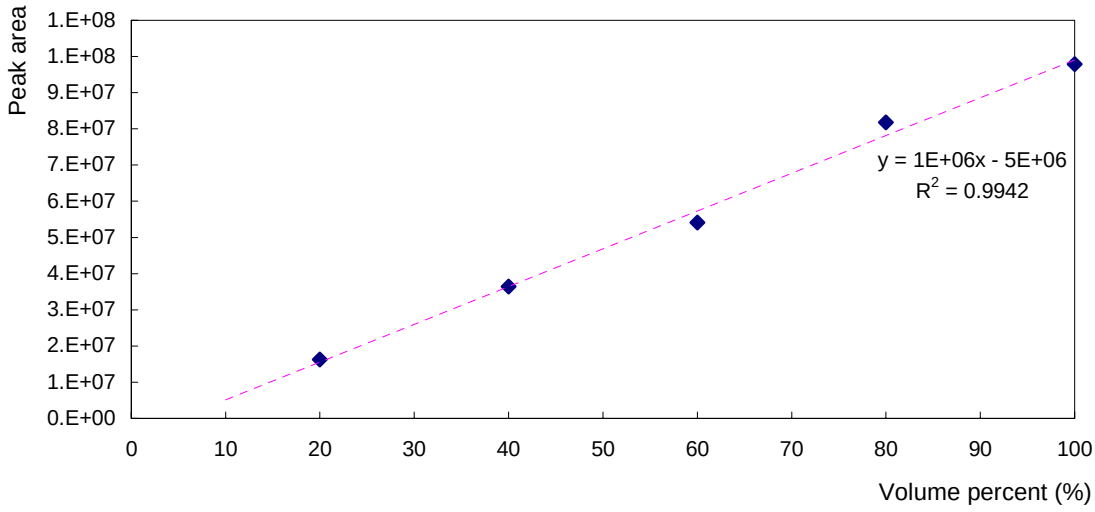

Figure B.18 Pure Isooctane injected in the GCMS

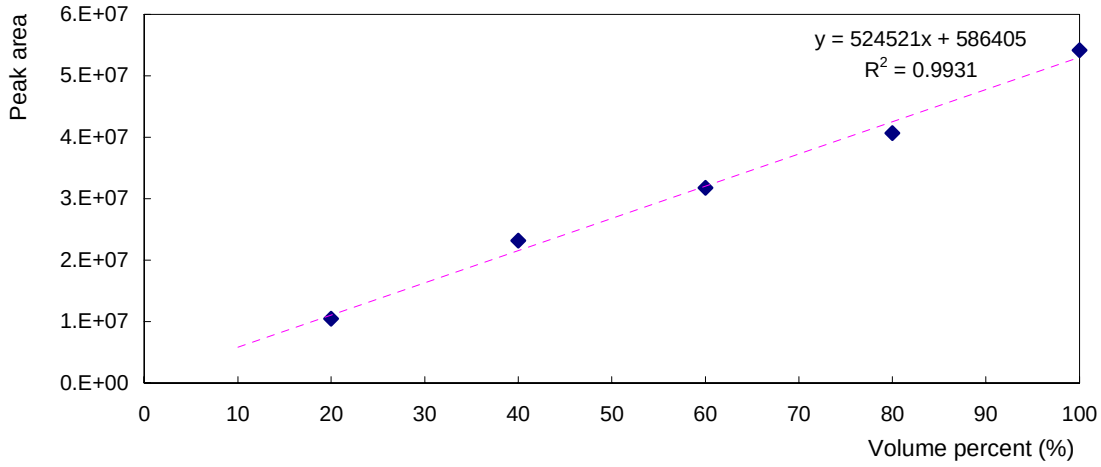

Figure B.19 Pure Heptane injected in the GCMS

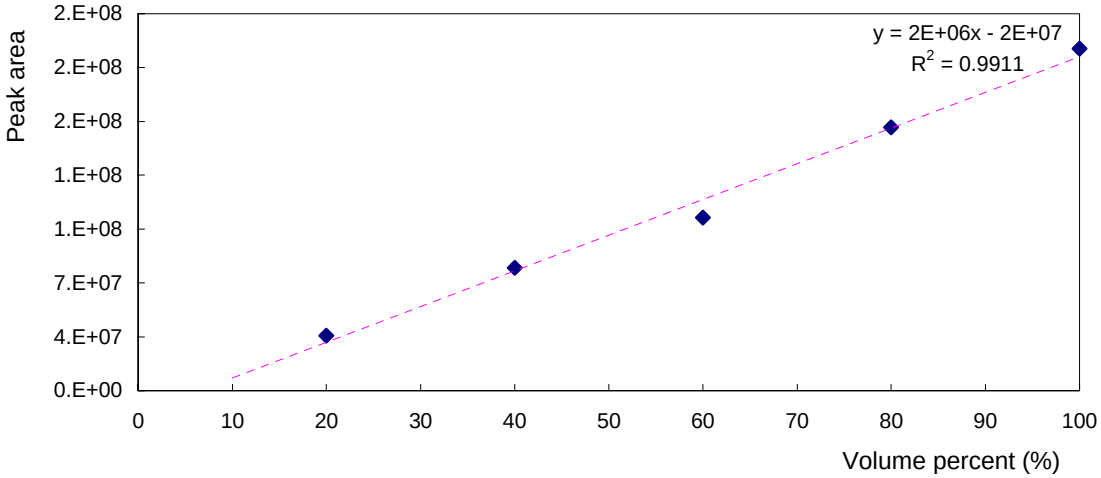

Figure B.20 Pure Toluene injected in the GCMS

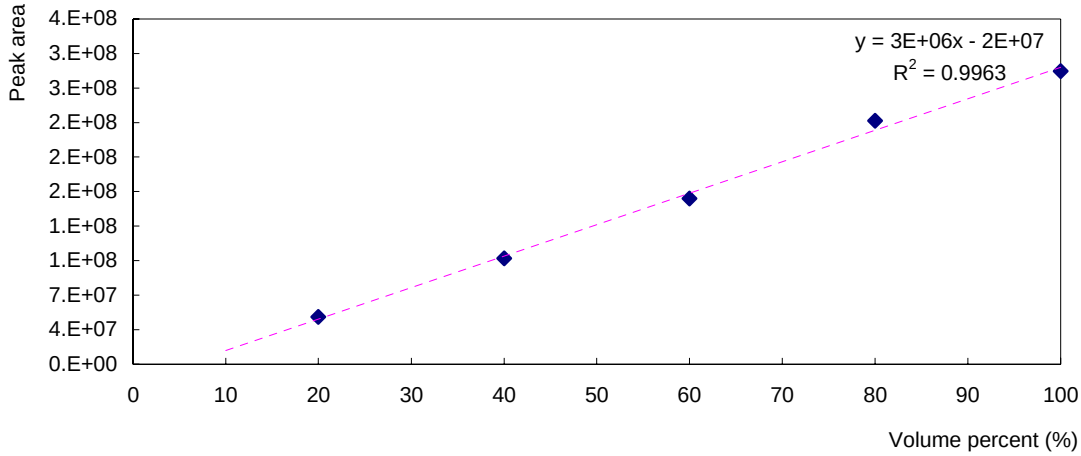

Figure B.21 Pure p-xylene injected in the GCMS

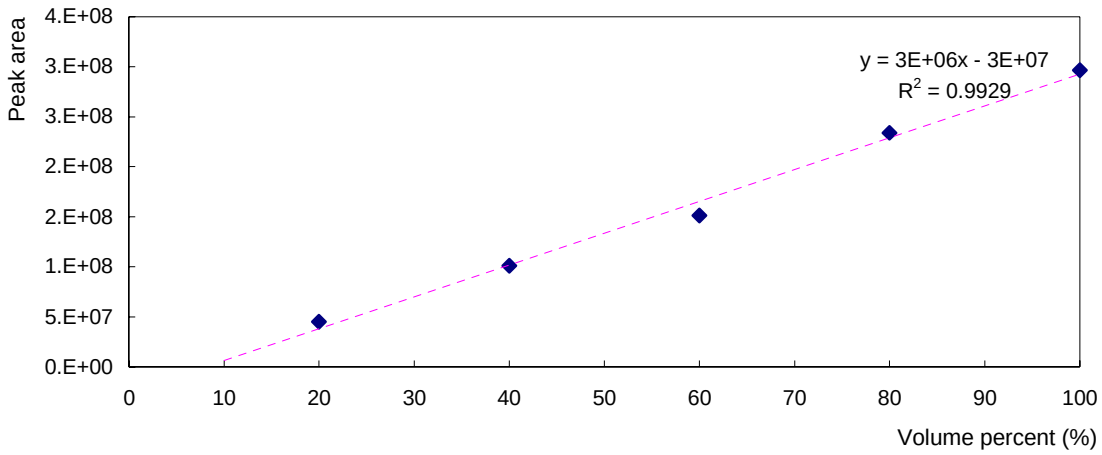

Figure B.22 Pure m-xylene injected in the GCMS

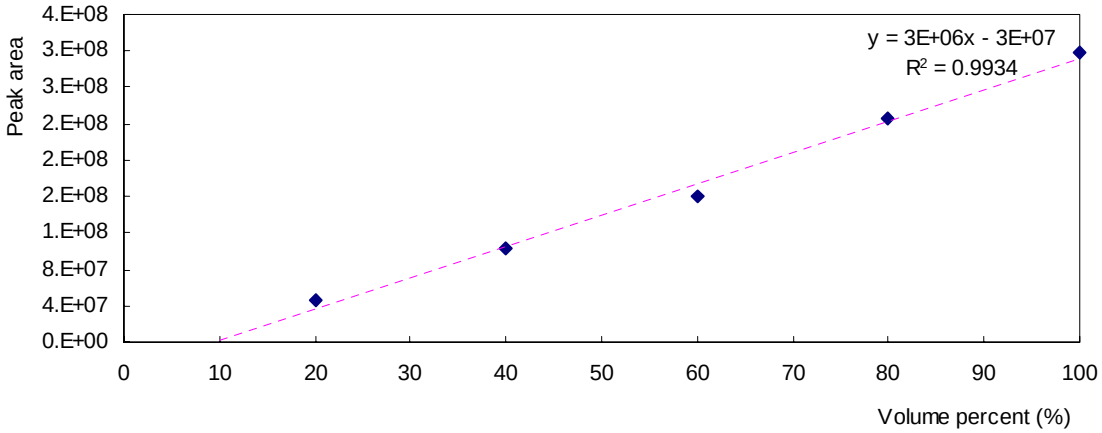

Figure B.23 o-xylene pure injected in the GCMS

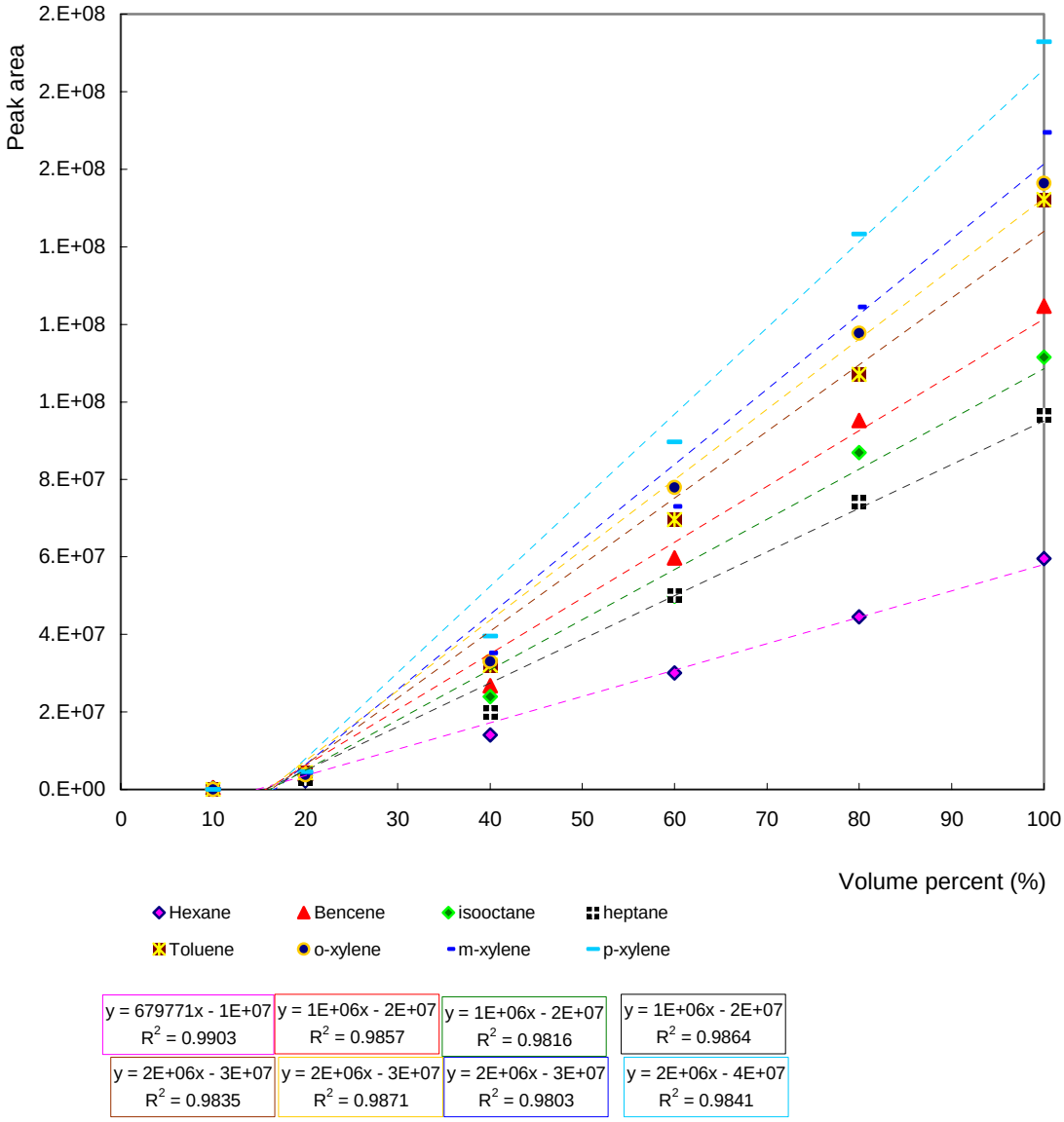

Figure B.24. Pure solvents dissolved in THF

APPENDIX C: Gaseous Hydrogen supply options

C.1.Near term supplies, centralized reforming [30]

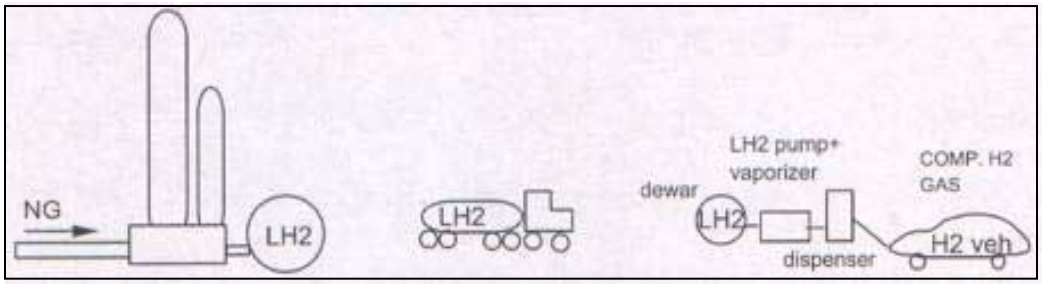

Figure C.1.1 Truck delivery

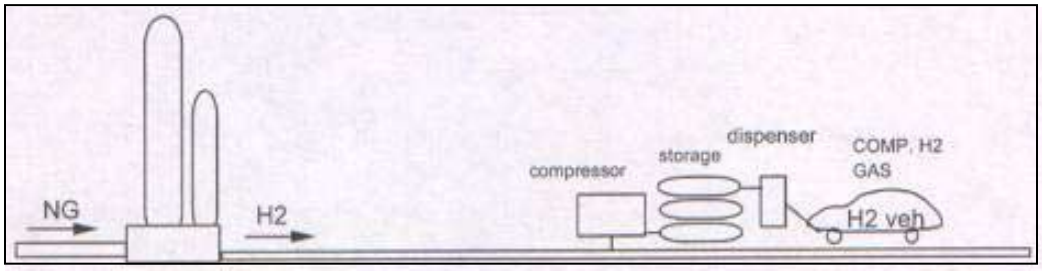

Figure C.1.2 Pipeline delivery

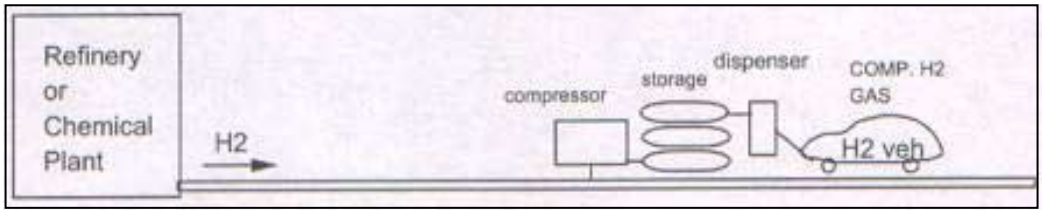

Figure C.1.3 Chemical by-product hydrogen

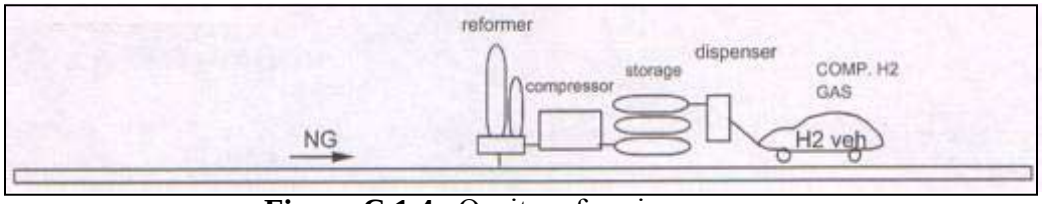

Figure C.1.4 Onsite reforming

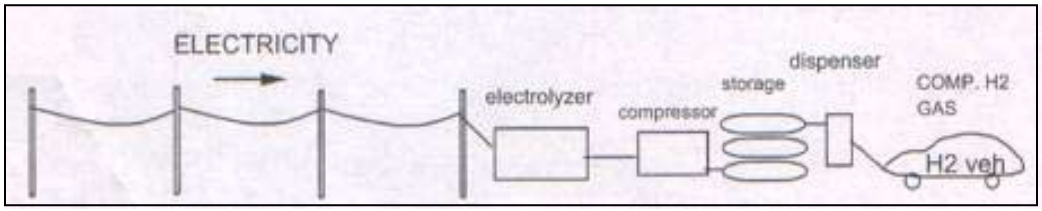

Figure C.1.5 Onsite electrolysis

C.2 Long term supplies

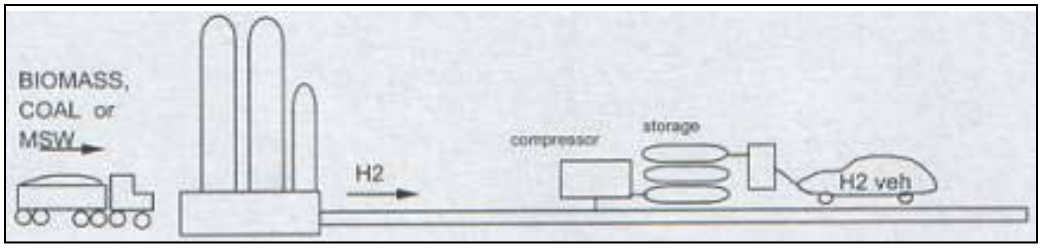

Figure C.2.1 H_2 via biomass, coal or MSW gasification

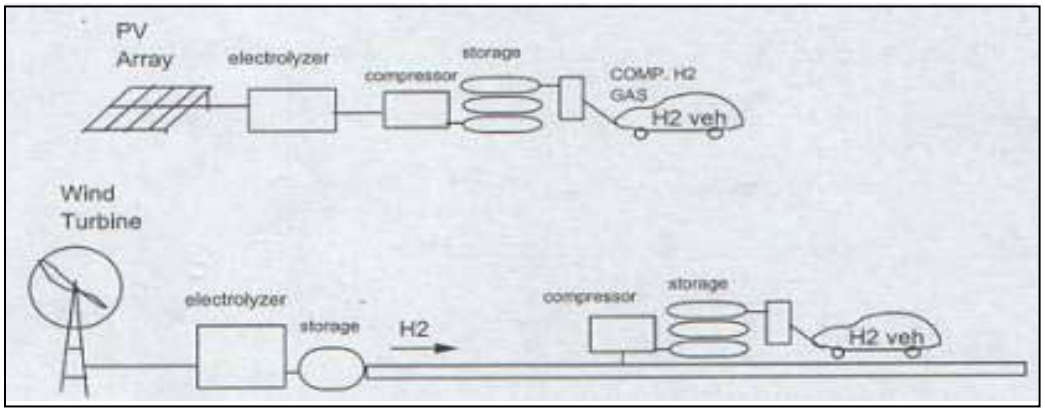

Figure C.2.2 Solar or wind electrolytic hydrogen

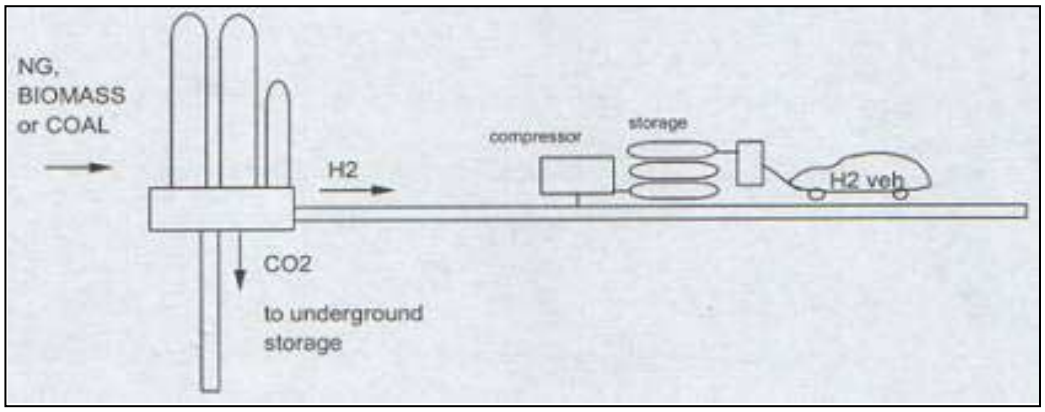

Figure C.2.3 H_2 from hydrocarbons with CO_2 sequestration

APPENDIX D: H_2O/C and O_2/C ratios calculation

E.1. Examples of Biodiesel and glycerol calculations for water, fuel and oxygen flows are presented below respectively.

- **Water**:

$$1.8\,\frac{\text{mL}\,H_2O}{\text{min}} \times \frac{1\,\text{g}\,H_2O}{1\,\text{mL}\,H_2O} \times \frac{1\,\text{mol}\,H_2O}{18\,\text{g}\,H_2O} \cong 0.1\,\text{mol}\,H_2O$$

- **Oxygen:**

$$n \equiv \frac{PV}{RT} \quad \rightarrow \quad \frac{1.0\,\text{atm} \times 298\text{cm}^3 \big/ \text{min}}{303°\text{K} \times 82.06} \cong 1.1985\text{x}10^{-2}\ \text{mol}\,O_2$$

- **Fuel (Biodiesel):**

$$0.5\frac{\text{mLBIO}}{\text{min}} \times \frac{0.878\,\text{g BIO}}{1\,\text{mL BIO}} \times \frac{1\,\text{mol BIO}}{298\,\text{g BIO}} \times \frac{19\,\text{mol C}}{1\,\text{mol BIO}} \cong 2.8179x10^{-2}\,\text{mol C}$$

Then, the water to carbon ratio and oxygen to carbon ratio could be calculated:

$$\therefore \quad \frac{0.1\text{mol}\,H_2O}{2.8179x10^{-2}\ \text{mol C}} \cong 3.5\,\text{mol}\,\frac{H_2O}{C} \quad \& \quad \frac{1.1985x10^{-2}\,\text{mol}\,O_2}{2.8179x10^{-2}\ \text{mol C}} \cong 0.4\,\text{mol}\,\frac{O_2}{C}$$

APPENDIX E: Biodiesel characterization

Biodiesel was identified by the GC-MS library with a 97% certainty as methyl ester, specifically methyl palmitate (see appendix G). Additionally, in the same analysis, biodiesel was defined as the combination of four characteristic peaks that appear qualitatively in the following order: 270, 294, 296 and 298 mass.

Figure IV.16 displays a typical spectrum of biodiesel, which shows five peaks, the first one corresponded to our control and solvent sample (tetrahydrofurane or THF) and the others are the four mentioned peaks. Also, examples of each peak and appearance order with its retention time and mass observed in every biodiesel chromatogram are shown in appendix G.

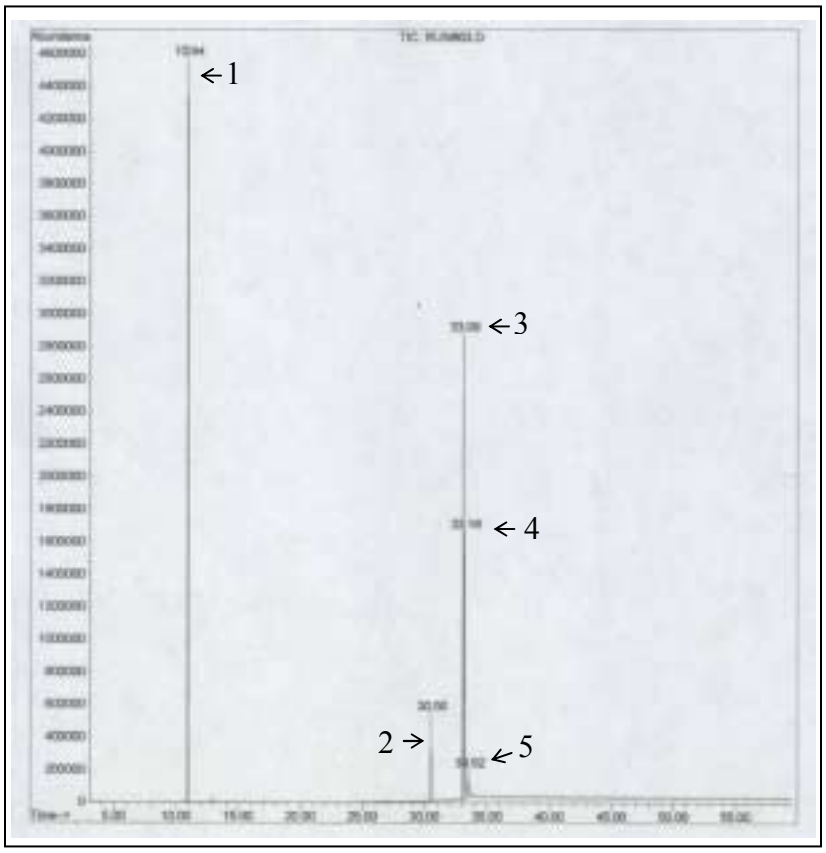

Figure E.1 Biodiesel typical spectrums. (1) THF, (2) 270mass, (3) 294mass, (4) 296mass and (5) 298mass

Analyzing each chromatogram it was determined that the biodiesel used was a combination of unsaturated and saturated fatty acids. Those four peaks are: palmitic (270), linoleic (294), oleic (296) and estearic (298). The peak abundances results in the biodiesel calibration curves makes it possible to define the fatty acid origin of our biodiesel. Table IV.7 contains the average percentages calculated for each mass. According with the literature research, the fatty origin of the biodiesel used in these experiments was either soy or corn vegetable oils (see table H.2).

Table E.1 Experimental approximate average composition in fatty acids of triglyceride in vegetable oils (%)

Ion mass	Fatty acids	Average composition (%)
270	16:0	11.11
294	18:0	3.70
296	18:1	31.48
298	18:2	53.70

A qualitative analysis was performed and helped establish the following equations relating volumetric percent with area under the peak in the chromatogram (see figure B.14):

Palmitic: $Y = 276184x - 5E+06$ (J.1)

Linoleic: $Y= 1E+06x - 2E+07$ (J.2)

Oleic: $Y= 628890x - 9E+06$ (J.3)

Estearic: $Y=121708x - 3E+06$ (J.4)

APPENDIX F: Typical GC-TCD Chromatograms

F.1. GC-TCD chromatograms for hydrogen identification using methanol as fuel.

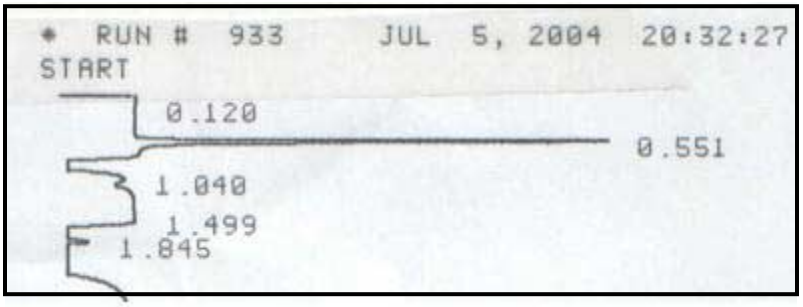

Figure F.1.1 Hydrogen chromatograph at O_2/C=0.39; H_2O/C=0.76 and 800°F

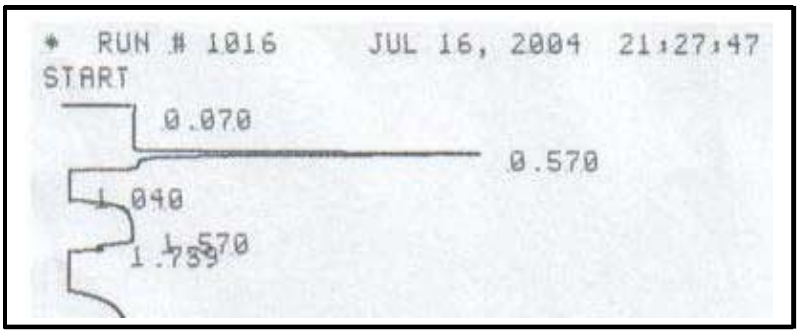

Figure F.1.2 Hydrogen chromatograph at O_2/C=0.39; H_2O/C=0.76; 700°F

F.2. GC-TCD chromatograms for oxygen, nitrogen, methane, monoxide and dioxide carbon

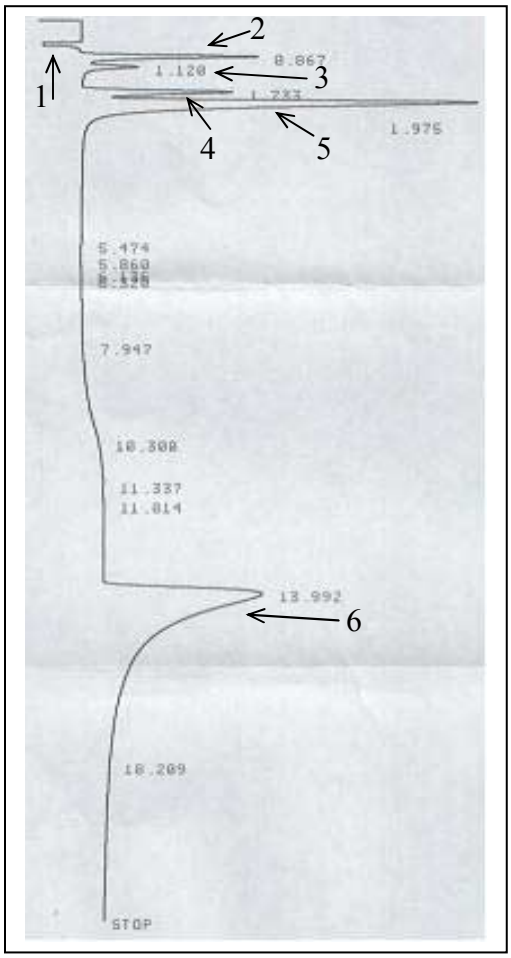

Figure F.2.1. O_2, CO and CO_2 chromatograph at O_2/C = 0.39, H_2O/C = 0.76 and 800°F. (1) Hydrogen, (2) Oxygen, (3) Nitrogen, (4) Methane, (5) Carbon monoxide and (6) Carbon dioxide

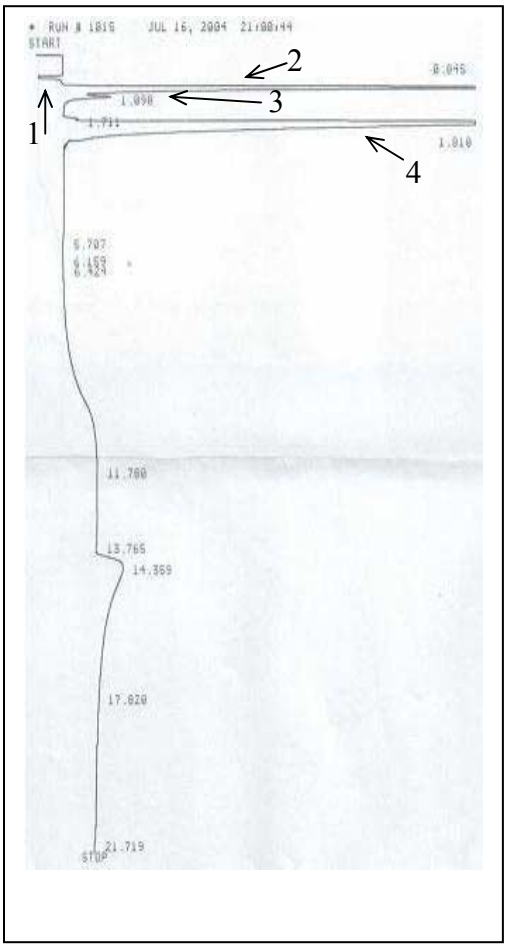

Figure F.2.2. O_2, CO and CO_2 chromatograph at O_2/C=0.39, H_2O/C = 0.76 and 700°F. (1) Hydrogen, (2) Oxygen, (3) Nitrogen, (4) Carbon monoxide

APPENDIX G: Typical GC-MS Chromatograms

G.1 Biodiesel Identifications

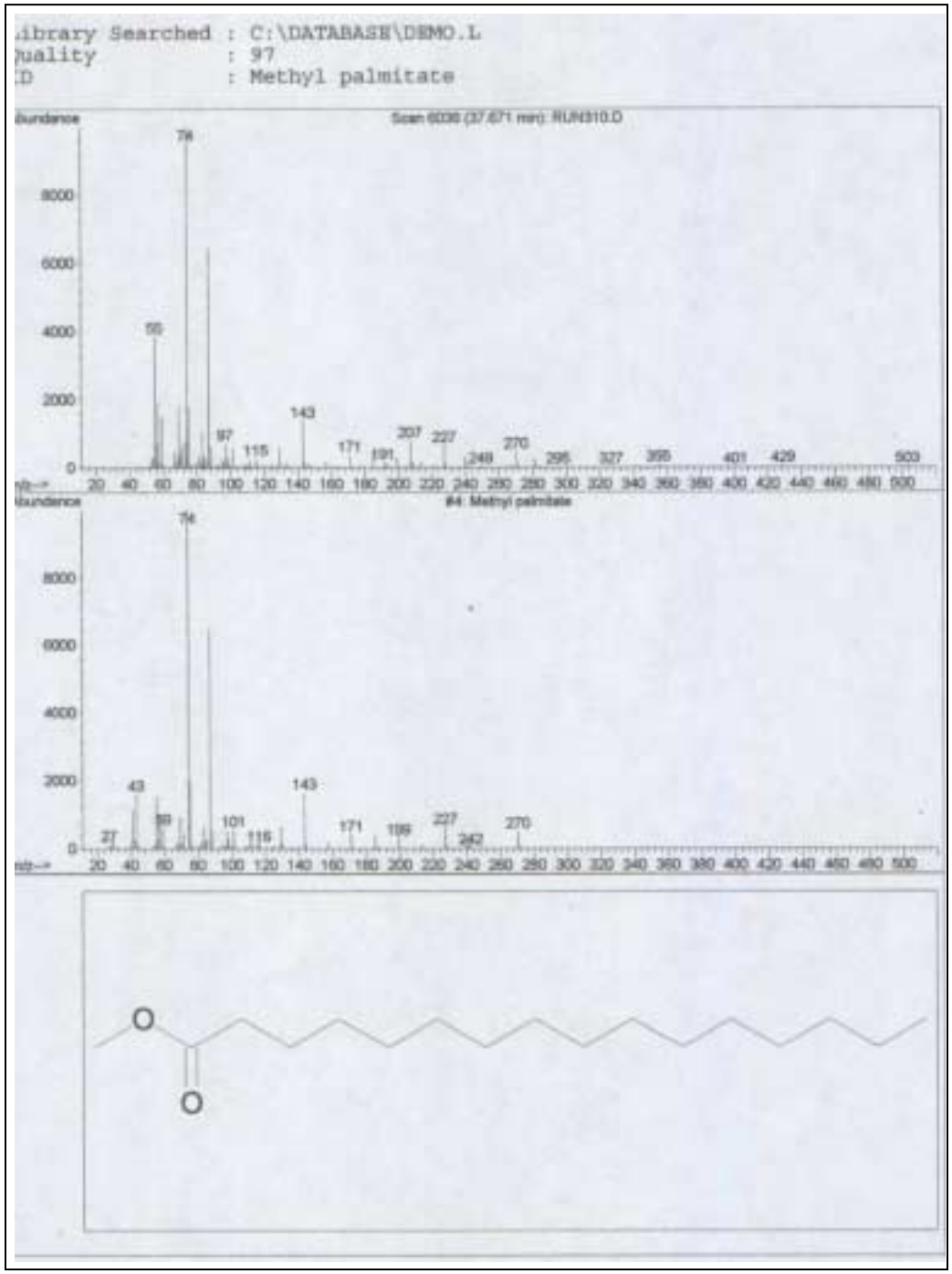

Figure G.1 Biodiesel characterization as methyl palmitate with a 97% of certainty

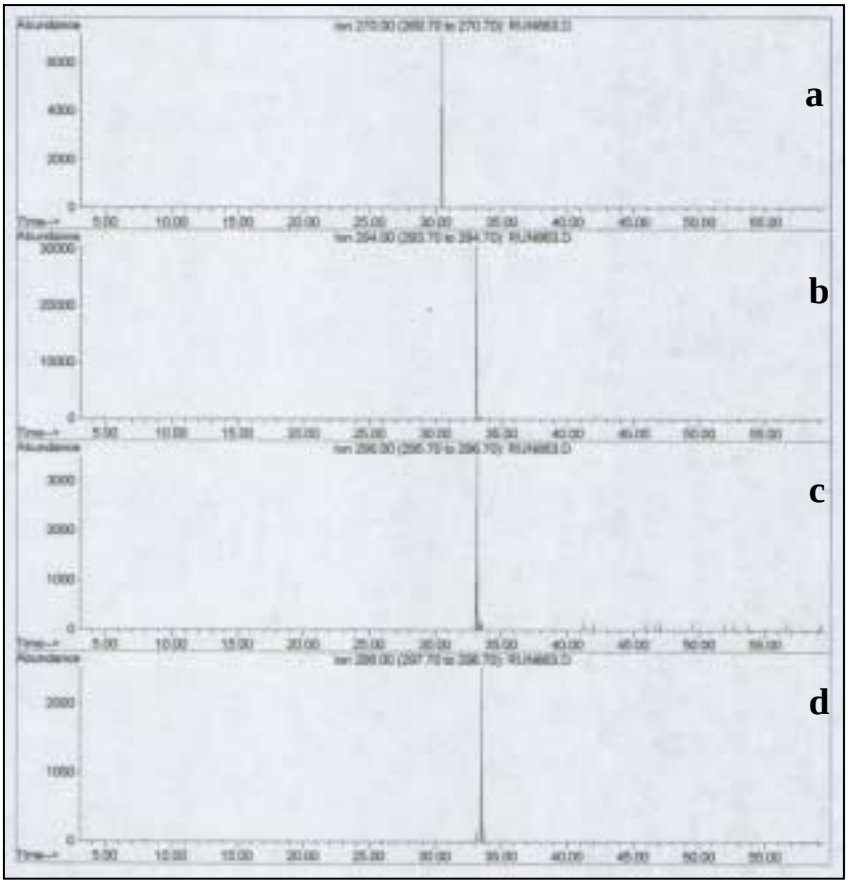

Figure G.2 Biodiesel mass and retention time distribution :(a) Ion270, (b)Ion 294, (c) Ion296 and (d) Ion298.

APPENDIX H: Additional information

Table H.1 Calibration curve of a stainless steel flow meter

L	**2**	**4**	**6**	**8**	**10**	**12**	**14**	**16**	**18**	**20**	**22**
FR	61	76	92	110	128	149	171	194	219	246	273
L	**24**	**26**	**28**	**30**	**32**	**34**	**36**	**38**	**40**	**42**	**44**
FR	302	330	359	387	415	443	470	496	522	548	573
L	**46**	**48**	**50**	**52**	**54**	**56**	**58**	**60**	**62**	**64**	**66**
FR	597	622	646	669	693	716	739	762	785	808	830
L	**68**	**70**	**72**	**74**	**76**	**78**	**80**	**82**	**84**	**86**	**90**
FR	853	875	898	920	942	965	987	1009	1031	1052	1096
L	**92**	**94**	**96**	**98**	**100**	**102**	**104**	**106**	**108**	**110**	**112**
FR	1118	1139	1160	1182	1203	1224	1245	1266	1287	1308	1328
L	**114**	**116**	**118**	**120**	**122**	**124**	**126**	**128**	**130**	**132**	**134**
FR	1349	1370	1390	1410	1431	1451	1472	1492	1512	1532	1552
L	**136**	**138**	**140**	**142**	**144**	**146**	**148**	**150**			
FR	1572	1592	1612	1632	1652	1671	1690	1709			

L = Location (mm) FR = Flow rate (cm^3 air)

Table H.2. Approximate average composition in fatty acids of triglyceride in vegetable oils (%)

Common name	**Fatty Acid**	**Corn**	**Olive**	**Soya**	**Sunflower**
Myristic	C14:0	-	-	0.5	0.5
Palmitic	**C16:0**	12	13	11	6
Estearic	**C18:0**	2.2	2.5	4	3
Oleic	**C18:1**	27	73	22	23
Linoleic	**C18:2**	57	8.5	53	64
Alphalinol	C18:3	<2.0	<1.5	8	<1.0
Arachidic	C20:0	<1.0	<0.5	<1.0	<1.0
Erutic	C22:1	-	<0.5	-	0.5

APPENDIX I: Reactors pictures

I.1 BSTR (Basket Stirred Tank Reactor)

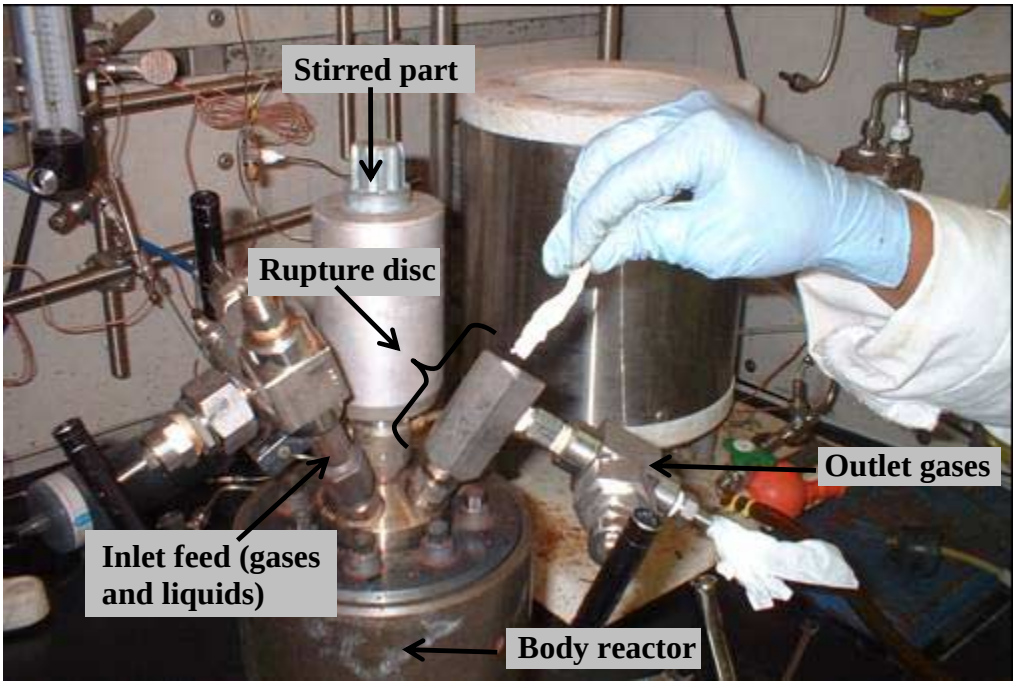

Figure I.1.1. Clean process after run with coke presence

Figure I.1.2. Coke presence in the gauge devices

BIBLIOGRAPHY

[1] Krumpelt M, Ahmed S, Kumar R, Doshi R. Partial Oxidation Catalyst. University of Chicago. US Patent 6,110,861 (1997)

[2] Borup R., Inbody T., Semelsberger T., Tafoya J. and Guidry D. Fuel composition effects on transportation fuel cell reforming. Catalysis today. (2004)

[3] Bae J-M., Ahmed S., Kumar R., Doss E. Microchennel development for autothermal reforming of hydrocarbons fuels. Power Sources. 139; 91-95(2005)

[4] Freni S., Calogero G., Cavallaro S. Hydrogen production from methane through catalytic partial oxidation reactions. Power Sources. 28-38 (2000)

[5] Garcia L., French R., Czernik S., Chorine E. Catalytic steam reforming of bio-oils for the production of hydrogen: effects of catalyst composition. Applied Catalysis. 225-239 (2000)

[6] Liu D-J., Kaun T., Liao H-K., Ahmed S. "Characterization of kilowatt-scale autothermal reformer for production of hydrogen from heavy hydrocarbons". Hydrogen Energy. 1035-1046(2004)

[7] Ayabe S., Omoto H., Utaka T., Kikuchi R., Sasaki K., Teraoka Y., Eguchi K. Catalytic Autothermal reforming of methane and propane over supported metal catalyst. Applied Catalysis. 261-269(2003)

[8] Chen G., Yuan Q., Li H., Li S. "CO selective oxidation in a micro channel reactor for PEM fuel cell". Chemical Engineering Journal. 101-106(2004)

[9] About Autos. Fuel Cell Future. - Goodbye, gasoline - hello, hydrogen http://about.edmunds.com/advice/specialreports/articles/102059/ (2004)

[10] Suzuki T., Miyamoto K., Kobayashi N. Aratani N. and Yogo T. (2002).R&D on hydrogen production by Autothermal Reforming. Shinnen Satte Laboratory. 2002

[11] Processing Crude oil. Chevron web page. http://www.chevron.com (2004)

[12] Wang X., Krause T., Kumar R. Sulfur Removal from reformate. Progress Report. Argonne National Laboratory. (2003)

[13] Farrell A., Keith D., Corbett J. A strategy for introducing hydrogen intro transportation. Energy Policy. 1357- 1367. (2003)

[14] Naidja A., Krishna C., Butcher T., Mahajan D. Cool flame partial oxidation and its role in combustion and reforming of fuels for fuel cell systems. Progress in energy and combustion science. 155-191 (2003)

[15] Krumplet M., Colucci J., Cabrera, C. Research Pre-proposal. Argonne Reformer Catalyst Characterization by X-Ray Photoelectron Spectroscopy. (2000)

[16] Pereira C., Bae J-M., Ahmed S. Krumpelt M. Liquid Fuel reformer development: Autothermal Reforming of Diesel Fuel. Proceedings of the 2000 Hydrogen Program Review, NREL/CP-570-28890. (2000)

[17] Rostrup-Nielsen J.R. Catalysis: Science and technology 5, Springer, Berlin (1984). Cited by Naidja A.

[18] Krumplet M. Converting hydrocarbon fuels into fuel for fuel cells. Seminary presentation. ANL. Boston (2003)

[19] Loffler D., Taylor K., Mason D. A light hydrocarbon fuel processor producing high-purity hydrogen. Journal of power sources 117. 84-91 (2003)

[20] Docter A., Lamm A. Gasoline fuel cell systems. Journal of power sources Vol 84. 194-200 (1999)

[21] Rampe T., Heinzel A., Vogel B. Hydrogen Generation from Biogenic and Fossil Fuels by Autothermal Reforming. J. of Power Sources Vol 86. 536-541 (2000)

[22] Moon D., Sreekumar K., Lee S., Lee B. and Kim H. Studies on gasoline fuel processor system for fuel-cell powered vehicles application. A.Cat. 215. 1-9 (2001)

[23] Krummenacher J., West K., Schmidt L. Catalytic Partial Oxidation of Higher Hydrocarbons at millisecond contact times: Decane, Hexadecane, and Diesel fuel. Journal of Catalysis 215. 332-343 (2002)

[24] Deluga G., Salge J., Schmidt L., Verykios X. Renewable Hydrogen from Ethanol by Autothermal Reforming. Science Vol 303. 993-997. (2004)

[25] Perez R. Autothermal Reforming (ATR) for fuel cells in automotive applications. Graduate Thesis. University of Puerto Rico at Mayagüez. (2004)

[26] http://www.virent.com/applications.htm. Conversion of Glycerol stream in a biodiesel plant. (2004).

[27] Anderson D., Masterson D., McDonald B., Sullivan L. Crown works iron company, Minneapolis, MN. Industrial Biodiesel Plant Design and Engineering: Practical Experience. Renewable energy management. (2003)

[28] Czernik S., French R., Feik C and Chornet E. Production of Hydrogen from Biomass-Derived Liquids. NREL/CP-570-28890. (2000)

[29] Yu S., Krebs J., Ferrandon M., Souleinmanova R., Myers D., Krause T. Water gas shift catalysis. ANL progress report. (2003)

[30] Borup R., Inbody M., Semelsberger T., Tafoya J., Vigil W., Guidry D. and Pacheco S. Testing of fuels in fuel cell reformers. Hydrogen, fuel cells and infrastructure Technologies. Alamos Laboratory. (2003)

[31] Ogden J. Review of small stationary reformers for hydrogen production. Center for Energy & Environmental Studies. Princeton Univ. IEA/H2/TR-02/002 (2002)

[32] Krishna C., Celebi Y., Butcher T., Long J., Waldee T., McDonald R. Research in future oil burner concepts. Proc 4th Natl Oil Heat Res Alliance Technology Conf. 37-66. (1989). Cited by Naidja *et al* [14]

[33] Lamini J., Dicks A. "Fuel cell systems explained". New York. Ed Wiley. (2000). Cited by Naidja *et al.*[14]

[34] Hirschernhofer J., Stauffer D., Engleman R. and Klett M. "Fuel Cell Handbook". 4th Ed. Fossil Energy Technology Center. (1998)

[35] http://www.cmt.anl.gov/science-technology/fuelcells/fuel-processor-engineering.shtml ANL, Fuel Processor Engineering. (2002)

[36] Mawdsley J., Ferrandon M., Rossignol C., Ralph J., Miller L., Kopasz J., and Krause T. "Catalysts for Autothermal Reforming". FY 2003 Progress Report. ANL

[37] Krause T., Ferrandon M., Mawdsley J., and Ralph J. IV.F.8 Catalysts for Autothermal Reforming. FY Progress Report. ANL (2004)

[38] Hadidi K., Bromberg L., Cohn D., Rabinovich A., Alexeev N., and Samokhin A. Plasma Catalytic Reforming of Biofuels. MIT (2003)

[39] Sirignano WA. Fuel droplet vaporization and spray combustion theory. Prog Energy Combust Sciences 9. 291–322 (1983). Cited by Naidaja *et al.*[14]

[40] Liu D., Krumpelt M., Chien H., and Sheen S.H. Catalysts and Fuel Mixing for Diesel Reformer in Fuel Cell Auxiliary Power Unit. Electrochemical Program. ANL

[41] Come G., Warth V., Glaude P., Fournet F., Batin-Leclerc F., Scacchi G. Computer-aided design of gas-phase oxidation mechanism-application to the modeling of n-heptane and isooctane oxidation. Proc Combust In.26 755–762 (1996). Cited by Naidaja *et al.*[14]

[42] Callahan C., Held T., Dryer F., Minetti R., Ribaucour M., Sauchet L., faravelli T., Gaffuri P., and Ranzi E. Experimental data and kinetic modeling of primary reference fuel mixtures. Proc Combust In. 25 730–746 (1996). Cited by Naidaja *et al.*[14]

[43] Wang D., Czernik S., Montane D., Mann M. and Chornet E. Biomass to hydrogen via fast pyrolysis and catalytic steam reforming of the pyrolysis oil or its fractions. Ind Engineering Chem Res Vol 36:1507–18. (1997). Cited by Naidaja *et al.*[14]

[44] Pietrogrande P, Bezzeccheri M. Fuel processing. In: Blomen LJM, Mugerwa MN, editors. (1993). Fuel cell systems. P. Press 121–56. Cited by Naidaja *et al.*[14]

[45] Sommer M., Lamn A., Doctor A., and Agar D. (2004). Modeling and dynamic simulation of a fuel cell system with an Autothermal gasoline reformer. J.Power Sources Vol 127 (313-318).

[46] Stutz M., Iseli C., and Poulikakos D. Effects of microreactor wall conduction on the reforming process of methane. Laboratory of Thermodynamics in Emerging Technologies, Inst. of Energy Technology, 2nd FC Research Symposium (2005)

[47] Arana L. High-Temperature microfluidic systems for thermally-Efficient fuel processing. PhD Thesis. MIT. (2003)

[48] Brown LF. A survey of processes for producing hydrogen fuel from different sources for automotive-propulsion fuel cells. DOE report # LA-13112-MS; Cited by Naidaja *et al.*[14] (1996)

[49] Krumpelt M., Ahmed S., Kumar R., Doshi R. Method for making hydrogen rich gas from hydrocarbon fuel University of Chicago US Patent 5,929,286 (1998)

[50] Palm C., Cremer P., Peters R. and Stolten D. Small-scale testing of a precious metal catalyst in the Autothermal reforming of various hydrocarbon feeds. Journal of Power Sources Vol 106- 231 (2002)

[51] Ersoz A., Olgun H., Ozdogan S., Gungor C., Akgun F. and Tırı M. ATR as a hydrocarbon fuel processing option for PEM fuel cell. J. of P. Sources Vol 118. (384–392) (2003)

[52] Krumplet M., Carter J.D., Wilkenhoener R., Lee S., Bae J. and Ahmed S. Catalytic Autothermal reforming for fuel cell systems. ANL. (2002)

[53] Institute for materials and processes in energy systems (IWV). Energy process engineering (IWV3). http://www.fz-juelich.de/iwv/iwv3/english/ (2003)

[54] Velu S., Satoh N., Chinnakonda G. and Suzuki K. Oxidative reforming of bio-ethanol over CuNIZnAl oxide catalysts for hydrogen production. Catalysis letters Vol 82. (145-152). (2002)

[55] Milne T., Elam C. and Evans R. Hydrogen from biomass. NREL. (2002)

[56] Zhang J. Investigation of CO tolerance in proton exchange membrane fuel cells. Warrester polytechnic institute. Graduate Thesis. (2004)

[57] Springmann S., Friedrich G., Himmen M., Sommer M., Eigenberger G. Isothermal Kinetic Measurements for Hydrogen Production from Hydrocarbon Fuels using a Novel Kinetic Reactor Concept. App. Catalysis. V235 (101-111) (2002)

[58] Liu D., Liao H., Miller L., Ahmed S. Diesel Reforming for Fuel Cell Application in a 1- to 5 – Kilowatt ATR reformer. Chemical Technology Division, Argonne National Laboratory. (2001)

[59] Krumplet M. Converting hydrocarbons fuels into fuel for fuel cells. ANL. (2003)

[60] NRC Institute for Fuel Cell Innovation. The Technology Fuel processing. http://ifci-iipc.nrc-cnrc.gc.ca/technology_fp.html. (2001)

[61] Office of industrial technologies. www.oit.doe.gov/chemicals. (2001)

[62] Wheeler F. Middle East Petrotech. Hydrogen Plants for the New Millennium. Conference and Exhibition. (2001)

[63] Chen Z., Yan Y., Said S. and Elnashaie H. Hydrogen Production and Carbon Formation during the Steam Reformer of Heptane in a Novel Circulating Fluidized Bed Membrane Reformer .Ind. Eng. Chem. Res. Vol 43 (1323-33). (2004)

[64] Brown L. A survey of processes for producing hydrogen fuel from different sources for automotive-propulsion fuel cells. Alamos Laboratory. (1996)

[65] Kumar R., Kastanas G., Barge S., Zamansky V., and Seeker R. Hydrogen Refueling System Based on Autothermal Cyclic Reforming. Proceeding of the 2002 US DOE Hydrogen Program Review, NREL/CP-610-32405. (2002)

[66] Kikuchi E., Tanaka S., Yamazaki Y., Morita Y. Bulletin Japan Petroleum Institute V 16. (1974)

[67] Aasberg K., Christensen T., Stub C., Dybkjær I. Recent developments in autothermal reforming and pre-reforming for synthesis gas production in GTL applications. Fuel Processing Technology. Vol 83 (253-261). (2003)

[68] Hartmann L., Lucks K., Köhne H. Mixture preparation by cool flames for diesel reforming technologies. Journal of power sources. Vol 118. (286-297). (2003)

[69] Johnson Matthey Fuel Cells. http://www.matthey.com/fuelcell/products.html

[70] Online Chemical Engineering Information. www.cheresources.com/ammonia.shtml

[71] Strategic Center for Coal. http://www.netl.doe.gov/coal

[72] Autothermal Reforming of Jet Fuel for SOFC APUs. University of Michigan. http://aiche.confex.com/aiche/2005/preliminaryprogram/abstract_17729.htm. (2005)

[73] Atlas web site. http://europa.eu.int/comm/energy_transport/atlas/homeu.html

[74] Cropper M. Fuel cells and hydrogen in Scandinavia – A survey of current developments. Fuel Cell today. (2004)

[75] USCAR. Web page. http://www.uscar.org/Media/2002issue2/hydrogen.htm. (2005)

[77] Chapter 2: Cars and the Environment. Driving Fuel Cell Vehicles—How Established Industries React to Radical Change. www.io.tudelft.nl

[78] Student Glossary. http://www.eere.energy.gov/biomass/student_glossary.html. EERE. (2005)

[79] Kopasz J., Liu D., Lottes S., Ahluwalia R., Novick V., Ahmed S. Progress Reports. ANL. (2003)

[80] Cortright R., Davda R., Dumesic A. Hydrogen from catalytic reforming of biomass-derived hydrocarbons in liquid water. Letters to nature, 418:964. (2002)

[81] Evans R., Boyd L., Elam C., Czernik S., French R., Feik C., Phillips S., Chornet E., Parent Y. Hydrogen from biomass-Catalytic Reforming of Pyrolysis Vapors. Hydrogen, fuel cells and infrastructure technologies. FY. (2003)

[82] Czernik S., French R., Magrini K., Evans R. Hydrogen from biomass: Process Research. NREL. (2004)

[83] Souza M., Aranda D., Schmal M. Coke formation on $Pt/ZrO_2/AlO_3$ catalysts during CH_4 reforming with CO_2. J. of Catalysis. V-204. (2001)

[84] Ahmed, S., Krumpelt, M. Hydrogen from Hydrocarbon Fuels for Fuel Cells. International Journal of Hydrogen energy, 26:291. (2001)

[85] Marty P., Grouset D. High temperature hybrid steam-reforming for hydrogen generation without catalyst. Journal of power sources. 118:66. (2003)

[86] Marquevich M., Coll R. and Montané D. Steam reforming of sunflower oil for hydrogen production. Ind. Eng. Chem. Res. 39: 2140. (2000)

[87] Marquevich M., Farriol X., Medina F. and Montané D. Hydrogen production by steam reforming of vegetable oils using Nickel-based catalysts. Ind. Eng. Chemical. 40:4757. (2001)

[88] Renewable power. Technical Reference Guide Hydrogen. (2000)

[89] Advantages and disadvantages of hydrogen. http://www.alternatefuels.com

[90] PEI wind-hydrogen symposium Hydrogen Energy Stations: The value proposition.. www.gov.pe.ca/photos/original/. (2003)

[91] The Future of the Hydrogen Economy. http://www.efcf.com. (2003)

[92] Knothe G., Rapid monitoring of transesterification and assessing Biodiesel fuel quality by NIR using a fiber optic. JAOCS, Vol 76;795. (1999)

[93] The hydrogen economy is coming, the question is where?. Forsberg C. Oak Ridge National Laboratory. Chemical Engineering Progress. Dec (2005)

[94] Oil wars or adaptation. http://www.grinningplanet.com. (2005)

[95] Garman D.; Ask the white house. Future of energy and personal transportation. http://www.whitehouse.gov/ask/20040312-2.html. (2004)